DISSERTATION

Impact of Renal Senescence on Kidney Allograft Outcome
-
Einfluss der renalen Seneszenz auf das Ergebnis von Nieren-Allotransplantaten

zur Erlangung des akademischen Grades
Medical Doctor - Doctor of Philosophy (MD/PhD)

vorgelegt der Medizinischen Fakultät
Charité – Universitätsmedizin Berlin

von

An He

Erstbetreuung: Univ. Prof. Dr. rer. nat. Katja Kotsch

Datum der Promotion: 23.03.2024

Table of contents

List of tables

List of figures

List of abbreviations

Acute rejection	AR
Bovine serum albumin	BSA
Cold ischemia time	CIT
C-reactive protein	CRP
Dendritic cells	DCs
Delayed graft function	DGF
Dimethylsulfoxid	DMSO
Double-negative	DN
Eurotransplant	ET
Fetal calf serum	FCS
Glomerular endothelial cells	gECs
Glomerular filtration rate	GFR
Granzyme B	GranB
Group 2 innate lymphoid cells	ILC2
Interleukin-33	IL-33
Immunofluorescence microscopy	IF
Ischemia-reperfusion injury	IRI
Mesentery lymph nodes	mLN
Mononuclear cells	MNCs
Organ Procurement and Transplantation Network	OPTN
Oxidative free radicals	OFR
Passenger leukocytes	PLs
Periodic acid schiff	PAS
Peroxisome proliferator-activated receptor γ activator-1	PPAR-γ

Penicillin/Streptomycin	P/S
Phorbol myristate acetat	PMA
Phosphate buffered saline	PBS
Proximal tubule epithelial cells	PTEC
Senescence-associated β-galactosidase	SA-β-gal
Senescence-associated secretory phenotype	SASP
Stress-induced premature senescence	SIPS
Standard criteria donors	SCD

Abstract

The increasing gap between available donor organs and the number of patients on the waiting list leads to the transplantation of so-called *expanded criteria donor* (ECD) organs. Advanced donor age is one of the main characteristics of ECD kidneys being associated with a higher risk of unfavorable outcome. So far, the underlying cellular mechanisms leading to restricted graft survival of older transplants as well as the recipients' immune response towards aged transplants remain largely unknown. In order to unravel the cellular composition of young versus aged grafts, a comprehensive analysis of the immunome of naïve murine kidneys was performed. Compared with young kidneys, older kidneys were characterized by increased frequencies of effector/memory T cells and group 2 innate lymphoid cells (ILC2s), whereas regulatory T cells (Treg) were decreased. Aged kidney-derived $CD4^+$ and $CD8^+$ T cells produced more IFNγ and showed a higher degranulation capacity than their young counterparts indicating a subclinical inflammation in senescent kidneys. This was further reflected by a significantly higher expression of MHC class II and the co-stimulatory molecules CD40 and CD80 on proximal tubular epithelial cells (PTECs). Applying a fully MHC-mismatch murine kidney transplantation model (C57BL/6 to BALB/c), an enhanced inflammatory, cytotoxic response towards the aged graft was observed compared with young donor grafts. This was indicated by significantly higher IFNγ, granzyme B, and perforin production by recipient-derived T cells. The induced inflammatory immune response to-wards the older kidney graft was successfully ameliorated by applying the senolytic drug ABT-263 to the donor prior to transplantation, resulting in significantly lower levels of IFNγ and IL-10 of graft-infiltrating T cell subsets. Moreover, ABT-263 graft pre-treatment of the aged donor resulted in a significant improvement of graft function on day 28 post kidney transplantation. In conclusion, chronological donor age is also reflected by changes within renal tissue, showing increased immunogenicity and provoking a stronger inflammatory response of the recipient. Pre-treatment strategies of aged grafts with senolytic drugs offer the potential to improve the outcome of ECD kidneys.

Zusammenfassung

Die steigende Diskrepanz zwischen verfügbaren Spenderorganen und Patienten auf der Warteliste resultiert in der zunehmenden Transplantation von Organen mit erweiterten Spenderkriterien, sogenannten *expanded criteria donor (ECD)* Organen. Ein höheres Spenderalter ist charakteristisch für ECD Organe, welche mit einem schlechteren Transplantatüberleben assoziiert sind. Bislang sind die zellulären Mechanismen für das schlechte Outcome älterer Spenderorgane als auch die zelluläre Antwort des Organempfängers gegen das alte Organ weitestgehend unbekannt. Um die zelluläre Komposition junger gegenüber alten Organen besser zu verstehen, wurde eine umfassende Analyse der lymphozytären Zusammensetzung muriner Nieren durchgeführt. Im Vergleich zu jungen Nieren wiesen ältere Organe höhere Frequenzen von effector/memory-Typ T-Zellen und sogenannten Gruppe 2 innate lymphoid cells (ILC2s) auf, wohingegen regulatorische T-Zellen deutlich reduziert waren. $CD4^+$ als auch $CD8^+$ T-Zellen älterer Nieren produzierten mehr IFNγ und zeigten eine höhere Degranulationskapazität - Charakteristika, die auf eine subklinische Inflammation in seneszenten Nieren hinweisen. Dies wurde auch durch die signifikant höhere Expression von MHC Klasse II-, als auch von kostimulatorischen Molekülen wie CD40 sowie CD80 auf proximalen tubulären Epithelzellen (PTECs) verdeutlicht. Unter Verwendung eines kompletten MHC-inkompatiblen murinen Nierentransplantationsmodells der Maus (C57BL/6 auf BALB/c) konnte eine erhöhte Inflammation und Zytotoxizität in älteren im Vergleich zu jungen Transplantaten dokumentiert werden, basierend auf höheren Frequenzen einwandernder IFNγ-, Granzym B- und Perforin-exprimierender Empfänger-T-Zellen. Die inflammatorische Immunantwort gegen ein älteres Organ konnte durch die Vorbehandlung des Spenders mit dem Senolytikum ABT-263 erfolgreich begrenzt werden. Diese führte zu einer signifikanten Reduktion der IFNγ- sowie IL-10-Produktion der infiltrierenden T-Zellen sowie zu einer verbesserten Nierenfunktion an Tag 28 post transplantationem. Zusammenfassend betrachtet führt das fortgeschrittene chronologische Alter potentieller Organspender zu einer Veränderung der lymphozitären Komposition residenter Immunzellen sowie zu einer erhöhten Immunogenität des renalen Spenderorgans. Dies führt zu einer erhöhten Immunantwort des Rezipienten gegen das Transplantat. Strategien zur Vorbehandlung älterer Organspender mit Senolytika sind daher vielversprechende Ansätze, um ein verbessertes Transplantatüberleben von ECD Organen zu erzielen.

1. Introduction

1.1 Renal transplantation, past and present

The first successful living-related kidney transplantation (KTx) was already carried out in 1954 between twins (Murray 2011). Since then, over the past seven decades, KTx was further developed into clinical practice in more than 80 countries as a treatment option for end-stage renal disease. Multiple studies have demonstrated that kidney transplant recipients experience better rates of life participation compared to dialysis patients (Sayin, Mutluay, and Sindel 2007; van den Ham et al. 2005). Advances in organ procurement and surgical techniques, development of immunosuppression regimens targeting early rejection, and prophylactic antibiotic therapies have led to major improvements in allograft outcomes during the past decades, reflected by an increase of the median survival for deceased donor transplants from 8.2 years in the era 1995–1999 to 11.7 years in the era 2014-2017 (Poggio et al. 2021). Out of all solid organs, kidney and liver were the most frequently transplanted organs, whilst small bowel transplants were the least frequent. In Europe, 5.687 and 1.183 kidney transplants were performed from deceased and living donors in 2022, respectively, while 13.276 patients were still on the waiting list (http://statistics.eurotransplant.org/). Thus, there is a great discrepancy between organ demand and supply, a circumstance that is further challenged by demographic changes in modern societies. For instance, the number of individuals with an advanced age >65 years is steadily increasing worldwide. Thus, an aging population and a higher incidence of patients diagnosed with e.g. progressive chronic kidney disease (CKD) constitutes a higher number of potential kidney transplant recipients. On the other hand, chronological donor age is also a major risk factor for allograft dysfunction, as grafts from older donors are more susceptible to ischemic injury and prone to develop delayed graft function (DGF) post-kidney transplantation, thus having an additional risk of unfavorable outcome (Perez-Saez et al. 2019).

1.2 Expanded criteria donors

The increasing gap between available donor organs and the increasing number of patients on the waiting list led to the usage of so-called expanded criteria donor organs (ECD). Expanded criteria donors were defined by the Organ Procurement and

Transplantation Network (OPTN) for marginal kidneys in 2002 (Metzger et al. 2003), referring to individuals aged 60 years or older or subjects aged 50-59 years with at least two of three additional risk factors: stroke, history of hypertension, or serum creatinine above 1.5 mg/dl before transplantation (Argani 2022)**.**

Recipients of ECD kidneys are characterized by a higher incidence of DGF rates, more acute rejection episodes and decreased long-term graft survival. A retrospective study from Hariharan et al. showed that transplant recipients who received a kidney graft with a donor age over 60 years had a significantly lower 5-year graft survival rate compared with recipients who received a kidney graft with a chronological age below 60 years (42.7% vs 61.4%) (Hariharan et al. 1997). Furthermore, at a 10-year follow-up, younger recipients (20 to 35 years) benefit from younger donor kidneys compared with older donor kidneys (Pippias et al. 2020). Several factors may explain these findings, including prolonged cold ischemia time (CIT), increased immunogenicity of aged grafts, and the impaired ability for kidney regeneration post-transplantation (Fang et al. 2022; Argani 2022). Even though ample evidence shows that ECD kidneys have a worse survival rate compared with standard criteria donor (SCD) kidneys (Querard et al. 2016), the usage of ECD kidneys has strongly increased during the last decade and accounts for nearly 50% of all deceased kidney donors in recent years. In 2022, 47% of all deceased donor kidney transplants performed in the Eurotransplant (ET) region were derived from donors >55 years (http://statistics.eurotransplant.org/). Therefore, a comprehensive understanding of the molecular mechanisms of ECD kidneys is of urgent need and instrumental for developing therapeutic strategies to improve renal allograft survival of these vulnerable organs.

1.3 Renal senescence

In general, an aging kidney is accompanied by a series of histological changes, including a decrease in total nephron size and number, glomerular basement membrane thickening, tubule interstitial changes, and increased glomerulosclerosis (Newbold, Sandison, and Howie 1992). At the immunological level, renal aging is characterized by the expression of senescence-associated β-galactosidase (SA-β-gal) and cyclin-dependent kinase inhibitor $p16^{INK4a}$ (Valieva et al. 2022; He and Sharpless 2017), and is associated with chronic, sterile, low-grade inflammation, defined as inflamm-aging. The term inflamm-

ageing represents a novel concept originally proposed by Claudio Franceschi at the beginning of this century which refers to an accumulation of unrepaired random molecular damage over time causing cellular defects and tissue dysfunction (Franceschi et al. 2000). Inflamm-aging is thought to be driven by immunosenescence (Walford 1964), characterizing cellular phenotypic and functional changes in the immune system reflected by two conflicting aspects: greater vulnerability to infectious disease and persistent systemic inflammation (Walford 1964). In principle, the number of senescent cells increases during immunosenescence; these cells are viable but exhibit altered morphology, greater heterogeneity, accumulation of lipofuscin granules, and SA-β-gal expression (Hayflick and Moorhead 1961). A substantial part of the senescent cells acquires a senescence-associated secretory phenotype (SASP) (Kuilman and Peeper 2009), mirrored by pro-apoptotic features and secretion of proinflammatory cytokines such as TNFα, IL-6, IL-8 and C-reactive protein (CRP) (Howcroft et al. 2013). Consequently, $SASP^+$ cells are believed to negatively influence the local tissue milieu by causing inflamm-aging. While it is considered that senescent cells are involved in the occurrence and progression of acute kidney injury (AKI), chronic renal disease and transplant rejection (Kooman et al. 2017; Infante et al. 2020; Valentijn et al. 2018), direct mechanistic data supporting this hypothesis are limited.

1.4 Immune cells and aging

The immune system is counteracted by intrinsic and extrinsic factors and changes accordingly start from early life while the onset of immunosenescence for healthy individuals commences around the age of 50 years (Rubelt et al. 2012). Age-associated changes in the immune system not only affect innate immunity, but also adaptive immune cells, resulting in impaired vaccine responses, increased susceptibility to infection and chronic kidney disease (Davis, Tato, and Furman 2017; Franceschi et al. 2017). Dendritic cells (DCs) are key components of innate immunity with a high potency of antigen presentation, but their ability of antigen retention and presentation is declining with age indicated by the downregulation of FcγRII (Aydar et al. 2003). In line with this, aged macrophages display reduced expression of pattern recognition receptors such as toll-like receptors (TLR); interestingly, this feature is accompanied by an enhanced capacity for inflammatory cytokine production, including TNFα and IL-6 (Chi et al. 2022). Phenotypic changes were also observed within the Natural Killer (NK) cell compartment

from the elderly with reduced expression of the natural cytotoxicity-associated receptors NKp46 and NKp30 (Almeida-Oliveira et al. 2011). Of note, enhanced expression of the activating cytotoxicity marker NKG2D in zero-hour biopsies of kidney transplants aged > 55 years has been associated with impaired graft function (Gunther et al. 2017), suggesting this marker being indicative for renal senescence.

T cells and B cells represent the main players in the adaptive immune system. For individuals with an age above 60 years, naïve T cell and B cell output is reduced, whereas memory T cells accumulate with loss of costimulatory molecule CD28 expression and upregulation of senescence signature molecules, including CD57 and killer cell lectin-like receptor G1 (KLRG1) (Frasca et al. 2016; Rodriguez et al. 2020). Whereas these features are collectively considered detrimental to host defense, immunosenescence might be beneficial in situations when immune cell activation is undesired. In that context, increased quantities of senescent $CD4^+CD28^-$ T cells in aged recipients correlate with superior acceptance of kidney allografts (Trzonkowski et al. 2010).

Studies on age-associated alterations within the recently described family of innate lymphoid cells (ILCs) are limited. ILCs are functionally related, innate counterparts of T helper cell subsets lacking a clonotypic antigen receptor and serving important roles in tissue homeostasis, maintenance, remodeling and antimicrobial immunity (Vivier et al. 2018). ILCs are defined by the absence of typical T-, B- or myeloid lineage markers and divided into three groups according to their different transcription factor- and cytokine profiles. Group 1 ILCs characteristically express Tbet and secrete IFNγ, whereas group 2 ILCs are $GATA3^+$ and express the signature cytokines IL-5 and IL-13. Group 3 innate lymphoid cells are $ROR\gamma t^+$ and predominantly produce IL-17 and IL-22. In human peripheral blood, ILC1 frequencies are stable throughout life, whereas ILC2 and ILC3 frequencies decline with age (Darboe et al. 2020). As ILC2s have been proposed to play an important role in tissue regeneration, the adoptive transfer of activated ILC2s has been successfully shown to revitalize the aged mouse brain by enhancing cognitive functions (Fung et al. 2020). The abundance of ILCs in multiple tissues, including the kidney (Cameron et al. 2019) and their emerging role in inflammatory and regenerative processes (Chen et al. 2020) emphasize the importance of a detailed investigation of this novel class of lymphocytes during aging.

1.5 Targeting senescence in potential renal grafts

The efficacy of immune surveillance diminishes with age, resulting in an accumulation and increase in the number of senescent cells (Munoz-Espin and Serrano 2014), particularly in transplant recipients under immunosuppressive medication to avoid allograft rejection (Hoffmann et al. 2015). These cells are associated with age-related pathologies such as glomerular disease and chronic allograft nephropathy (Sturmlechner et al. 2017; Childs et al. 2015). Furthermore, because senescent cells are unable to replace other damaged cells during wound healing, senescence reduces the ability of tissue regeneration as already shown for renal tubular injury (Bonventre and Yang 2011). Increased levels of mRNA expression of various potential senescence markers including $p21^{Cip1}$ and $p16^{INK4a}$ have been observed in pre-transplant biopsies and were correlated with unfavorable outcomes in renal transplantation (Koppelstaetter et al. 2008; Melk et al. 2009). Therefore, it might be beneficial to implement methods to modify vulnerable aged donor kidneys to enhance their resistance to ischemia-reperfusion injury (IRI) in order to improve their outcome. In this context, several potential therapeutic targets have been reported. Statins, for example, can upregulate the expression of telomere repeat-binding factor, a key protein for telomere capping, therefore preventing senescence in cells (Spyridopoulos et al. 2004). PPAR-γ agonists have been shown to reduce proteinuria, improvement of glomerular filtration rate (GFR) and decrease renal oxidative stress, thus alleviating cell senescence in the aging kidney (Yang et al. 2009). Reducing the number of renal senescent cells by senolytic drugs can also decrease aging-related diseases. ABT-263 (a specific inhibitor of the anti-apoptotic proteins BCL-2 and BCL-xL), is a potent senolytic drug that can selectively kill senescent cells in aged mice and promote rejuvenation of stem cells of several tissues, allowing tissue regeneration (Chang et al. 2016).

Despite these findings and insights into the effects of aging on the kidney, the precise mechanisms behind age-related changes that affect the long-term survival of renal allografts remain unknown. Hence, for this study, we employed an experimental mouse kidney transplantation model to investigate how kidney-resident lymphocytes are affected by aging, and to examine how aged kidneys influence the alloimmune response of the recipient. Our findings may have important implications for the development of targeted therapeutic approaches.

2. Aim of the study

The application of aged donor kidneys in clinical transplantation is growing rapidly, but the immunological factors leading to the compromised long-term survival of these organs have not been fully addressed. Kidney-resident immune cells and parenchymal cells induce an alloimmune response after transplantation, but so far little is known about the difference between these cells in young as compared to aged organs, especially with respect to the impact on the inflammatory response and graft function after transplantation. The same applies to potential therapeutic interventions to rejuvenate organs from old donors. Hence, the following objectives have been addressed in this study:

1. Determining the “immunome” in young vs. aged murine kidneys (and multiple other organs) by comprehensive characterization of key lymphocyte subsets.
2. Impact of young vs. aged renal transplants on the alloimmune response and resulting graft function in a murine kidney transplantation model.
3. Characterization of age-dependent changes in murine renal parenchymal cells.
4. Evaluating the effects of the senolytic agent ABT-263 on the renal “immunome” and parenchymal cells in aged mice.
5. Impact of ABT-263 donor pre-treatment on renal function in context with murine kidney transplantation.

3. Material and Methods

3.1 Material

3.1.1 Mice

C57BL/6 (CD45.2, H-2K^{b}), C57BL/6.SJL-Ptprca Pepcb/BoyJ (CD45.1, H-2K^{b}) and BALB/c (CD45.2, H-2K^{d}) mice, were purchased from Charles River Laboratory (Sulzfeld, Germany). Young C57BL/6 (C57BL/6JRj; CD45.2, H-2K^{b}), and old C57BL/6 (C57BL/6JRj; CD45.2, H-2K^{b}), 20 months, were purchased from Janvier-Labs (les Sorinières, France). For all experiments, only male mice, 8-12 weeks (if not otherwise indicated), weighing 24-35 g were used. Animals were kept under standard conditions and received human care in compliance with the 'Principles of Laboratory Animal Care' prepared by the National Academy of Sciences and published by the National Institutes of Health (NIH Publication No. 86–23, revised 1985). All animal experiments were approved and in accordance with guidelines from the Landesamt für Gesundheit und Soziales Berlin, Germany.

3.1.2 Chemicals and reagents

Chemicals and reagents are summarized in Table 1.

3.1.3 Equipment

Equipment used for experiments is summarized in Table 2.

3.2 Methods

3.2.1 Murine kidney transplantation

Murine kidney transplantations were performed as previously described with a slightly modified technique (Ashraf et al. 2019). After induction of anesthesia with isoflurane inhalation, an abdominal midline cross-incision was performed to fully expose the left urinary system. The left adrenal vein, lumbar vein, and gonadal vessels were carefully cauterized and cut to mobilize the left kidney, aorta, and inferior vena cava. The kidney was flushed in situ with HTK solution (CUSTODIOL, Dr. Franz Köhler Chemie GmbH, Germany) and procured en-bloc including the renal vein, the renal artery along with a small aortic cuff, and the ureter. Following the left nephrectomy of the recipient, the donor's kidney was implanted below the level of native renal vessels. End-to-side anastomoses between the donor and recipient vessels were performed using 10-0 nylon sutures (ETHILON, Johnson & Johnson Medical, Belgium). The last stitches were tied to

the short ends of the proximal or distal tie gently without tension. The ureter was directly anastomosed into the bladder using a pull-through technique for urinary tract reconstruction (He/Sarwar et al. 2022).

Table 1: Used chemicals and reagents (He/Sarwar et al, AJT. 2022)

Chemicals and reagents	Manufacturer
4% Histofix	Carl Roth, Karlsruhe, Germany
Albumin Fraction V	Carl Roth, Karlsruhe, Germany
Bepanthen eye ointment	Bayer, Leverkusen, Germany
Brefeldin A	Cayman, Michigan, USA
Bovine serum albumin (BSA)	Carl Roth, Karlsruhe, Germany
Buprenovet sine (Buprenorphine)	Bayer, Leverkusen, Germany
CASY Clean	OLS, Bremen, Germany
CASY Ton	OLS, Bremen, Germany
Corn Oil	Merck, Darmstadt, Germany
CD45 Micro Beads	Miltenyi, Bergisch Gladbach, Germany
Collagenase II	Gibco, Thermo Fisher, Darmstadt, Germany
Collagenase IV	Gibco, Thermo Fisher, Darmstadt, Germany
Dimethylsulfoxid (DMSO)	Honeywell, Seelze, Germany
DMEM F12 Advanced Medium	Corning, Falcon, Kaiserslautern, Germany
DNase I	Sigma Aldrich, Merck, Darmstadt, Germany
FACS Clean	Thermo Fisher, Darmstadt, Germany
FACS Flow	Thermo Fisher, Darmstadt, Germany
FACS Rinse	Thermo Fisher, Darmstadt, Germany
FcR blocking Reageant mouse	Miltenyi, Bergisch Gladbach, Germany
Fetal calf serum (FCS)	Gibco, Thermo Fisher, Darmstadt, Germany
Fix/Perm kit	BD, Heidelberg, Germany
Interleukin-33, carrier-free	Biolegend, San Diego, USA
Ionomycin	Sigma Aldrich, Darmstadt, Germany
Isoflurane	FEM Apotheke, Berlin, Germany
Isopentane	AppliChem, Darmstadt, Germany
Heparin-Natrium	B. Braun Melsungen AG, Melsungen, Germany
Histopaque 1083	Sigma Aldrich, Darmstadt, Germany
Monensin	Biolegend, San Diego, USA
Navitoclax (ABT-263)	Hycultec, Passau, Germany
Oligo (dT) primer	Thermo Fisher Scientific, Schwerte, Germany
Paraformaldehyde 2% (methanol- and RNAse-free)	Electron Microscopy Sciences, Hatfield, PA,USA
Penicillin/Streptomycin (P/S)	Sigma Aldrich, Merck, Darmstadt, Germany
Phorbol myristat acetat (PMA)	Sigma Aldrich, Darmstadt, Germany
Phosphate buffered saline (PBS)	Biochrom, Berlin, Germany
RPMI-1640 medium	Corning, Falcon, Kaiserslautern, Germany
Sodium chloride (NaCl) 0.9 %	B. Braun Melsungen AG, Melsungen, Germany

Table 2: Used equipment (He/Sarwar et al, AJT. 2022)

Equipment	Manufacturer
10-0 Nylon suture ETHILON	Johnson & Johnson, New Jersey, United States
5-0 Polypropylene suture PROLENE	Johnson & Johnson, New Jersey, United States
7-0 Braided silk suture	FST, Vancouver, Canada
2 ml Plastic pipet	VWR, Darmstadt, Germany
5 ml Plastic pipet	Sarstedt, Nürnbrecht, Germany
10 ml Plastic pipet	Fisher Scientific, Schwerte, Germany
25 ml Plastic pipet	Fisher Scientific, Schwerte, Germany
1.5 ml Reaction tube	Brand, Wertheim, Germany
5 ml Reaction tube	Sarstedt, Nurnbrecht, Germany
15 ml Reaction tube	Corning, Falcon, Kaiserslautern, Germany
50 ml Reaction tube	Corning, Falcon, Kaiserslautern, Germany
Bench EnvairEco Safe basic Plus	Envair, Emmendingen, Germany
Bench HeraSafe	Kendro, Langenselbold, Germany
CASY Cell counter & analyzer	OLS, Bremen, Germany
CASY Cups	OLS, Bremen, Germany
Cauterizer Surtron	LED SpA, Munich, Germany
Centrifuge 5415 R	Eppendorf, Hamburg, Germany
Centrifuge Multifuge 3 S-R	Thermo Fisher Scientific, Schwerte, Germany
Centrifuge Megafuge ST Plus	Thermo Fisher Scientific, Schwerte, Germany
Clamp Applying Forcep	FST, Vancouver, Canada
FACS tubes	Corning, Falcon, Kaiserslautern, Germany
Fortessa X-20 cell analyzer	BD, Heidelberg, Germany
Forcep Curve	FST, Vancouver, Canada
Forcep Straight	FST, Vancouver, Canada
Freezer -80°C	Heraeus, Hanau, Germany
Incubator	Eppendorf, Hamburg, Germany
Isoflurane Diffuser	Norvap, Barrowford, UK
LS Column	Miltenyi, Bergisch Gladbach, Germany
Oxgen Generator EverFlo	Philips, Amsterdam, Netherland
Pipetboy	Neolab, Heidelberg, Germany
Pipets ACURA 825	Socorex, Ecublens, Switzerland
Pump Novis	Neolab, Heidelberg, Germany
Scissor Staight	FST, Vancouver, Canada
Scissor Vannas spring	FST, Vancouver, Canada
Stero Microscope SZX10	Olympus Deutschland, Hamburg, Germany
Strainer 100um	Corning, Falcon, Kaiserslautern, Germany
Strainer 40um	Corning, Falcon, Kaiserslautern, Germany
Syringes 0.5 ml	BD, Heidelberg, Germany
Syringes 1 ml	BD, Heidelberg, Germany
Syringes 2 ml	BD, Heidelberg, Germany
Syringes 5 ml	BD, Heidelberg, Germany
Syringes 10 ml	BD, Heidelberg, Germany
Vascular Clamp	Aesculap, Tuttlingen, Germany
Vortex Shaker VF2	Neolab, Heidelberg, Germany
Warm Plate	Labtect, Göttingen, Germany

Cold and warm ischemia of the graft was kept at 20 and 30 minutes, respectively. To assess the effect of acute rejection (AR) on graft function, the contralateral naive kidney was removed 24 hours before the harvest. For short-term survival groups, mice were sacrificed and harvested 7 days after surgery. For long-term survival groups, mice were sacrificed and harvest 28 days after surgery. For prolonged cold ischemia groups, the donor kidneys were stored in HTK solution at 4 °C for 6 hours (He/Sarwar et al. 2022).

3.2.2 In vivo treatment

To induce senescent cells apoptosis, ABT-263 (50 mg/kg/day, Navitoclax, Hycultech GmbH) was applied by oral gavage in two cycles, with a one-week interval in between. Control animals received corn oil. Animals were sacrificed on either day 7 (short-term survival) or day 28 (long-term survival). The contralateral kidney was removed 1 day before the animals were euthanized in order to assess serum creatinine and urea, which are indicators of graft function (He/Sarwar et al. 2022). For the in vivo expansion of kidney ILC2s, carrier-free recombinant murine IL-33 (300 ng/mouse/day, Biolegend) was administered to the mouse intraperitoneally (i.p) for 5 consecutive days prior transplantation (He/Sarwar et al. 2022).

3.2.3 Tissue harvest

Whole animal perfusion was performed during tissue harvesting as described previously (Gage, Kipke, and Shain 2012). Briefly, after induction of anesthesia, a big cross incision was made to expose abdominal organs. Blood was collected through the vena cava. The portal vein was cut for a perfusate outlet. The pleural cavity was exposed by cutting the rib cage until the collarbone. The needle was inserted into the left ventricle through the posterior end and perfusate was pumped into the heart until all organs were pale and the perfusate from the outlet was clear. The kidney membrane was removed after harvesting (He/Sarwar et al. 2022).

3.2.4 Graft function assessment

Serum was collected by centrifuge of the whole blood at 4 °C, 3000 rpm for 10 minutes. Samples were stored in aliquots at −20°C until serum creatinine and urea were measured using the CREP2 Creatinine Plus version 2 and Urea/BUN assays, respectively, on a Roche/Hitachi Cobas C 701/702 system (Roche Diagnostics) (He/Sarwar et al. 2022).

3.2.5 Cell isolation

For isolation of MNCs from kidneys, tissues were minced and digested in 10 ml of RPMI medium supplemented with collagenases IV (Gibco/Invitrogen, Worthington) and DNase I (Roche Diagnostics) for 45 min at 37°C. Following digestion, recovered kidney leukocytes were enriched by CD45 microbeads over MACS LS columns (Miltenyi Biotec, Inc.). Leukocytes from lymph nodes and spleen were isolated by density gradient centrifugation. For isolation and culture of PTECs, kidneys were minced into pieces, processed through a 180 µm stainless steel sieve and collected in DMEM/F12 medium. Flow-through was applied to a 100 µm cell strainer from which renal tubular segments and glomeruli were recovered by reverse flushing with the medium. After centrifugation, tubular segments were digested using collagenase II for 20 min at 37°C in a shaking water bath. Thereafter, cells were either immediately analyzed by FACS or transferred to 6 well plates for outgrow cultures; 80% confluence of PTECs was reached after 5–6 days. Glomerular endothelial cells (gECs) were isolated as already published (Dumas et al. 2021). Briefly, glomeruli were digested using Trypsin–EDTA 0.25% (Life Technologies) for 23 min at 37°C in a shaking water bath, with pellet resuspension every 5 min. gECs were harvested by filtering the suspension through a 40 µm strainer. Cells were recorded by FACS LSR Fortessa X-20 and analyzed by FlowJo software 10.0 (He/Sarwar et al. 2022).

3.2.6 Cell counting

To count cell numbers, 10 µl of cell suspension was added to 10 ml CASY ton and measured in a CASY cell counter (Omni Life Science, Bremen, Germany). The given counts of living cells were used for further calculations (He/Sarwar et al. 2022).

3.2.7 Cell staining

To phenotype isolated MNCs, following a 10 mins Fc receptor block, 1 x 10^6 freshly isolated leukocytes were stained extracellularly with a mixture of various antibodies (see table 3) for 20 min at RT in the dark. Afterward, cells were washed at 500 xg for 6 min at 4°C. For intracellular antibody staining, cells were fixed and permeabilized by a Fix/Perm kit (Thermo Fisher). After washing at 500 xg for 6 min at 4 °C, cells were stained with a mixture of intracellular antibodies (Table 3) for 30 min at RT in the dark. Stained cells were washed at 500 xg for 6 min at 4 °C and measured on a BD Fortessa X-20 flow cytometer (Becton Dickinson). For functional analysis, 2.5 x 10^6 cells were stimulated with

phorbol 12-myristate 13-acetate (PMA, 50 ng), ionomycin calcium salt (1 µg) in the presence of brefeldin A (5 µg/ml), and monensin (2 µM) for retaining intracellular molecules for 4 hrs at 37°C and 5% CO_2 before staining (He/Sarwar et al. 2022).

Table 3: Antibodies used for phenotyping (He/Sarwar et al, AJT. 2022)

Antibody	Clone	Fluorochrome	Manufacturer
B220	RA3-6B2	APCCy7	Biolegend, San Diego, USA
B220	RA3-6B2	BV510	Biolegend, San Diego, USA
CD103	2E7	PE	Biolegend, San Diego, USA
CD107a	1D4B	PE	Biolegend, San Diego, USA
CD11b	M1/70	BV785	Biolegend, San Diego, USA
CD11c	N418	APCCy7	Biolegend, San Diego, USA
CD127	A7R34	BV785	Biolegend, San Diego, USA
CD25	PC61	BV605	BD, Heidelberg, Germany
CD25	PC61	PE	Biolegend, San Diego, USA
CD3	REA641	PerCP-Vio700	Miltenyi, Bergisch Gladbach, Germany
CD4	RM4-5	BV711	Biolegend, San Diego, USA
CD44	IM7	APC-eFluor 780	ThermoFisher,Darmstadt, Germany
CD45	30-F11	BV-510	Biolegend, San Diego, USA
CD45	30-F11	UV395	BD, Heidelberg, Germany
CD49a	Ha31/8	BV711	BD, Heidelberg, Germany
CD62L	MEL-14	BV421	Biolegend, San Diego, USA
CD69	H1.2F3	PE-Cy7	Biolegend, San Diego, USA
CD69	H1.2F3	BV421	Biolegend, San Diego, USA
CD8	53-6.7	BV605	Biolegend, San Diego, USA
CXCR6	SA051D1	PE-Dazzle	Biolegend, San Diego, USA
EOMES	Dan11mag	Alexa488	ThermoFisher,Darmstadt, Germany
FoxP3	MF-14	AF 647	Biolegend, San Diego, USA
GATA3	REA174	PE	Miltenyi, Bergisch Gladbach, Germany
Granzyme B	NGZB	PE-Cy7	eBioscience, ThermoFisher, Germany
IFNγ	XMG1.2	BV650	Biolegend, San Diego, USA
IL-5	REA1009	APC	Miltenyi, Bergisch Gladbach, Germany
IL-10	JES5-16E3	PE	Biolegend, San Diego, USA
IL-13	eBio13A	PE-Cy7	ThermoFisher,Darmstadt, Germany
IL-17	TC11-18H10.1	BV421	Biolegend, San Diego, USA
Ki67	SolA15	PE-Cy7	eBioscience, ThermoFisher, Germany
KLRG1	2F1	PE-Dazzle	Biolegend, San Diego, USA
KLRG1	2F1	BV711	BD, Heidelberg, Germany
L/D	-	BV510	Biolegend, San Diego, USA
MHCII	M5/114.15.2	BV650	Biolegend, San Diego, USA
NKp46	29A1.4	A700	BD, Heidelberg, Germany
NKp46	29A1.4	APC	Biolegend, San Diego, USA
RORγt	Q31-378	BV421	BD, Heidelberg, Germany
ST2	DIH9	PE-Dazzle	Biolegend, San Diego, USA
T-bet	4B10	PerCP-Cy5.5	Biolegend, San Diego, USA

3.2.8 Flow cytometry

Flow cytometric (FACS) analysis allows for the examination of single cells. Cells were labeled with fluorescently labeled antibodies against surface and intracellular markers of interest, allowing expression analysis using a flow cytometer. Single cells pass a light ray at fast speed, and depending on their structure, size, and staining, the cells exhibit a specific signal that may be examined (Cossarizza et al., 2017). An exemplary gating strategy for analysis of $CD4^+$, $CD8^+$, NK cells and subsets, DN T cells, effector memory T cells, regulatory T cells is depicted in He/Sarwar et al. 2022, Supplemental Figure 1; exemplary gating for PTECs and ECs is depicted in He/Sarwar et al. 2022, Supplemental Figure 2 and Figure 3. Innate lymphoid cell analysis was performed according to the gating strategy shown in Figure 1, below.

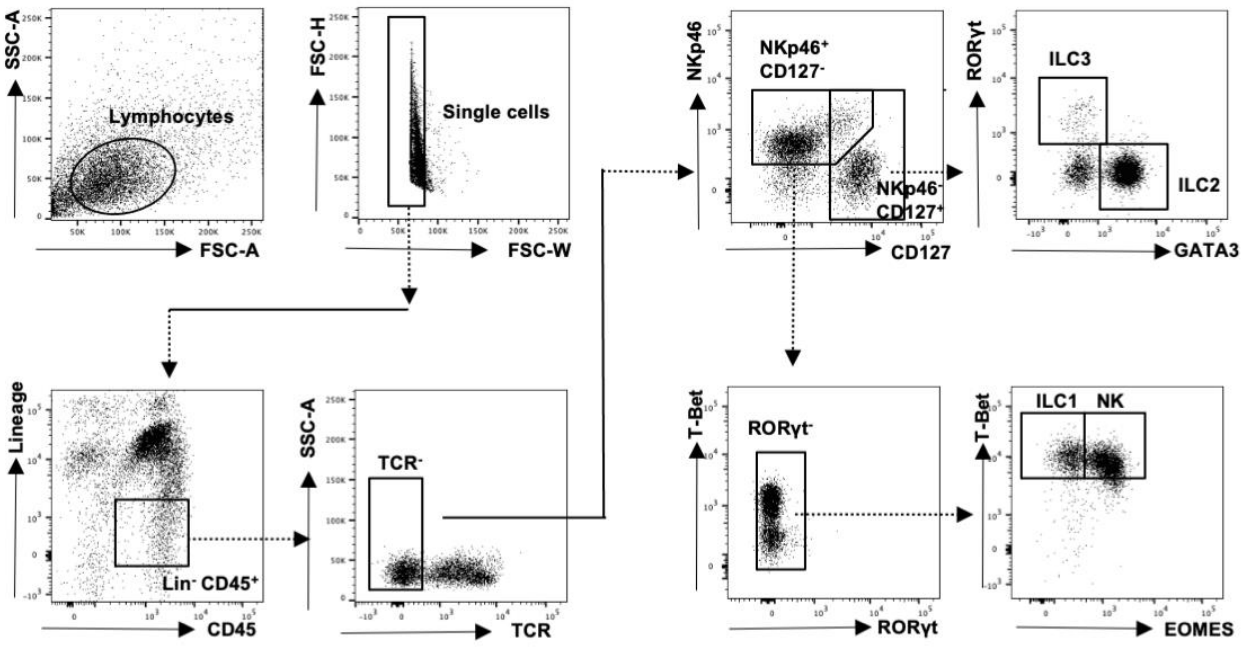

Figure 1. **Gating strategy for flow cytometric analysis of innate lymphoid cells**. Cell subsets were detected by FACS. Lymphocytes were gated, followed by single cells and $Lineage^-CD45^+$ ($DUMP^-$) TCR^- cells. Within the TCR^- subset, $NKp46^-CD127^+$ and $NKp46^+CD127^-$ cells were identified. Within $NKp46^-CD127^+$ cells, ILC2s are gated as $GATA3^+$ cells, ILC3s are gated as $ROR\gamma t^+$ cells. $ROR\gamma t^-$ cells were identified within $NKp46^-CD127^+$ cells, ILC1s are gated as $EOMES^-$, NK cells are gated as $EOMES^+$.

3.2.9 Histology and immunofluorescence microscopy

Formalin-fixed and paraffin-embedded kidney allograft tissues were cut into 1 µm thick sections. Following preparation, sections were stained with periodic acid schiff (PAS) and counterstained with hematoxylin. Samples were under evaluation for necrosis, acute

tubular damage, and glomerulitis. Semiquantitative scores in alignment with the Banff criteria were adapted and designed for each lesion. The following scores were used (Table 4). Scoring was performed in a blinded fashion based on the whole slide of each sample. Staining of ß-galactosidase was performed according to the manufacturer's instructions (Abcam).

Table 4: Evaluation and scoring criteria of kidney allografts

Scoring / Evaluation	0	1	2	3
Acute tubular damage	non	mild	moderate	severe
Necrosis	non	1–10% of tissue	11–20% of tissue	more than 20% of tissue
Interstitial inflammation in non-fibrotic cortex	⩽10%	11–25%	26–50%	more than 50%
Glomerulitis	non	present in at least one glomerulus		

Immunofluorescence microscopy (IF) was done as previously published (Stamatiades et al. 2016). Briefly, kidney allografts were excised and a ¼ of each kidney was fixed in PLP fixative overnight at 4°C on a rotating mixer. Following extensive washing with PBS, kidneys were dehydrated were in 30% sucrose in PBS overnight at 4°C, followed by snap frozen in OCT and stored at −80°C. 16 µm kidney cryosections were mounted on Superfrost Plus microscope slides (Fisher) and dried overnight at room temperature (RT). Sections were blocked and stained in a humidified box in the dark at RT overnight with purified or directly conjugated antibodies (Table 3). The next morning, following washes with PBS, sections were stained with the respective secondary antibody for 1h at RT, counterstained with Hoechst and mounted with Fluoromount-G (eBiosciences). Samples were scanned on a Zeiss LSM780 confocal microscope using a dry 20× 0.8 N.A. objective. Tiled, z-stacks were acquired at 1024 × 1024 pixels, with line averaging of 4 and pinhole size 1, and were stitched together using Zen Blue software (Zeiss). Fuji (version 1.53r) was used to process the acquired images and generate maximal intensity projection snapshots (He/Sarwar et al. 2022).

3.2.10 Analysis and statistics

Data generated by flow cytometry were analyzed using FlowJo Version 10. Statistical analysis was performed using GraphPad Prism 8. Cytobank software was used for further

analyses, including viSNE, heatmaps, or FlowSOM. T-test or Mann Whitney U-test (two groups) or Kruskal–Wallis test (multiple groups) based on the normality test results of the data, was used for calculating statistical significance. All present bar graphs show means. Statistical significance was considered for the following p-values: ns=$p > 0.05$, * $p \leqslant 0.05$, ** $p \leqslant 0.01$, *** $p \leqslant 0.001$, ****$p \leqslant 0.0001$ (He/Sarwar et al. 2022).

4. Results

4.1 Aged lymphoid and non-lymphoid organs display a distinct composition of key immune cell subsets

To assess differences in immune cell composition between young (3 months) and aged (20 months) mice, fresh mononuclear cells (MNCs) from lymphoid (lymph nodes, spleen) and non-lymphoid (kidney) organs were isolated, fluorescently labelled for typical cell-lineage determining markers and analyzed by flow cytometry. Lymphocyte subsets were identified by manual gating using FlowJo software (exemplified in He/Sarwar et al. 2022, Supplemental Figure 1), revealing that $CD3^+CD8^+$ T cell frequencies were significantly increased in all aged organs, whereas those of $CD3^+CD4^+$ T cells were decreased in old kidneys and lymph nodes (Figure 2A). Furthermore, significantly lower frequencies of $CD3^+CD4^-CD8^-$ double-negative (DN) T cells together with $NKp46^+$ NK cells were observed in aged kidneys and spleens compared to their young counterparts. Interestingly, DN T cells and NK cell frequencies were both increased in mLNs (He/Sarwar et al. 2022. Figure 1C). In addition, aged kidneys and lymph nodes were also characterized by significantly higher $CD11c^+$MHC II^+ dendritic cell (DC) frequencies (exemplary gating strategy in He/Sarwar et al. 2022, Supplemental Figure 2) than young organs, whereas aged spleens harbored fewer DCs (He/Sarwar et al. 2022, Figure 1C). Further characterization of T cell subsets revealed increased frequencies of the effector memory subset ($CD44^+CD62L^-$) within aged renal $CD8^+$ and $CD4^+$ T cells (Figure 2B).

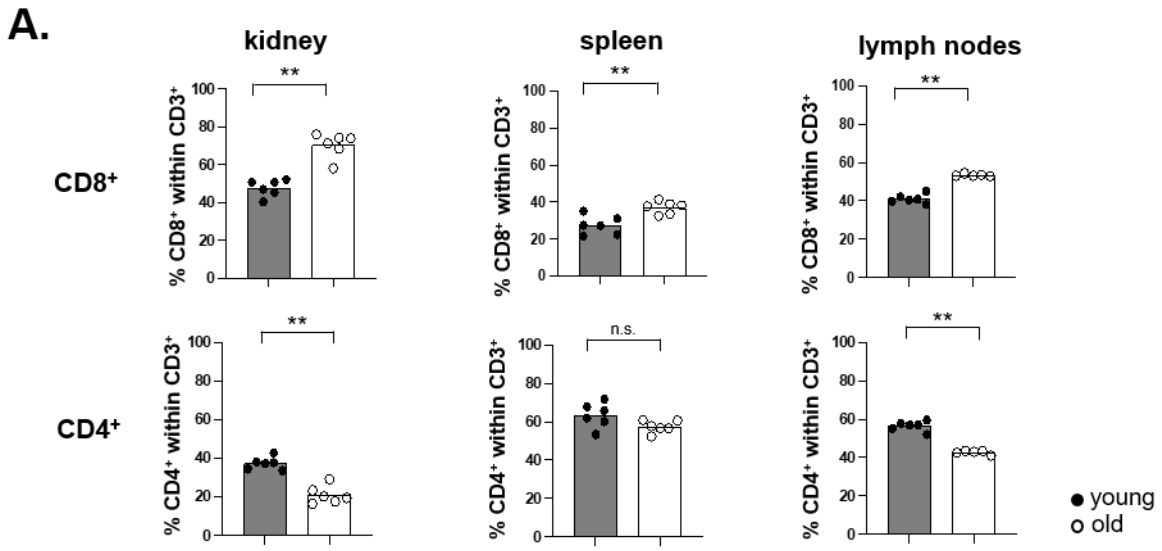

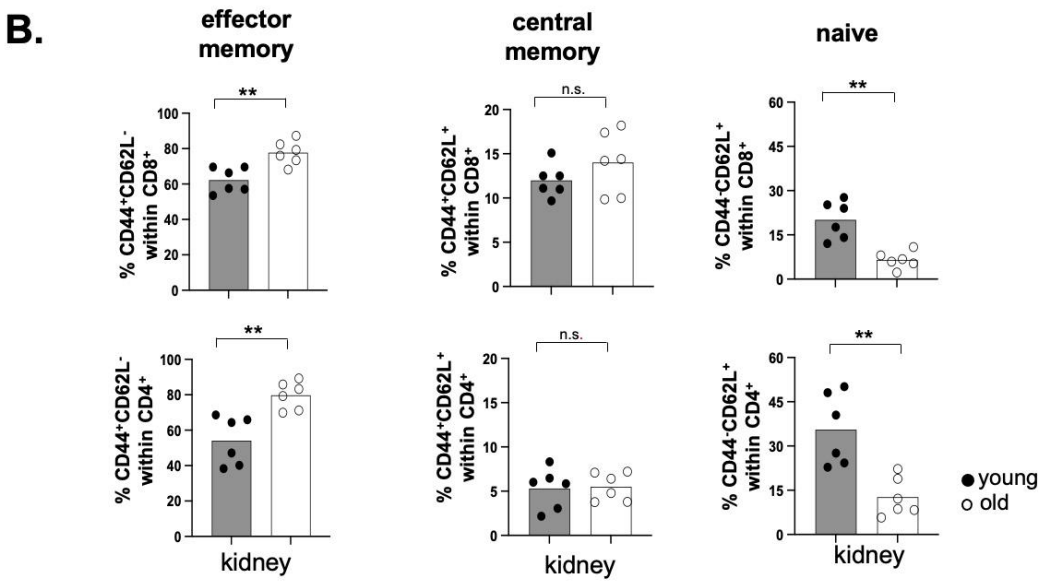

Figure 2. Aging leads to lymphocyte re-composition in various organs. (A) Frequencies of $CD3^+CD8^+$ and $CD3^+CD4^+$ T cells from young (3 months) and aged (20 months) naïve C57BL/6 murine kidneys, spleens, and mesentery lymph nodes (6 mice per group) as examined by FACS. (B) Frequencies of T cell subpopulations within the total $CD8^+$ and $CD4^+$ T cell populations as indicated and isolated from young (3 months) and aged (20 months) kidneys: $CD44^+CD62L^-$ effector memory T cells, $CD44^+CD62L^+$ central memory T cells and $CD44^-CD62L^+$ naïve T cells (6 mice per group). Statistically significant differences were tested with Mann–Whitney U test and presented as means, *p < .05; **p < .01; n.s. = not significant. Source: He/Sarwar et al. 2022.

On the contrary, natural regulatory T cells (Treg), defined as $CD4^+CD25^+FoxP3^+$, were significantly reduced in aged kidneys, showing less proliferation as indicated by lower portions of $Ki67^+$ cells (He/Sarwar et al. 2022. Figure 1E). Of note, we also found that group 1 innate lymphoid cell (ILC1s) frequencies were reduced, whereas group 2 innate lymphoid cells (ILC2s) and group 3 innate lymphoid cells (ILC3s) were significantly increased, in aged kidneys with all ILC subsets showing less proliferative capacity based on Ki67 analysis (Figure 3). In summary, aging leads to a re-composition of the immunome in aged kidneys, shifting towards an effector memory phenotype, accompanied by a loss of regulatory T cells and an enrichment of the kidney-dominating ILC2 population.

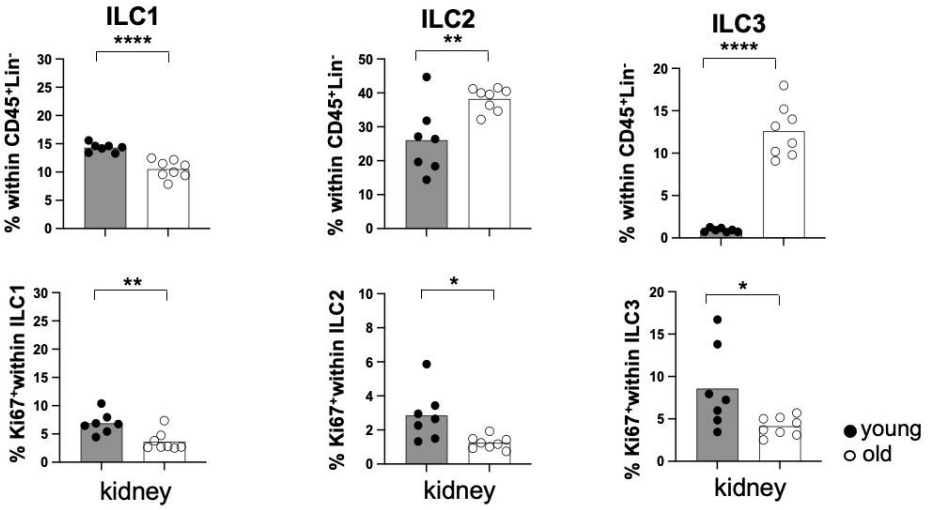

Figure 3. Aging leads to innate lymphoid cell re-composition in the kidney. Frequencies of NKp46^{+}Tbet^{+}EOMES^{-} group 1 innate lymphoid cells, CD127^{+}GATA3^{+} group 2 innate lymphoid cells, and CD127^{+}RORγt^{+} group 3 innate lymphoid cells within the CD45^{+}Lin^{-} population in young (3 months) and aged (20 months) kidneys (6-7 mice per group). Statistically significant differences were tested with Mann–Whitney U test and presented as means, *p < .05; **p < .01, ****p < .001; n.s. = not significant. Unpublished own data.

4.2 Aged renal lymphocytes acquire an inflammatory effector function profile

To study functional alterations induced by aging, MNC were activated ex vivo with PMA and ionomycin in the presence of the protein transport inhibitor Brefeldin A, allowing to assess of cytokine expression and cytotoxic capacity intracellularly by FACS (gating strategy depicted in He/Sarwar et al. 2022, Supplementary Figure 4). Within aged kidney-derived CD8^{+} and CD4^{+} T cells, we observed significantly higher portions of CD107a^{+} and IFNγ^{+} cells, but lower portions of granzyme B producers. An increase in frequencies of IL-10^{+} cells was only detectable for the renal CD4^{+} population isolated from aged mice. (Figure 3). Frequencies of perforin^{+} and IL-17^{+} CD8^{+} and CD4^{+} T cells were comparable between young and aged kidneys (He/Sarwar et al. 2022. Figure 3A). However, IL-17 producers were enriched in the DN T cells from aged kidneys, along with reduced portions of IFNγ producers. Aged kidney derived NK cells showed similar frequencies of degranulating CD107a^{+} cells as compared to young organs but contained fewer portions of IFNγ^{+}, GranB^{+}, and perforin^{+} cells, indicating an impairment of classical NK effector functions, along with higher frequencies of IL-17^{+} and IL-10^{+} cells (for data on DN T cells and NK cells, refer to He/Sarwar et al. 2022, Figure 3A). To conclude, intra-renal lymphocytes showed multiple functional shifts of their effector molecule profiles in aged organs (Figure 4).

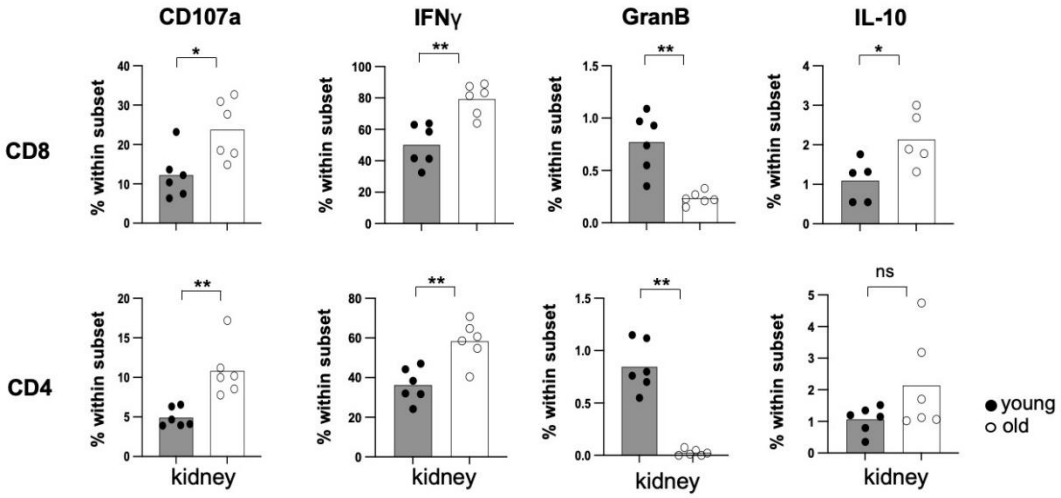

Figure 4. Aged kidney-resident lymphocytes show an inflammatory effector profile. (A) Frequencies of CD107a-, IFNγ-, Granzyme B- and IL-10-expressing cells within the total $CD8^+$ or $CD4^+$ T cell populations isolated from young (3 months) and aged (20 months) naïve kidneys. Statistically significant differences were tested with Mann–Whitney U test and presented as means, *p < .05; **p < .01; n.s. = not significant. Source: He/Sarwar et al. 2022.

4.3 Aged renal proximal tubular epithelial cells and glomerular endothelial cells upregulate MHC class II and co-stimulatory molecules

Enhanced age-dependent, glomerular inflammation might be principally associated with altered activatory states of endothelial cell (EC) subsets. We therefore isolated glomerular endothelial cells (gECs) and parenchymal endothelial cells (pECs) from naïve young and aged kidneys. Strikingly, aged kidneys contained significantly higher portions of MHC class II^+ gECs, whereas upregulation of CD40, and CD80 less pronounced (Figure 5A;

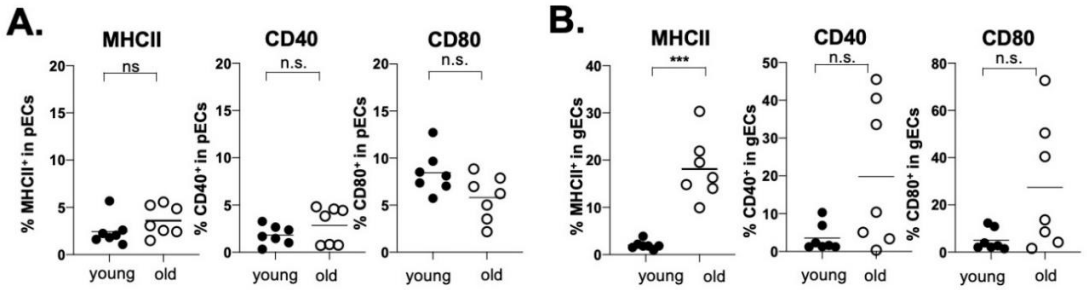

Figure 5. Aged kidney gECs are characterized by augmented expression of activating and co-stimulatory molecules. (A) Frequencies of $MHCII^+$, $CD40^+$, and $CD80^+$ cells within freshly isolated gECs and (B) pECs from naïve young and old C57BL/6 kidneys as determined by FACS. Statistically significant differences were tested with Mann–Whitney U test and presented as means, ***p < .001; n.s. = not significant. Source: He/Sarwar et al. 2022.

gating strategy depicted in He/Sarwar et al. 2022, Supplemental Figure 3). No differences between young and old organs were observed for pECs (Figure 5B).

Next, we examined whether the phenotype of proximal tubular epithelial cells (PTECs) was influenced by aging. Similar to gECs, isolated PTECs from aged naïve kidneys showed higher frequencies of MHC II^+, $CD40^+$, and $CD80^+$ cells with only the latter comparison not reaching significance (Figure 6).

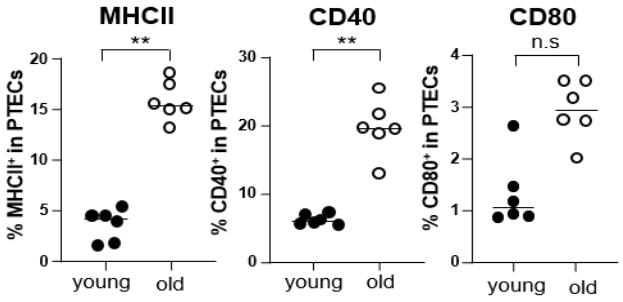

Figure 6. Aged kidney PTECs show enhanced expression of activating and co-stimulatory molecules. Statistically significant differences were tested with Mann–Whitney U test and presented as means, **p < .01; n.s. = not significant. Source: He/Sarwar et al. 2022.

In summary, these experiments demonstrate that aging is associated with enhanced immunogenicity/costimulation capacity of renal endothelial and epithelial cells from distinct micro-anatomical locations.

4.4 Aged kidney allografts trigger a more inflammatory immune response

As a prerequisite for studying the impact of young vs. aged donor organs in a fully MHC-mismatched model of murine kidney transplantation, lymphocyte infiltration kinetics of the graft post-transplantation were analyzed. BALB/c derived donor lymphocytes could be identified based on expression of the congenic marker CD45.2, while C57BL/6 recipient cells express CD45.1. The composition of intra-renal leukocytes showed that, while donor-derived leukocytes were still detectable on day 3 post-transplantation, the kidney was almost completely repopulated by $CD45.1^+$ recipient-derived cells on day 7 (Figure 7). Since the recipients´ immune response was in the focus of this study, most cellular readouts were consequently conducted at day 7. In addition, in some experiments, kidney function was assessed on day 28, based on previous experience in this experimental model (Dangi et al. 2020).

In the next step, kidneys from either young (3 months) or aged (20 months) C57BL/6 donor mice were transplanted into young (3 months) BALB/c recipients (Figure 8). This

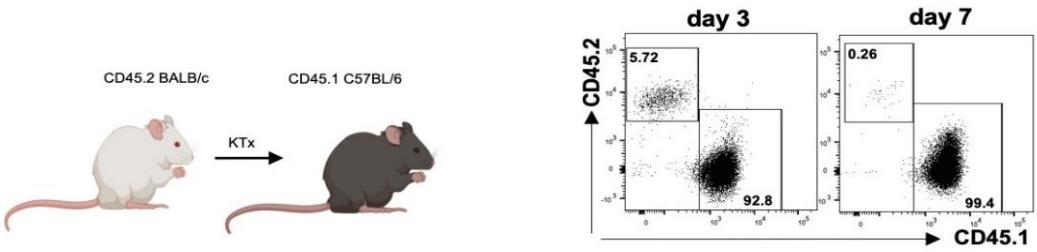

Figure 7. Early infiltration of recipient-derived leukocytes into the graft post-transplantation. Kidney transplantation was performed using CD45.2$^+$ BALB/c as donors and CD45.1$^+$ C57BL/6 mice as recipients. Representative FACS dot plots depict leukocyte distribution in the graft on day 3 and day 7 post-transplantation. Source: He/Sarwar et al. 2022.

strain combination was chosen due to the fact that only aged C57BL/6, but not BALB/c mice are commercially available. On day 7 post-transplantation, significantly higher frequencies of CD4$^+$ T cells infiltrated into the graft (He/Sarwar et al. 2022, Figure 5A) which was not observed in the spleen or lymph nodes (He/Sarwar et al. 2022, Supplemental Figure 7). CD4$^+$ T cells were enriched for CD44$^+$CD62L$^-$ effector memory cells in aged over young grafts (Figure 8).

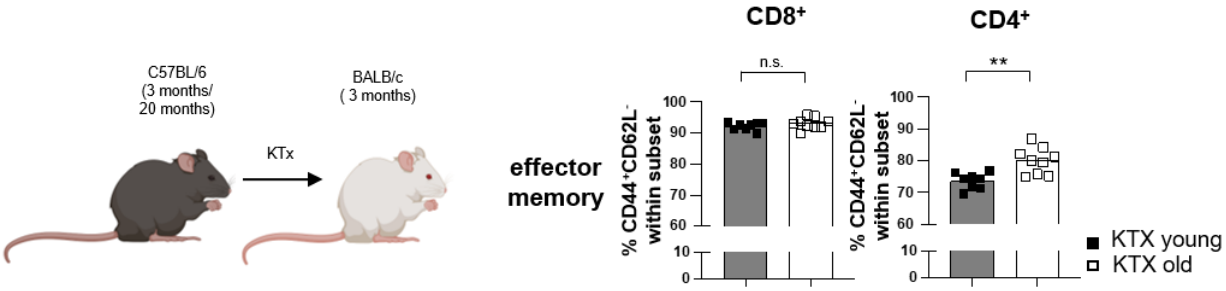

Figure 8. Aged kidneys are infiltrated by higher frequencies of effector memory CD4$^+$ T cells. Experimental setup (left). Frequencies of effector memory CD8$^+$ and CD4$^+$ T cells isolated from young or old kidney grafts on day 7 post-transplantation (right) (n=8-9). Statistically significant differences were tested with Mann–Whitney U test and presented as means, *p < .05; **p < .01; n.s. = not significant. Source: He/Sarwar et al. 2022.

Further characterization of recipient-derived T cells in the aged kidney graft revealed elevated frequencies of CD107a, GranB, and perforin expressing cells within the CD8$^+$ compartment, whereas portions IFNγ$^+$ and IL-10$^+$ cells were upregulated in both CD8$^+$ and CD4$^+$ T cells (Figure 9). Some of the aforementioned features also applied to graft-derived DN T- and NK cells (He/Sarwar et al. 2022, Figure 5C). In summary, infiltrating recipient-derived T cells isolated from aged kidney grafts were characterized by an augmented proinflammatory, cytotoxic immune response.

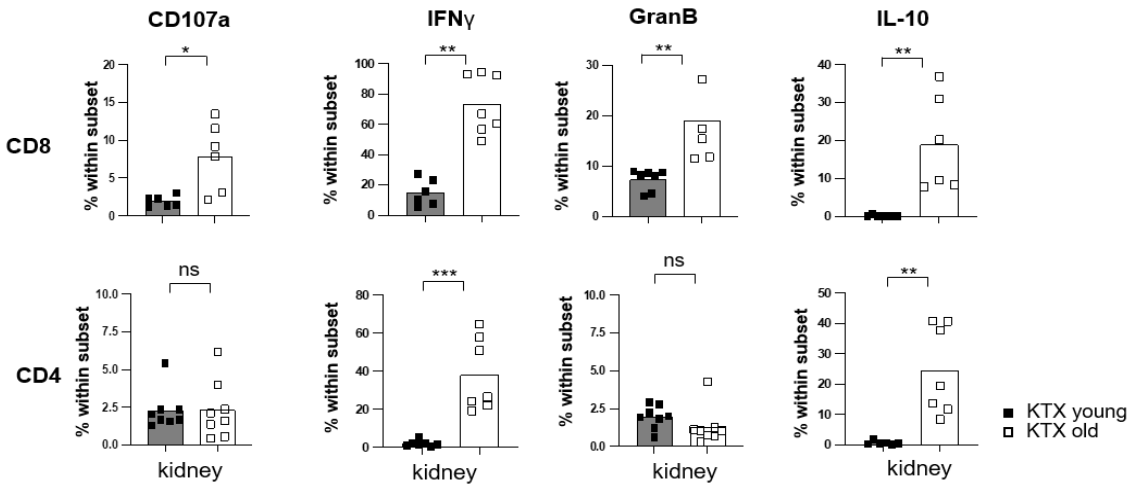

Figure 9. Aged kidneys trigger an inflammatory intra-renal milieu post-transplantation. Functional profile of $CD8^+$ and CD4 T^+ cells isolated from young or old kidney grafts on day 7 after transplantation with the cytokines and cytotoxic features as indicated (n = 5-8). Statistically significant differences were tested with Mann–Whitney U test and presented as means, *p < .05; **p < .01, ***p < .001; n.s. = not significant. Source: He/Sarwar et al. 2022.

Classical histological analysis of kidney allografts from aged donors revealed a higher incidence of glomerulitis compared with young counterparts, but no difference for tubular damage, necrosis, and interstitial inflammation was observed (Figure 10A, 10B).

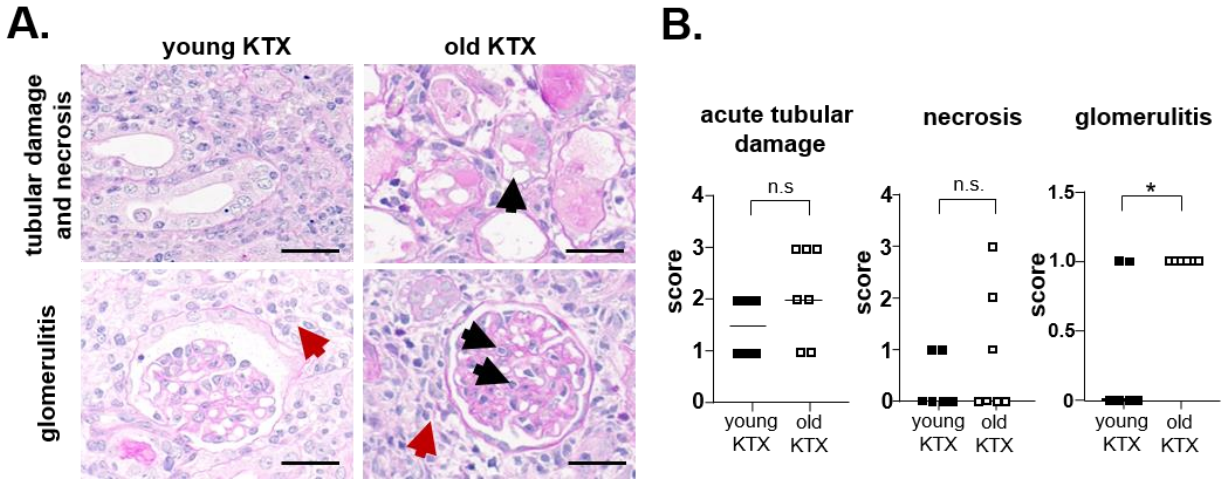

Figure 10. Aged kidney allografts exhibit more glomerulitis post-transplantation. (A) Representative histological images of tubular damage, necrosis (black arrow), glomerulitis (black arrow), and interstitial inflammation (red arrows) in young and old kidney allografts on day 7 post-transplantation. 400x magnification, bar represents 20 µm. (B) Statistical analysis of tubular damage, necrosis and glomerulitis scores of young and old kidney allografts on day 7 post-transplantation. Statistically significant differences were tested with Mann–Whitney U test and presented as means, *p < .05; n.s. = not significant. Source: He/Sarwar et al. 2022.

4.5 Senolytic drugs reduce inflammation of aged kidneys and improve allograft function

The application of senolytics represents a potent strategy to modify aged organs. ABT-263 (Navitoclax), a specific inhibitor of the anti-apoptotic proteins BCL-2 and BCL-xL, can selectively induce apoptosis in senescent cells (Mylonas et al. 2021), bearing the potential to counteract age-related renal inflammation. Therefore, we first examined ABT-263-induced effects on senescent gEC cells after systemically treating naïve aged C57BL/6 mice (representing the donor in our kidney transplantation model). ABT-263 was dissolved in corn oil and administered in two cycles by oral gavage with a 1-week interval in-between. Corn oil alone was administered to control animals (Figure 11).

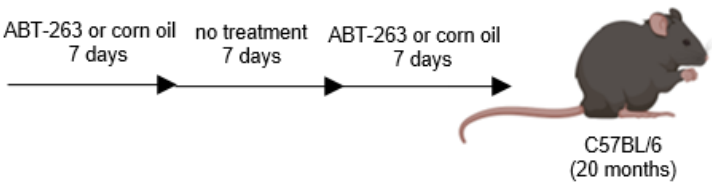

Figure 11. Diagram of the experimental setup of ABT-263 treatment. ABT-263 (50 mg/kg/day) was ad- ministered in two cycles by oral gavage with a 1-week interval in-between (own illustration).

Importantly, pretreatment of ABT-263 resulted in a lower number of MHC class II^+ gECs in the aged kidney as compared to untreated aged organs (Figure 12A). This difference was significant for the two-group comparison (old ABT-263 treated vs. old untreated), but not in the three-group comparison including young mice. In line with the aforementioned, kidney $CD4^+$ and $CD8^+$ T cells produced less IFNγ and displayed lower cytotoxic capacity based on the degranulation marker CD107a (Figure 12B), indicating a less inflammatory/cytotoxic phenotype.

Next, we examined the impact of ABT-263 donor pre-treatment in the context of kidney transplantation. Therefore, aged C57BL/6 donor mice were ABT-263 pre-treated or not as before; kidneys from both groups were transplanted into BALB/c recipients, respectively (Figure 13A). Mice were sacrificed on day 7 for cellular analysis and graft function, the contralateral kidney was removed 1 day before animals were sacrificed in order to analyze serum creatinine and urea being indicative of graft function; in some experiments, functional parameters were also assessed on day 28.

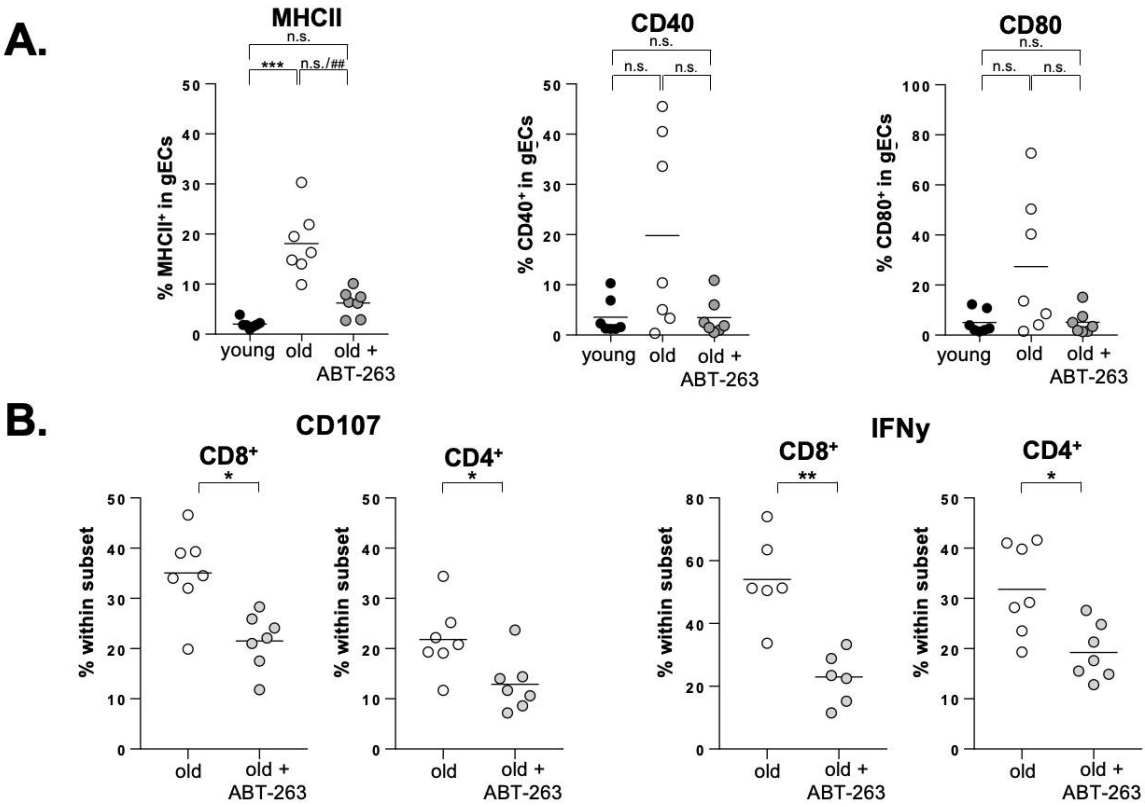

Figure 12. ABT-263 modulates the immunogenicity of the old kidney. (A) Ex vivo surface expression of MHCII, CD40, and CD80 on glomerular endothelial cells isolated from naïve young (n = 6), or aged corn oil (n = 7) versus ABT-236 treated aged C57BL/6 mice (n = 6). (B) Frequencies of CD107a$^+$ and IFNγ$^+$ CD8$^+$ and CD4$^+$ T cells isolated from aged corn oil (n = 7) versus ABT-236 treated aged C57BL/6 mice (n = 7). Statistically significant differences were tested with Mann–Whitney U where ## indicates $p < .01$ in a two-group comparison or, alternatively by Kruskal–Wallis-test in a multiple-group comparison and presented as means. *$p < .05$; **$p < .01$; ***$p < .001$; n.s. = not significant. Source: He/Sarwar et al. 2022.

Of note, ABT-263 treatment resulted in lower frequencies of MHCII, CD40, and CD80 expressing cells as compared to the untreated group, although not statistically significant due to the small sample size (Figure 13B). Functional characterization of graft infiltrating CD4$^+$, CD8$^+$, and DN T showed significantly less frequencies of IFNγ- and IL-10 producers. With respect to IFNγ, this observation also applied to NK cells (Figure 13C).

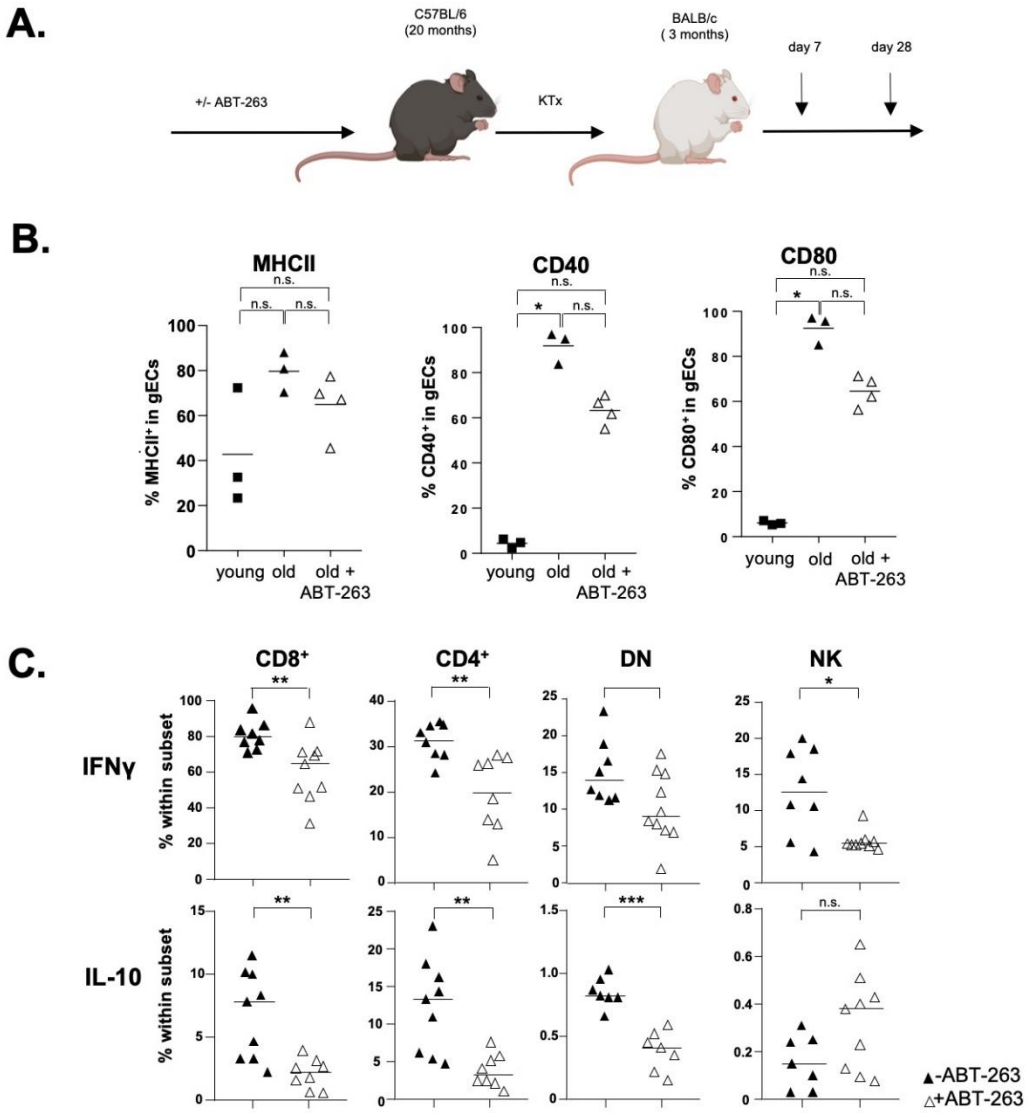

Figure 13. ABT-263 treatment ameliorates intra-graft inflammation of senescent kidneys post-transplantation. (A) Diagram of the experimental setup of ABT-263 treatment. (B) Frequencies of cells expressing the indicated molecules within total glomerular endothelial cells directly isolated from young (n = 3) and aged control (n = 3) versus ABT-263 treated aged C57BL/6 grafts (n = 4) transplanted into BALB/c recipients. Analysis was conducted on day 7 post-transplantation. (C) Frequencies of IFNγ- and IL-10 expressing $CD8^+$ and $CD4^+$ T, DN T cells and NK cells isolated from aged control or ABT-263 pre-treated grafts. Statistically significant differences were tested with Mann–Whitney U test or unpaired t-test and presented as means. *p < .05, **p < .01; ***p < .001; n.s. = not significant. Source: He/Sarwar et al. 2022.

We only noted a minor impact of ABT-263 treatment on graft function on day 7 post-transplantation as reflected by similar creatinine and urea levels compare to controls (Figure 14, left), potentially owing to small sample size. To further address the long-term effect of ABT-263 on kidney function, experiments were conducted as before with readout of kidney function at day 28. Importantly, the ABT-263 treated group showed significantly

better graft function indicated by reduced serum creatinine and urea compared with the untreated group (Figure 14, right).

Figure 14. ABT-263 treatment improves graft function of senescent kidneys post-transplantation. Analysis of graft function according to serum creatinine and urea on day 7 and (left panel) or day 28 post kidney transplantation (right panel) with n = 4 -10 animals/group. Statistically significant differences were tested with Mann–Whitney U test or unpaired t-test and presented as means. *p < .05; n.s. = not significant. Source: He/Sarwar et al. 2022.

4.6 Enriched group 2 innate lymphoid cells were depleted following the allogeneic response

ILC2s have been identified as reno-protective cells in experimental models of IRI and glomerulosclerosis (Cao et al. 2018; Riedel et al. 2017). Our analysis revealed that relative frequencies of ILC2s within the total ILC compartment were strongly enriched in aged compared with young kidneys from naïve C57BL/6 mice (Figure 15A and 15B). Interestingly, ILC2s from aged animals showed significantly reduced ex vivo proliferation as reflected by Ki67 expression (Figure 15B, right panel). In order to evaluate whether the enrichment of intra-renal ILC2s in the donor graft shows persistence post kidney transplantation, thus having a potential reno-protective effect, we transplanted kidneys from either young (3 months) or aged (20 months) C57BL/6 donor mice into young (3 months) BALB/c recipients.

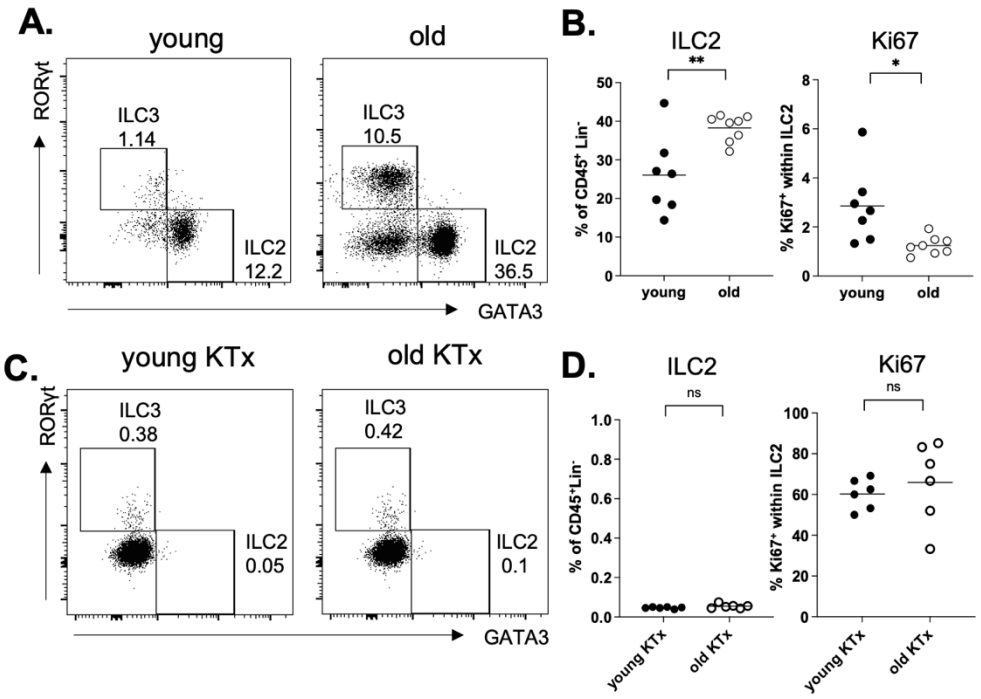

Figure 15. Enriched ILC2s in aged kidneys were depleted following allogeneic kidney transplantation. (A) Representative FACS dot plots of ILC subset composition from kidneys of young (3 months) vs. old (20 months) C57BL/6J mice. ILC2s were gated as $CD45^+Lin^-CD127^+GATA3^+$, ILC3s as $CD45^+Lin^-CD127^+ROR\gamma t^+$. (B) Statistical analysis of renal ILC2 frequencies within the $CD45^+Lin^-$ compartment and those expressing Ki67 from young and old mice. (C) Representative FACS dot plots of ILC subset composition from graft of young (3 months) donor vs. old (20 months) donor C57BL/6J mice transplanted into BALB/c recipients. (D) Statistical analysis of ILC2s from graft of young (3 months) donor vs. old (20 months) donor C57BL/6J mice transplanted into BALB/c recipients and those expressing Ki67. Statistically significant differences were tested with Mann–Whitney U test or unpaired t-test and presented as means. **p < .01; *p < .05; n.s. = not significant.

Interestingly, the readout on day 7 post-transplantation revealed that even though the ILC2 number was significantly increased in old donor kidneys, they were depleted post-transplantation, showing comparable cell numbers with the young allograft (Figure 14C). The remaining ILC2s showed strongly upregulated, albeit comparable levels of proliferation in old vs. young grafts as indicated by Ki67 (Figure 14D). In summary, these preliminary experiments demonstrated that potentially reno-protective ILC2s were equally depleted upon the allogeneic immune response, regardless of their frequencies before transplantation.

5. Discussion

Associations between advanced organ donor age and inferior transplantation outcomes in humans have been identified in a plethora of studies, dating back to the 1990ies (Alexander, Bennett, and Breen 1994). However, comprehensive information on cellular changes that characterize a senescent organ and might mechanistically explain clinical observations is still limited. In this study, we have identified a profound age-related re-composition of key immune cell subsets within the naïve murine kidney, affecting dendritic-, innate lymphoid-, NK- and T cells, with the latter showing an enhanced proinflammatory, cytotoxic programming. Moreover, being particularly relevant in the context of allotransplantation, we noted senescent parenchymal cells, including PTECs and gECs, to be more immunogenic as reflected by upregulation of MHC class II and/or costimulatory molecules.

Enhanced immunogenicity of aged murine organs has recently been described by Iske et al., focusing on dendritic cells isolated from spleen and lymph nodes. Of note, in coculture assays, senescent DCs augmented inflammatory cytokine production by T cells (Iske et al. 2020), a feature that we verified for both aged renal $CD4^+$ and $CD8^+$ subsets after polyclonal stimulation and that equally applied to cytotoxic capacity. Interestingly, although not exhibiting similar levels of (co-) stimulatory molecule levels as DCs, renal PTECs bear the potential to activate $CD4^+$ T cells and induce an inflammatory phenotype (Breda et al. 2019), thereby principally supporting the idea that an age-enhanced costimulatory capacity of parenchymal cells could augment proinflammatory cytokine production by T cells. We further observed age-dependent shifts in the relative quantitative contribution of subpopulations to the overall T cell compartment, reflected by an increase of the $CD8^+$ subset in both naïve kidneys and lymphoid organs. These data are consistent with reports on altered CD4:CD8 ratios associated with age or chronic low-grade inflammatory conditions such as obesity in human peripheral blood (Zanni et al. 2003). An aging immune system is further characterized by the progressive expansion of the memory and/or effector T cell compartment (Nikolich-Zugich 2014). The enrichment of renal effector memory-type cells at the expense of the naïve T cell population therefore extends findings based on human peripheral blood (Moro-Garcia, Alonso-Arias, and Lopez-Larrea 2013) and is principally in line with the observation that tissues, including human kidneys, are enriched for memory-type T cells (Dornieden et al. 2021).

It initially remained tempting to speculate which of the aforementioned features of a senescent kidney might contribute to altered outcomes in a fully mismatched model of kidney transplantation. In this context, Starzl and others demonstrated that passenger leukocytes from the allograft may shape the recipients´ immune response (Starzl and Zinkernagel 1998). Analysis of passenger leucocytes indicated that donor-derived T cells and ILCs can persist for years in human small intestinal transplants (Bartolome-Casado et al. 2021; Weiner et al. 2017). Similar findings were made for natural regulatory T cells in human lung transplants that ameliorated vasculopathy in a murine cardiac allograft model (Harper et al. 2019). Importantly, however, direct analysis of donor vs. recipient-derived cells in our kidney model revealed that on d7 post transplantation, organs were almost completely re-populated by recipient´s leukocytes. Together with related results on rapid depletion of donor T cells in experimental murine liver transplantation (Tay et al. 2013), these data suggest that the impact of senescent kidney-derived donor leukocytes on transplantation outcomes in the fully mismatched setting is likely small. At the same time, it appears more likely that age-related changes within parenchymal cells might influence the recipients´ alloimmune response towards the graft and, thereby, graft function. Indeed, although not consistently showing significance due to sample size, PTECs and gECs isolated from old compared to young kidney transplants showed strong upregulation of MHC class II and/or the costimulatory molecules CD40 and CD80. In favor of an undesirable role for intra-graft MHC-II expression, donor kidneys from MHC class II knockout mice exhibit lower histopathological scores along with reduced $CD4^+$ T cell infiltration and cytokine expression, leading to improved graft function (Mannon et al. 2002). For sustained upregulation of MHC class II expression, PTECs depend on stimulation with IFNγ (Wuthrich et al. 1990). Since we could show that T cell infiltrates in aged kidney grafts are biased towards higher production of this prototypical Th1 associated cytokine, it appears conceivable that senescent parenchymal cells form an inflammatory feedback loop with T cells, thereby creating an intra-renal microenvironment boosting allo-immunity. Direct visualization of this crosstalk in *in vitro* experiments was not feasible due to the rapid loss of MHC class II expression on PTECs in culture.

Our classical histological analysis identified glomerulitis scores to be significantly upregulated in aged transplants. Of note, Baker et al demonstrated that depletion of senescent cells in naïve mice delays glomerulosclerosis, being a key characteristic of age-related kidney diseases (Baker et al. 2016). Murine studies have further shown that

the application of senolytic drugs to deplete senescent cells alleviates multiple disorders in experimental models, including acute kidney injury, obesity-induced metabolic dysfunction, Alzheimer's disease and chronic lung diseases (Schafer et al. 2017; Musi et al. 2018; Palmer et al. 2019; Mylonas et al. 2021). These results prompted us to treat aged kidney donors before transplantation by oral gavage with Navitoclax (ABT-263), a potent and broad-spectrum Bcl-2 family protein inhibitor to induce apoptosis of senescent cells (Cooley et al. 2023). Analysis of the non-transplanted, contralateral kidney already revealed a reduction in frequencies of MHC-II$^+$ gECs, along with significantly lower portions of IFNγ$^+$ and cytotoxic CD4$^+$ and CD8$^+$ T cells. Enhanced immunogenicity of gECs was not significantly downregulated in allografts of aged ABT-263 treated vs. untreated donors due the small sample size; however, a trend towards lower frequencies of MHC II$^+$, CD40$^+$ and CD80$^+$ cells was observed. More importantly, grafts of pretreated donors showed a clear reduction of IFNγ$^+$ T- and NK cells and improved graft function at day 28 as reflected by reduced serum creatinine and urea levels. Together, these findings suggest an overall reduction of the allo-inflammatory state, thus supporting the concept to deplete senescent cells for graft optimization as an attractive therapeutic option that warrants further study. So far, a similar approach has only been applied in experimental cardiac transplantation, leading to prolonged allograft survival. Mechanistically, the authors found mitochondrial DNA, released from senescent cells, to trigger toll-like receptor 9, thereby boosting inflammation, a phenomenon also characterized by upregulation of MHC class II levels (Iske et al. 2020). A more detailed knowledge of possible short-term effects of senolytics (e.g. taking effect within hours) might enable their application in graft preconditioning regimens in context with organ perfusion systems that are progressively entering clinical routine (Franzin et al. 2021). Related fields for therapeutical application of senolytic drugs encompass certain complications associated with chronic graft versus host disease after hematopoietic stem cell transplantation that has been shown to be fueled by senescent cells (Yamane et al. 2020). Overall, ongoing studies with ABT-263 and related therapeutics in human hematopoietic malignancies will provide important information on pharmacokinetics and safety profiles (Joly et al. 2022).

The influence of senescence on innate lymphoid cells (ILCs) is rarely studied. Our data demonstrate that compared with young kidney ILCs, aged kidneys harbor a higher frequency of ILC2s and ILC3s, but lower portions of NK cells and ILC1s. Among all ILC subsets, ILC2 is the dominant population in the kidney, and enriched ILC2s in the kidney

have been reported to be reno-protective during ischemia-reperfusion injury and glomerulosclerosis (Cao et al. 2018; Riedel et al. 2017). Although ILC2s are dominating aged organs, their numerical increase pre-transplantation is obviously not preventing graft inflammation and function as compared to young organs. This is likely due to the broad depletion of all donor-derived leukocytes by day 7 post transplantation, preventing potential anti-inflammatory effects. Furthermore, kidney grafts, within the time frame of our analyses, are not considerably re-populated by recipient-derived ILC2s. In summary, these preliminary experiments demonstrated that potentially reno-protective ILC2s were equally depleted upon the allogeneic immune response, regardless of their frequencies before transplantation. Further experiments should address whether maintaining a sufficient number of ILC2s in the aged allograft could result in better graft function post-transplantation.

We are aware that our study has several limitations. First, we were unable to show in coculture experiments that senescent parenchymal cells (PTECs or/and gECs) are sufficiently promoting inflammatory cytokine production and cytotoxicity in allo-sensitized T cells due to rapid MHC class II downregulation of PTECs in vitro. Novel techniques such as multiplexed fluorescence microscopy (Dornieden et al. 2021) might not only allow us to visualize such interactions directly in renal allografts but also to better characterize subtle changes in the cellular architecture with higher accuracy. Second, although ABT-263 has been shown effective in our study, alternative senolytics, such as Dasatinib and Quercetin have been proven effective in murine models and first clinical (Xu et al. 2018; Hickson et al. 2019). Therefore, screening of other available drugs for optimal depletion efficiency within the kidney, along with an acceptable safety profile, is required. Furthermore, in this study, we were mainly interested in how organ age impacts the acute inflammatory phase following kidney transplantation. Thus, no immunosuppressive medication was applied. Further investigation of the efficiency of ABT-263 or other senolytics in a more clinically relevant long-term setting is required that involves the administration of immunosuppressive medication.

In summary, our comprehensive analyses identify key phenotypic and functional changes in the aging kidney that impact transplantation outcomes. More importantly, our strategy to deplete senescent renal cells paves the way for innovative therapeutical modulation concepts, bearing the potential to extend the progressively limited organ donor pool in the future.

6. Further work

SARS-CoV2 mRNA Vaccine-Specific B-, T- and Humoral Responses in Adolescents After Kidney Transplantation

Sattler A*, Thumfart J*, Tóth L, Schrezenmeier E, Proß V, Stahl C, Siegle J, **He A**, Thole LML, Ludwig C, Straub-Hohenbleicher H, Friedersdorff F, Jahrsdörfer B, Schrezenmeier H, Bufler P, Kotsch K. Transpl Int. 2022 Aug 4;35:10677; * equally contributing first authors

Summary

Due to the low reactogenicity of available vaccines, protection of adult kidney transplant recipients against SARS-CoV2 was shown to be severely compromised. In addition, the late approval of vaccination for this group led to limited data on their vaccination outcomes. In this study, we recruited kidney transplanted adolescents aged 12-18 years and healthy controls 6 weeks after standard two-dose BNT162b2 ("Comirnaty"; Pfizer/BioNTech) vaccination, and performed comprehensive analysis on their vaccination-specific humoral-, T- and B-cell responses. Although 75% (15/20) of transplanted adolescents developed neutralizing titers, and 90% (18/20) of them displayed IgG seroconversion. However, compared to controls, both features were significantly diminished in magnitude. In line with this, patients had a quantitative reduction in spike-specific B cells and an enrichment of non-isotype-class-switched $IgD^{+}27^{+}$ memory cells. While the frequencies of spike-specific $CD4^{+}$ T cells were comparable in both groups, transplant recipients had significantly reduced cytokine production and memory differentiation.

In summary, our data reveal limitation in all arms of vaccine-specific immunity in adolescents patients, but the majority demonstrated strong humoral responses despite the fact that antimetabolite-based therapy was linked to poor vaccination results in adults.

Reference list

https://www.eurotransplant.org/statistics/statistics-

library/>https://statistics.eurotranplant.org/

Stand: 15.04.2023, 18:18 Uhr.

Alexander, J. W., L. E. Bennett, and T. J. Breen. 1994. 'Effect of donor age on outcome of kidney transplantation. A two-year analysis of transplants reported to the United Network for Organ Sharing Registry', *Transplantation*, 57: 871-6.

Almeida-Oliveira, A., M. Smith-Carvalho, L. C. Porto, J. Cardoso-Oliveira, S. Ribeiro Ados, R. R. Falcao, E. Abdelhay, L. F. Bouzas, L. C. Thuler, M. H. Ornellas, and H. R. Diamond. 2011. 'Age-related changes in natural killer cell receptors from childhood through old age', *Hum Immunol*, 72: 319-29.

Argani, H. 2022. 'Expanded Criteria Donors', *Exp Clin Transplant*, 20: 13-19.

Ashraf, M. I., A. Sarwar, A. A. Kuhl, E. Hunger, A. Sattler, F. Aigner, H. Regele, M. Sauter, K. Klingel, S. Schneeberger, T. Resch, and K. Kotsch. 2019. 'Natural Killer Cells Promote Kidney Graft Rejection Independently of Cyclosporine A Therapy', *Front Immunol*, 10: 2279.

Aydar, Y., P. Balogh, J. G. Tew, and A. K. Szakal. 2003. 'Altered regulation of Fc gamma RII on aged follicular dendritic cells correlates with immunoreceptor tyrosine-based inhibition motif signaling in B cells and reduced germinal center formation', *J Immunol*, 171: 5975-87.

Baker, D. J., B. G. Childs, M. Durik, M. E. Wijers, C. J. Sieben, J. Zhong, R. A. Saltness, K. B. Jeganathan, G. C. Verzosa, A. Pezeshki, K. Khazaie, J. D. Miller, and J. M. van Deursen. 2016. 'Naturally occurring p16(Ink4a)-positive cells shorten healthy lifespan', *Nature*, 530: 184-9.

Bartolome-Casado, R., O. J. B. Landsverk, S. K. Chauhan, F. Saetre, K. T. Hagen, S. Yaqub, O. Oyen, R. Horneland, E. M. Aandahl, L. Aabakken, E. S. Baekkevold, and F. L. Jahnsen. 2021. 'CD4(+) T cells persist for years in the human small intestine and display a T(H)1 cytokine profile', *Mucosal Immunol*, 14: 402-10.

Bonventre, J. V., and L. Yang. 2011. 'Cellular pathophysiology of ischemic acute kidney injury', *J Clin Invest*, 121: 4210-21.

Breda, P. C., T. Wiech, C. Meyer-Schwesinger, F. Grahammer, T. Huber, U. Panzer, G. Tiegs, and K. Neumann. 2019. 'Renal proximal tubular epithelial cells exert immunomodulatory function by driving inflammatory CD4(+) T cell responses', *Am J Physiol Renal Physiol*, 317: F77-F89.

Cameron, G. J. M., S. H. Jiang, S. Loering, A. V. Deshpande, P. M. Hansbro, and M. R. Starkey. 2019. 'Emerging therapeutic potential of group 2 innate lymphoid cells in acute kidney injury', *J Pathol*, 248: 9-15.

Cao, Q., Y. Wang, Z. Niu, C. Wang, R. Wang, Z. Zhang, T. Chen, X. M. Wang, Q. Li, V. W. S. Lee, Q. Huang, J. Tan, M. Guo, Y. M. Wang, G. Zheng, D. Yu, S. I. Alexander, H. Wang, and D. C. H. Harris. 2018. 'Potentiating Tissue-Resident Type 2 Innate Lymphoid Cells by IL-33 to Prevent Renal Ischemia-Reperfusion Injury', *J Am Soc Nephrol*, 29: 961-76.

Chang, J., Y. Wang, L. Shao, R. M. Laberge, M. Demaria, J. Campisi, K. Janakiraman, N. E. Sharpless, S. Ding, W. Feng, Y. Luo, X. Wang, N. Aykin-Burns, K. Krager, U. Ponnappan, M. Hauer-Jensen, A. Meng, and D. Zhou. 2016. 'Clearance of senescent cells by ABT263 rejuvenates aged hematopoietic stem cells in mice', *Nat Med*, 22: 78-83.

Chen, W. Y., L. C. Li, Y. H. Wu, J. L. Yang, and H. T. Tzeng. 2020. 'Emerging Roles of Interleukin-33-responsive Kidney Group 2 Innate Lymphoid Cells in Acute Kidney Injury', *Int J Mol Sci*, 21.

Chi, M., Z. Tian, K. Ma, Y. Li, L. Wang, M. I. Nasser, and C. Liu. 2022. 'The diseased kidney: aging and senescent immunology', *Immun Ageing*, 19: 58.

Childs, B. G., M. Durik, D. J. Baker, and J. M. van Deursen. 2015. 'Cellular senescence in aging and age-related disease: from mechanisms to therapy', *Nat Med*, 21: 1424-35.

Cooley, J. C., N. Javkhlan, J. A. Wilson, D. G. Foster, B. L. Edelman, L. A. Ortiz, D. A. Schwartz, D. W. Riches, and E. F. Redente. 2023. 'Inhibition of antiapoptotic BCL-2 proteins with ABT-263 induces fibroblast apoptosis, reversing persistent pulmonary fibrosis', *JCI Insight*, 8.

Dangi, A., S. Yu, F. T. Lee, M. Burnette, J. J. Wang, Y. S. Kanwar, Z. J. Zhang, M. Abecassis, E. B. Thorp, and X. Luo. 2020. 'Murine cytomegalovirus dissemination but not reactivation in donor-positive/recipient-negative allogeneic kidney transplantation can be effectively prevented by transplant immune tolerance', *Kidney Int*, 98: 147-58.

Darboe, A., C. M. Nielsen, A. S. Wolf, J. Wildfire, E. Danso, B. Sonko, C. Bottomley, S. E. Moore, E. M. Riley, and M. R. Goodier. 2020. 'Age-Related Dynamics of Circulating Innate Lymphoid Cells in an African Population', *Front Immunol*, 11: 594107.

Davis, M. M., C. M. Tato, and D. Furman. 2017. 'Systems immunology: just getting started', *Nat Immunol*, 18: 725-32.

Dornieden, T., A. Sattler, A. Pascual-Reguant, A. H. Ruhm, L. G. Thiel, Y. S. Bergmann, L. M. L. Thole, R. Kohler, A. A. Kuhl, A. E. Hauser, S. Boral, F. Friedersdorff, and K. Kotsch. 2021. 'Signatures and Specificity of Tissue-Resident Lymphocytes Identified in Human Renal Peritumor and Tumor Tissue', *J Am Soc Nephrol*, 32: 2223-41.

Dumas, S. J., E. Meta, N. V. Conchinha, L. Sokol, R. Chen, M. Borri, L. A. Teuwen, K. Veys, M. Garcia-Caballero, V. Geldhof, L. Treps, P. de Zeeuw, K. D. Falkenberg, C. Dubois, M. Parys, Lpmh de Rooij, K. Rohlenova, J. Goveia, L. Schoonjans, M. Dewerchin, G. Eelen, X. Li, J. Kalucka, and P. Carmeliet. 2021. 'Protocols for endothelial cell isolation from mouse tissues: kidney, spleen, and testis', *STAR Protoc*, 2: 100523.

Fang, X., Y. Wang, R. Liu, C. Zhu, C. Wu, F. He, S. Yang, and D. Wang. 2022. 'Long-term outcomes of kidney transplantation from expanded criteria donors with Chinese novel donation policy: donation after citizens' death', *BMC Nephrol*, 23: 325.

Franceschi, C., M. Bonafe, S. Valensin, F. Olivieri, M. De Luca, E. Ottaviani, and G. De Benedictis. 2000. 'Inflamm-aging. An evolutionary perspective on immunosenescence', *Ann N Y Acad Sci*, 908: 244-54.

Franceschi, C., S. Salvioli, P. Garagnani, M. de Eguileor, D. Monti, and M. Capri. 2017. 'Immunobiography and the Heterogeneity of Immune Responses in the Elderly: A Focus on Inflammaging and Trained Immunity', *Front Immunol*, 8: 982.

Franzin, R., A. Stasi, M. Fiorentino, S. Simone, R. Oberbauer, G. Castellano, and L. Gesualdo. 2021. 'Renal Delivery of Pharmacologic Agents During Machine Perfusion to Prevent Ischaemia-Reperfusion Injury: From Murine Model to Clinical Trials', *Front Immunol*, 12: 673562.

Frasca, D., A. Diaz, M. Romero, and B. B. Blomberg. 2016. 'The generation of memory B cells is maintained, but the antibody response is not, in the elderly after repeated influenza immunizations', *Vaccine*, 34: 2834-40.

Fung, I. T. H., P. Sankar, Y. Zhang, L. S. Robison, X. Zhao, S. S. D'Souza, A. E. Salinero, Y. Wang, J. Qian, M. L. Kuentzel, S. V. Chittur, S. Temple, K. L. Zuloaga, and Q. Yang. 2020. 'Activation of group 2 innate lymphoid cells alleviates aging-associated cognitive decline', *J Exp Med*, 217.

Gage, G. J., D. R. Kipke, and W. Shain. 2012. 'Whole animal perfusion fixation for rodents', *J Vis Exp*.

Gunther, J., T. Resch, H. Hackl, A. Sattler, S. Ebner, P. V. Ritschl, M. Biebl, R. Ollinger, S. Schneeberger, G. Brandacher, H. Schwelberger, B. Zelger, D. Stauch, A. Pascher, J. Pratschke, and K. Kotsch. 2017. 'Identification of the activating cytotoxicity receptor NKG2D as a senescence marker in zero-hour kidney biopsies is indicative for clinical outcome', *Kidney Int*, 91: 1447-63.

Hariharan, S., M. A. McBride, L. E. Bennett, and E. P. Cohen. 1997. 'Risk factors for renal allograft survival from older cadaver donors', *Transplantation*, 64: 1748-54.

Harper, I. G., O. Gjorgjimajkoska, J. H. Y. Siu, J. Parmar, A. Mulder, F. H. J. Claas, S. A. Hosgood, M. L. Nicholson, R. Motallebzadeh, and G. J. Pettigrew. 2019. 'Prolongation of allograft survival by passenger donor regulatory T cells', *Am J Transplant*, 19: 1371-79.

Hayflick, L., and P. S. Moorhead. 1961. 'The serial cultivation of human diploid cell strains', *Exp Cell Res*, 25: 585-621.

He, S., and N. E. Sharpless. 2017. 'Senescence in Health and Disease', *Cell*, 169: 1000-11.

Hickson, L. J., L. G. P. Langhi Prata, S. A. Bobart, T. K. Evans, N. Giorgadze, S. K. Hashmi, S. M. Herrmann, M. D. Jensen, Q. Jia, K. L. Jordan, T. A. Kellogg, S. Khosla, D. M. Koerber, A. B. Lagnado, D. K. Lawson, N. K. LeBrasseur, L. O. Lerman, K. M. McDonald, T. J. McKenzie, J. F. Passos, R. J. Pignolo, T. Pirtskhalava, I. M. Saadiq, K. K. Schaefer, S. C. Textor, S. G. Victorelli, T. L. Volkman, A. Xue, M. A. Wentworth, E. O. Wissler Gerdes, Y. Zhu, T. Tchkonia, and J. L. Kirkland. 2019. 'Senolytics decrease senescent cells in humans: Preliminary report from a clinical trial of Dasatinib plus Quercetin in individuals with diabetic kidney disease', *EBioMedicine*, 47: 446-56.

Hoffmann, U., C. Neudorfl, K. Daemen, J. Keil, M. Stevanovic-Meyer, F. Lehner, H. Haller, C. Blume, and C. S. Falk. 2015. 'NK Cells of Kidney Transplant Recipients Display an Activated Phenotype that Is Influenced by Immunosuppression and Pathological Staging', *PLoS One*, 10: e0132484.

Howcroft, T. K., J. Campisi, G. B. Louis, M. T. Smith, B. Wise, T. Wyss-Coray, A. D. Augustine, J. E. McElhaney, R. Kohanski, and F. Sierra. 2013. 'The role of inflammation in age-related disease', *Aging (Albany NY)*, 5: 84-93.

Infante, B., R. Franzin, D. Madio, M. Calvaruso, A. Maiorano, F. Sangregorio, G. S. Netti, E. Ranieri, L. Gesualdo, G. Castellano, and G. Stallone. 2020. 'Molecular Mechanisms of AKI in the Elderly: From Animal Models to Therapeutic Intervention', *J Clin Med*, 9.

Iske, J., M. Seyda, T. Heinbokel, R. Maenosono, K. Minami, Y. Nian, M. Quante, C. S. Falk, H. Azuma, F. Martin, J. F. Passos, C. U. Niemann, T. Tchkonia, J. L. Kirkland, A. Elkhal, and S. G. Tullius. 2020. 'Senolytics prevent mt-DNA-induced inflammation and promote the survival of aged organs following transplantation', *Nat Commun*, 11: 4289.

Joly, F., M. Fabbro, P. Follana, J. Lequesne, J. Medioni, A. Lesoin, J. S. Frenel, S. Abadie-Lacourtoisie, A. Floquet, L. Gladieff, B. You, C. Gavoille, E. Kalbacher, M. Briand, P. E. Brachet, F. Giffard, L. B. Weiswald, P. A. Just, C. Blanc-Fournier, A. Leconte, B. Clarisse, A. Leary, and L. Poulain. 2022. 'A phase II study of Navitoclax (ABT-263) as single agent in women heavily pretreated for recurrent epithelial ovarian cancer: The MONAVI - GINECO study', *Gynecol Oncol*, 165: 30-39.

Kooman, J. P., M. J. Dekker, L. A. Usvyat, P. Kotanko, F. M. van der Sande, C. G. Schalkwijk, P. G. Shiels, and P. Stenvinkel. 2017. 'Inflammation and premature aging in advanced chronic kidney disease', *Am J Physiol Renal Physiol*, 313: F938-F50.

Koppelstaetter, C., G. Schratzberger, P. Perco, J. Hofer, W. Mark, R. Ollinger, R. Oberbauer, C. Schwarz, C. Mitterbauer, A. Kainz, H. Karkoszka, A. Wiecek, B. Mayer, and G. Mayer. 2008. 'Markers of cellular senescence in zero hour biopsies predict outcome in renal transplantation', *Aging Cell*, 7: 491-7.

Kuilman, T., and D. S. Peeper. 2009. 'Senescence-messaging secretome: SMS-ing cellular stress', *Nat Rev Cancer*, 9: 81-94.

Mannon, R. B., R. Griffiths, P. Ruiz, J. L. Platt, and T. M. Coffman. 2002. 'Absence of donor MHC antigen expression ameliorates chronic kidney allograft rejection', *Kidney Int*, 62: 290-300.

Melk, A., B. M. Schmidt, H. Braun, A. Vongwiwatana, J. Urmson, L. F. Zhu, D. Rayner, and P. F. Halloran. 2009. 'Effects of donor age and cell senescence on kidney allograft survival', *Am J Transplant*, 9: 114-23.

Metzger, R. A., F. L. Delmonico, S. Feng, F. K. Port, J. J. Wynn, and R. M. Merion. 2003. 'Expanded criteria donors for kidney transplantation', *Am J Transplant*, 3 Suppl 4: 114-25.

Moro-Garcia, M. A., R. Alonso-Arias, and C. Lopez-Larrea. 2013. 'When Aging Reaches CD4+ T-Cells: Phenotypic and Functional Changes', *Front Immunol*, 4: 107.

Munoz-Espin, D., and M. Serrano. 2014. 'Cellular senescence: from physiology to pathology', *Nat Rev Mol Cell Biol*, 15: 482-96.

Murray JE. Ronald Lee Herrick Memorial: June 15, 1931-December 27, 2010. Am J Transplant. 2011 Mar;11(3):419.

Musi, N., J. M. Valentine, K. R. Sickora, E. Baeuerle, C. S. Thompson, Q. Shen, and M. E. Orr. 2018. 'Tau protein aggregation is associated with cellular senescence in the brain', *Aging Cell*, 17: e12840.

Mylonas, K. J., E. D. O'Sullivan, D. Humphries, D. P. Baird, M. H. Docherty, S. A. Neely, P. J. Krimpenfort, A. Melk, R. Schmitt, S. Ferreira-Gonzalez, S. J. Forbes, J. Hughes, and D. A. Ferenbach. 2021. 'Cellular senescence inhibits renal regeneration after injury in mice, with senolytic treatment promoting repair', *Sci Transl Med*, 13.

Newbold, K. M., A. Sandison, and A. J. Howie. 1992. 'Comparison of size of juxtamedullary and outer cortical glomeruli in normal adult kidney', *Virchows Arch A Pathol Anat Histopathol*, 420: 127-9.

Nikolich-Zugich, J. 2014. 'Aging of the T cell compartment in mice and humans: from no naive expectations to foggy memories', *J Immunol*, 193: 2622-9.

Palmer, A. K., M. Xu, Y. Zhu, T. Pirtskhalava, M. M. Weivoda, C. M. Hachfeld, L. G. Prata, T. H. van Dijk, E. Verkade, G. Casaclang-Verzosa, K. O. Johnson, H. Cubro, E. J. Doornebal, M. Ogrodnik, D. Jurk, M. D. Jensen, E. N. Chini, J. D. Miller, A. Matveyenko, M. B. Stout, M. J. Schafer, T. A. White, L. J. Hickson, M. Demaria, V. Garovic, J. Grande, E. A. Arriaga, F. Kuipers, T. von Zglinicki, N. K. LeBrasseur,

J. Campisi, T. Tchkonia, and J. L. Kirkland. 2019. 'Targeting senescent cells alleviates obesity-induced metabolic dysfunction', *Aging Cell*, 18: e12950.

Perez-Saez, M. J., O. Lafuente Covarrubias, D. Hernandez, F. Moreso, E. Melilli, J. Juega, E. de Sousa, P. Lopez-Sanchez, M. L. Rodriguez-Ferrero, N. Maruri-Kareaga, M. D. Navarro, R. Valero, M. A. Mazuecos, F. Llamas, P. Martin-Moreno, A. Fernandez-Garcia, J. Espi, C. Jimenez, A. Ramos, E. Gavela, J. Pascual, J. M. Portoles, and Geodas Group. 2019. 'Early outcomes of kidney transplantation from elderly donors after circulatory death (GEODAS study)', *BMC Nephrol*, 20: 233.

Pippias, M., K. J. Jager, A. Asberg, S. P. Berger, P. Finne, J. G. Heaf, J. Kerschbaum, M. Lempinen, A. Magaz, Z. A. Massy, and V. S. Stel. 2020. 'Young deceased donor kidneys show a survival benefit over older donor kidneys in transplant recipients aged 20-50 years: a study by the ERA-EDTA Registry', *Nephrol Dial Transplant*, 35: 534-43.

Poggio, E. D., J. J. Augustine, S. Arrigain, D. C. Brennan, and J. D. Schold. 2021. 'Long-term kidney transplant graft survival-Making progress when most needed', *Am J Transplant*, 21: 2824-32.

Querard, A. H., Y. Foucher, C. Combescure, E. Dantan, D. Larmet, M. Lorent, L. M. Pouteau, M. Giral, and F. Gillaizeau. 2016. 'Comparison of survival outcomes between Expanded Criteria Donor and Standard Criteria Donor kidney transplant recipients: a systematic review and meta-analysis', *Transpl Int*, 29: 403-15.

Riedel, J. H., M. Becker, K. Kopp, M. Duster, S. R. Brix, C. Meyer-Schwesinger, L. A. Kluth, A. C. Gnirck, M. Attar, S. Krohn, B. Fehse, R. A. K. Stahl, U. Panzer, and J. E. Turner. 2017. 'IL-33-Mediated Expansion of Type 2 Innate Lymphoid Cells Protects from Progressive Glomerulosclerosis', *J Am Soc Nephrol*, 28: 2068-80.

Rodriguez, I. J., N. Lalinde Ruiz, M. Llano Leon, L. Martinez Enriquez, M. D. P. Montilla Velasquez, J. P. Ortiz Aguirre, O. M. Rodriguez Bohorquez, E. A. Velandia Vargas, E. D. Hernandez, and C. A. Parra Lopez. 2020. 'Immunosenescence Study of T Cells: A Systematic Review', *Front Immunol*, 11: 604591.

Rubelt, F., V. Sievert, F. Knaust, C. Diener, T. S. Lim, K. Skriner, E. Klipp, R. Reinhardt, H. Lehrach, and Z. Konthur. 2012. 'Onset of immune senescence defined by unbiased pyrosequencing of human immunoglobulin mRNA repertoires', *PLoS One*, 7: e49774.

Sayin, A., R. Mutluay, and S. Sindel. 2007. 'Quality of life in hemodialysis, peritoneal dialysis, and transplantation patients', *Transplant Proc*, 39: 3047-53.

Schafer, M. J., T. A. White, K. Iijima, A. J. Haak, G. Ligresti, E. J. Atkinson, A. L. Oberg, J. Birch, H. Salmonowicz, Y. Zhu, D. L. Mazula, R. W. Brooks, H. Fuhrmann-Stroissnigg, T. Pirtskhalava, Y. S. Prakash, T. Tchkonia, P. D. Robbins, M. C. Aubry, J. F. Passos, J. L. Kirkland, D. J. Tschumperlin, H. Kita, and N. K. LeBrasseur. 2017. 'Cellular senescence mediates fibrotic pulmonary disease', *Nat Commun*, 8: 14532.

Spyridopoulos, I., J. Haendeler, C. Urbich, T. H. Brummendorf, H. Oh, M. D. Schneider, A. M. Zeiher, and S. Dimmeler. 2004. 'Statins enhance migratory capacity by upregulation of the telomere repeat-binding factor TRF2 in endothelial progenitor cells', *Circulation*, 110: 3136-42.

Stamatiades EG, Tremblay ME, Bohm M, Crozet L, Bisht K, Kao D, Coelho C, Fan X, Yewdell WT, Davidson A, Heeger PS, Diebold S, Nimmerjahn F, Geissmann F. Immune Monitoring of Trans-endothelial Transport by Kidney-Resident Macrophages. Cell. 2016 Aug 11;166(4):991-1003.

Sturmlechner, I., M. Durik, C. J. Sieben, D. J. Baker, and J. M. van Deursen. 2017. 'Cellular senescence in renal ageing and disease', *Nat Rev Nephrol*, 13: 77-89.

Tay, S. S., B. Lu, F. Sierro, V. Benseler, C. M. McGuffog, G. A. Bishop, P. J. Cowan, G. W. McCaughan, K. M. Dwyer, D. G. Bowen, and P. Bertolino. 2013. 'Differential migration of passenger leukocytes and rapid deletion of naive alloreactive CD8 T cells after mouse liver transplantation', *Liver Transpl*, 19: 1224-35.

Trzonkowski, P., A. Debska-Slizien, M. Jankowska, A. Wardowska, M. Carvalho-Gaspar, L. Hak, G. Moszkowska, B. Bzoma, N. Mills, K. J. Wood, J. Mysliwska, and B. Rutkowski. 2010. 'Immunosenescence increases the rate of acceptance of kidney allotransplants in elderly recipients through exhaustion of CD4+ T-cells', *Mech Ageing Dev*, 131: 96-104.

Valentijn, F. A., L. L. Falke, T. Q. Nguyen, and R. Goldschmeding. 2018. 'Cellular senescence in the aging and diseased kidney', *J Cell Commun Signal*, 12: 69-82.

Valieva, Y., E. Ivanova, A. Fayzullin, A. Kurkov, and A. Igrunkova. 2022. 'Senescence-Associated beta-Galactosidase Detection in Pathology', *Diagnostics (Basel)*, 12.

van den Ham, E. C., J. P. Kooman, A. M. Schols, F. H. Nieman, J. D. Does, F. M. Franssen, M. A. Akkermans, P. P. Janssen, and J. P. van Hooff. 2005. 'Similarities in skeletal muscle strength and exercise capacity between renal transplant and hemodialysis patients', *Am J Transplant*, 5: 1957-65.

van der Putten, C., E. B. M. Remmerswaal, M. L. Terpstra, N. D. van der Bom, J. Kers, I. J. M. Ten Berge, S. E. Geerlings, R. A. W. van Lier, F. J. Bemelman, and M. C. van Aalderen. 2021. 'CD8 and CD4 T Cell Populations in Human Kidneys', *Cells*, 10.

Vivier, E., D. Artis, M. Colonna, A. Diefenbach, J. P. Di Santo, G. Eberl, S. Koyasu, R. M. Locksley, A. N. J. McKenzie, R. E. Mebius, F. Powrie, and H. Spits. 2018. 'Innate Lymphoid Cells: 10 Years On', *Cell*, 174: 1054-66.

Walford, R. L. 1964. 'The Immunologic Theory of Aging', *Gerontologist*, 4: 195-7.

Weiner, J., J. Zuber, B. Shonts, S. Yang, J. Fu, M. Martinez, D. L. Farber, T. Kato, and M. Sykes. 2017. 'Long-term Persistence of Innate Lymphoid Cells in the Gut After Intestinal Transplantation', *Transplantation*, 101: 2449-54.

Wuthrich, R. P., L. H. Glimcher, M. A. Yui, A. M. Jevnikar, S. E. Dumas, and V. E. Kelley. 1990. 'MHC class II, antigen presentation and tumor necrosis factor in renal tubular epithelial cells', *Kidney Int*, 37: 783-92.

Xu, M., T. Pirtskhalava, J. N. Farr, B. M. Weigand, A. K. Palmer, M. M. Weivoda, C. L. Inman, M. B. Ogrodnik, C. M. Hachfeld, D. G. Fraser, J. L. Onken, K. O. Johnson, G. C. Verzosa, L. G. P. Langhi, M. Weigl, N. Giorgadze, N. K. LeBrasseur, J. D. Miller, D. Jurk, R. J. Singh, D. B. Allison, K. Ejima, G. B. Hubbard, Y. Ikeno, H. Cubro, V. D. Garovic, X. Hou, S. J. Weroha, P. D. Robbins, L. J. Niedernhofer, S. Khosla, T. Tchkonia, and J. L. Kirkland. 2018. 'Senolytics improve physical function and increase lifespan in old age', *Nat Med*, 24: 1246-56.

Yamane, M., S. Sato, E. Shimizu, S. Shibata, M. Hayano, T. Yaguchi, H. Kamijuku, M. Ogawa, T. Suzuki, S. Mukai, S. Shimmura, H. Okano, T. Takeuchi, Y. Kawakami, Y. Ogawa, and K. Tsubota. 2020. 'Senescence-associated secretory phenotype promotes chronic ocular graft-vs-host disease in mice and humans', *FASEB J*, 34: 10778-800.

Yang, H. C., S. Deleuze, Y. Zuo, S. A. Potthoff, L. J. Ma, and A. B. Fogo. 2009. 'The PPARgamma agonist pioglitazone ameliorates aging-related progressive renal injury', *J Am Soc Nephrol*, 20: 2380-8.

Zanni, F., R. Vescovini, C. Biasini, F. Fagnoni, L. Zanlari, A. Telera, P. Di Pede, G. Passeri, M. Pedrazzoni, M. Passeri, C. Franceschi, and P. Sansoni. 2003. 'Marked increase with age of type 1 cytokines within memory and effector/cytotoxic CD8+

T cells in humans: a contribution to understand the relationship between inflammation and immunosenescence', *Exp Gerontol*, 38: 981-7.

Statutory Declaration

“I, An He, by personally signing this document in lieu of an oath, hereby affirm that I prepared the submitted dissertation on the topic [Impact of Renal Senescence on Kidney Allograft Outcome - Einfluss der renalen Seneszenz auf das Ergebnis von Nieren-Allotransplantaten], independently and without the support of third parties, and that I used no other sources and aids than those stated.
All parts which are based on the publications or presentations of other authors, either in letter or in spirit, are specified as such in accordance with the citing guidelines. The sections on methodology (in particular regarding practical work, laboratory regulations, statistical processing) and results (in particular regarding figures, charts and tables) are exclusively my responsibility.

Furthermore, I declare that I have correctly marked all of the data, the analyses, and the conclusions generated from data obtained in collaboration with other persons, and that I have correctly marked my own contribution and the contributions of other persons (cf. declaration of contribution). I have correctly marked all texts or parts of texts that were generated in collaboration with other persons.

My contributions to any publications to this dissertation correspond to those stated in the below joint declaration made together with the supervisor. All publications created within the scope of the dissertation comply with the guidelines of the ICMJE (International Committee of Medical Journal Editors; http://www.icmje.org) on authorship. In addition, I declare that I shall comply with the regulations of Charité – Universitätsmedizin Berlin on ensuring good scientific practice.

I declare that I have not yet submitted this dissertation in identical or similar form to another Faculty.

The significance of this statutory declaration and the consequences of a false statutory declaration under criminal law (Sections 156, 161 of the German Criminal Code) are known to me.”

Date Signature

Declaration of contribution to the top-journal publication for a MD/PhD degree

An He contributed the following to the below listed publications:

Publication 1: **He A***, Sarwar A*, Thole LML, Siegle J, Sattler A, Ashraf MI, Proß V, Stahl C, Dornieden T, Bergmann Y, Ritschl PV, Ebner S, Hublitz KW, Stamatiades EG, Bülow RD, Boor P, Kotsch K. **Renal inflamm-aging provokes intra-graft inflammation following experimental kidney transplantation**. Am J Transplant. 2022 Nov; * equally contributing first authors

Contribution:

- Experimental design
- Mouse
    - Animal caring pre-, and post-transplantation
    - Medication preparing and feeding
    - Murine kidney transplantation: 2nd round to 4th round of ABT-263 treated vs. ctrl KTx: Including data for Figure 4C; Figure 5B; Figure 6C; Figure 8A, 8B, 8C, 8D, 8E; Figure 9B, 9C.
    - Tissue harvesting
- Experimental performance
    - Lymphocyte isolation, staining, flow cytometry measurement
    - Cell Isolation,staining and flow cytometry: lymphocyte isolation from 2nd to 4th round of ABT-263 treated vs. ctrl KTx; PTEC and EC cell isolation, cell culture and co-culture experiment. Including data for Figure 6D, 6E, 6F; Figure 7C; Figure 8B, 8C, 8D, 8E; Figure 9A.
    - Immunofluorescence microscopy: Collection and preparation of samples (snap freezing) were done by the author. All other procedures for immunofluorescence microscopy were done in a close collaboration with Dr. Efstathios Stamatiades and Karolin Hublitz (Institute of Microbiology, CBF, Charité, Berlin).

    - Histology: Collection and preparation of samples were done by the author. All other procedures of histology were done in a close collaboration with Univ.-Prof. med. Peter Boor and Dr. med. Roman Bülow (Institute of Pathology, UKA, Aachen).
- Data analysis
- Creation of figures, statistics: Including figure for Figure 6D, 6E, 6F; Figure 7C, 7D; Figure 8B, 8C, 8D, 8E; Figure 9A, 9B,9C; Figure 10.

Publication 2: Sattler A*, Thumfart J*, Tóth L, Schrezenmeier E, Proß V, Stahl C, Siegle J, **He A**, Thole LML, Ludwig C, Straub-Hohenbleicher H, Friedersdorff F, Jahrsdörfer B, Schrezenmeier H, Bufler P, Kotsch K. **SARS-CoV2 mRNA Vaccine-Specific B-, T- and Humoral Responses in Adolescents After Kidney Transplantation**. Transpl Int. 2022 Aug; * equally contributing first authors

Contribution:

- Experimental performance
    - Lymphocyte isolation
    - Staining

_____

Signature, date and stamp of first supervising university professor / lecturer

_____

Signature of doctoral candidate

Received: 8 November 2021 | Revised: 14 June 2022 | Accepted: 14 July 2022

DOI: 10.1111/ajt.17154

ORIGINAL ARTICLE

AJT

Renal inflamm-aging provokes intra-graft inflammation following experimental kidney transplantation

An He[1] | Attia Sarwar[1] | Linda Marie Laura Thole[1] | Janine Siegle[1] | Arne Sattler[1] | Muhammad Imtiaz Ashraf[2] | Vanessa Proß[1] | Carolin Stahl[1] | Theresa Dornieden[1] | Yasmin Bergmann[1] | Paul Viktor Ritschl[2] | Susanne Ebner[3] | Karolin Wiebke Hublitz[4] | Efstathios Gregorios Stamatiades[4] | Roman David Bülow[5] | Peter Boor[5] | Katja Kotsch[1]

[1]Department of General- and Visceral Surgery, Campus Benjamin Franklin, Charité-Universitätsmedizin Berlin, corporate member of Freie Universität Berlin, Humboldt-Universität zu Berlin, and Berlin Institute of Health (BIH), Berlin, Germany

[2]Department of Surgery, Campus Charité Mitte, Campus Virchow-Klinikum, Charité-Universitätsmedizin Berlin, corporate member of Freie Universität Berlin, Humboldt-Universität zu Berlin, and Berlin Institute of Health (BIH), Berlin, Germany

[3]Department of Visceral, Transplant and Thoracic Surgery, Medical University of Innsbruck, Innsbruck, Austria

[4]Institute of Microbiology, Infectious Diseases and Immunology, Campus Benjamin Franklin, Charité-Universitätsmedizin Berlin, Freie Universität Berlin, Humboldt-Universität zu Berlin, Berlin, Germany

[5]Institute of Pathology & Department of Nephrology, University Clinic of RWTH Aachen, Aachen, Germany

Correspondence
Katja Kotsch, Department of General- and Visceral Surgery, Campus Benjamin Franklin, Charité–Universitätsmedizin Berlin, Freie Universität Berlin, Humboldt-Universität zu Berlin, Hindenburgdamm 30, 12203 Berlin, Germany.
Email: katja.kotsch@charite.de

Abstract

Donor age is a major risk factor for allograft outcome in kidney transplantation. The underlying cellular mechanisms and the recipient's immune response within an aged allograft have yet not been analyzed. A comprehensive immunophenotyping of naïve and transplanted young versus aged kidneys revealed that naïve aged murine kidneys harbor significantly higher frequencies of effector/memory T cells, whereas regulatory T cells were reduced. Aged kidney-derived $CD8^+$ T cells produced more IFNγ than their young counterparts. Senescent renal $CD8^+$ T and NK cells upregulated the cytotoxicity receptor NKG2D and the enrichment of memory-like $CD49a^+CXCR6^+$ NK cells was documented in aged naïve kidneys. In the C57BL/6 to BALB/c kidney transplantation model, recipient-derived T cells infiltrating an aged graft produced significantly more IFNγ, granzyme B and perforin on day 7 post-transplantation, indicating an enhanced inflammatory, cytotoxic response towards the graft. Pre-treatment of aged kidney donors with the senolytic drug ABT-263 changed the recipient-derived effector molecule profile to significantly reduced levels of IFNγ and IL-10 compared to controls. Graft function after ABT-263 pre-treatment was significantly improved 28 days post kidney transplantation. In conclusion, renal senescence also occurs at the immunological level (inflamm-aging) and aged organs provoke an altered recipient-dominated immune response in the graft.

KEYWORDS
inflamm-aging, kidney transplantation, senescence, senolytic drug

Abbreviations: CKD, chronic kidney disease; DC, dendritic cell; DGF, delayed graft function; GBM, glomerular basement membrane; PTECs, proximal tubule epithelial cells; SASP, senescence-associated secretory phenotype; Trm, tissue-resident memory T cells.

An He and Attia Sarwar equally contributed as first authors.

Funding information
Chinese Scholarship Council; Deutsche Forschungsgemeinschaft, Grant/Award Number: DFG-Ko2270/4-1, DFG-Ko2270/5-1, 22900939 and 45402465; European Research Council, Grant/Award Number: 101001791; Federal Ministry of Education and Research, Grant/Award Number: STOP-FSGS-01GM1901A; Sonnenfeldstiftung

1 | INTRODUCTION

Worldwide, the number of individuals with an advanced age >65 years is steadily increasing. This results in a higher number of patients diagnosed with progressive chronic kidney disease (CKD) constituting a potential kidney transplant recipient group.[1,2] Chronological donor age is also a major risk factor for allograft dysfunction, as grafts from older donors are more susceptible to ischemic injury and prone to develop delayed graft function (DGF) post kidney transplantation.[3–5] Aged donor kidneys are characterized by structural changes, including glomerular basement membrane (GBM) permeability, changes in podocyte morphology and nephron loss, resulting in reduced glomerular filtration rate and altered homeostasis.[6–12]

Renal aging also entails chronic, sterile low-grade inflammation paralleled with the development of fibrosis occurring at different molecular and cellular levels including DNA damage, dysfunctional telomeres, and protein aggregation.[13] One major mechanism is mediated via *cyclin-dependent kinase inhibitor* p16INK4a resulting in growth arrest of viable cells and changes in the cell's secretory phenotype, called senescence-associated secretory phenotype (SASP).[14–16] In addition, the reduced regenerative capacity of stem cells and their progeny accelerates cellular senescence.[17]

Despite these findings, the exact mechanisms of age-dependent alterations in the kidney impacting long-term overall graft survival still remain unclear. Although it has been speculated that the SASP present in older allografts creates a pro-inflammatory milieu, literature on this topic is scarce. Some experimental data suggested that parenchymal changes seen in older allografts are associated with enhanced immunogenicity, therefore accelerating rejection, whereas other studies failed to detect such differences.[18,19] The process of progressive, multidimensional, physiological degeneration of the immune system resulting in a low-grade chronic inflammation has been described as inflamm-aging.[20,21] However, it has not been addressed as to how kidney-resident lymphocytes may undergo senescence. In this context we recently demonstrated that frequencies of tissue-resident memory CD8$^+$ T cells (T_{rm}) residing in human kidneys correlate with chronological age and that CD4$^+$ T_{rm} correlate with kidney function.[22] Here, using experimental mouse models, we show how age impacts immunity in the naïve kidney, but also assess how aged organs shape the recipients´ allo-response, with possible implications for therapeutic targeting.

2 | MATERIALS AND METHODS

2.1 | Animals

Young BALB/c and C57BL/6 mice (8–12 weeks) and C57BL/6 mice (20 months) were purchased from Charles River Laboratories (Charles River). Male mice weighing 24–30 g were used. Animals were housed under standard conditions and received human care in compliance with the 'Principles of Laboratory Animal Care' prepared by the National Academy of Sciences and published by the National Institutes of Health (NIH Publication No. 86–23, revised 1985). All animal experiments were approved by the Landesamt für Gesundheit und Soziales Berlin, Germany.

2.2 | Kidney and heart transplantation

Renal transplantations were performed as previously described.[23] Briefly, after procurement of the left donor kidney, end-to-side anastomoses between the donor renal vessels and the recipient's abdominal aorta and inferior vena cava were performed following a knotless technique. Animals were either sacrificed on day 7 or on day 28 without receiving immunosuppression. For long-term

FIGURE 1 Aging affects the lymphocyte composition in various organs. (A) Visualization of t-distributed stochastic neighbor embedding (viSNE, left panel) considering the markers CD4, CD8, CD44, CD62L, CD103, CD69 and KLRG1 indicates the clustering of viable CD3$^+$ T cell subsets in C57BL/6 kidneys according to age; viSNE plots were generated on concatenated FCS files ($n = 5–6$) using an equal amount of 17.674 CD3$^+$events per file and Cytobank default parameters (1000 iterations, perplexity of 30, 0.5 Theta). Subsequent FlowSOM analysis of T cell subsets (right panel) performed on viSNE map using CD4, CD8, CD44, and CD62L for hierarchical clustering. (B) Representative images depicting kidney histology of young and old naïve (i.e., not transplanted) kidney showing slightly more acute tubular injury in kidneys of old mice. Bar represents 50 μm. (C) Frequencies of manually gated CD8$^+$, CD4$^+$, double negative (DN), NK cells from kidney and lymphoid organs (spleen, lymph nodes) derived from young (3 months) and aged (20 months) C57BL/6 mice (5–6 animals/group). (D, E) Frequencies of manually gated CD8$^+$, CD4$^+$ naïve, memory T cells and T_{regs} derived from young (3 months) and aged (20 months) C57BL/6 mice (5–6 animals/group). Statistically significant differences were tested with Mann–Whitney U test and presented as means, $^*p < .05$; $^{**}p < .01$; n.s. = not significant.

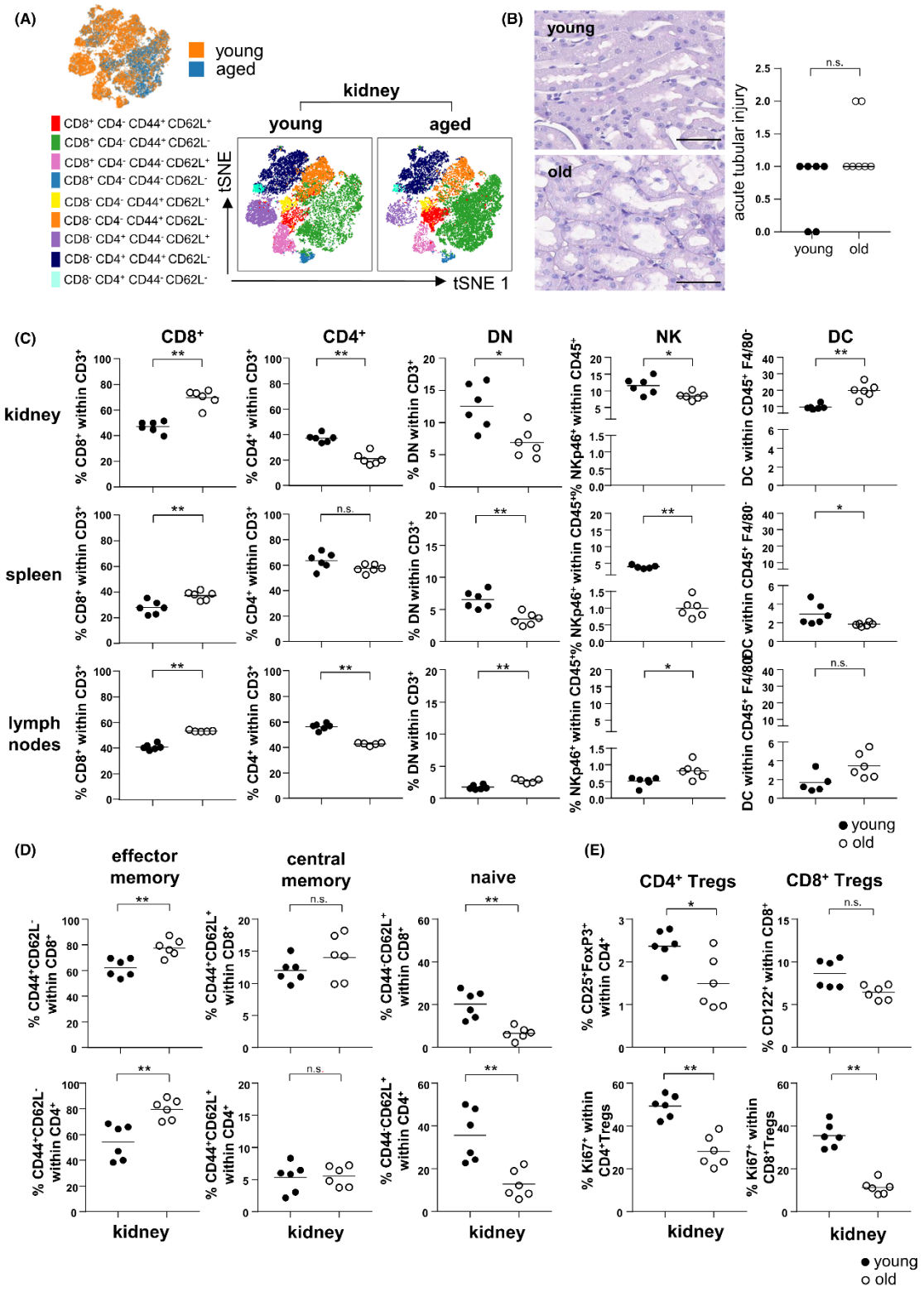
(A)
young
aged
kidney
young
aged
CD8+ CD4- CD44+ CD62L+
CD8+ CD4- CD44+ CD62L-
CD8+ CD4- CD44- CD62L+
CD8+ CD4- CD44- CD62L-
CD8- CD4- CD44+ CD62L+
CD8- CD4- CD44+ CD62L-
CD8- CD4+ CD44- CD62L+
CD8- CD4+ CD44+ CD62L-
CD8- CD4+ CD44- CD62L-
tSNE
tSNE 1
(B)
young
old
acute tubular injury
n.s.
young
old
(C)
CD8+
CD4+
DN
NK
DC
kidney
spleen
lymph nodes
% CD8+ within CD3+
% CD4+ within CD3+
% DN within CD3+
% NKp46+ within CD45+
DC within CD45+ F4/80-
% NKp46+ within CD45+
young
old
(D)
effector memory
central memory
naive
% CD44+CD62L- within CD8+
% CD44+CD62L+ within CD8+
% CD44-CD62L+ within CD8+
% CD44+CD62L- within CD4+
% CD44+CD62L+ within CD4+
% CD44-CD62L+ within CD4+
kidney
(E)
CD4+ Tregs
CD8+ Tregs
% CD25+FoxP3+ within CD4+
% CD122+ within CD8+
% Ki67+ within CD4+Tregs
% Ki67+ within CD8+Tregs
kidney
young
old

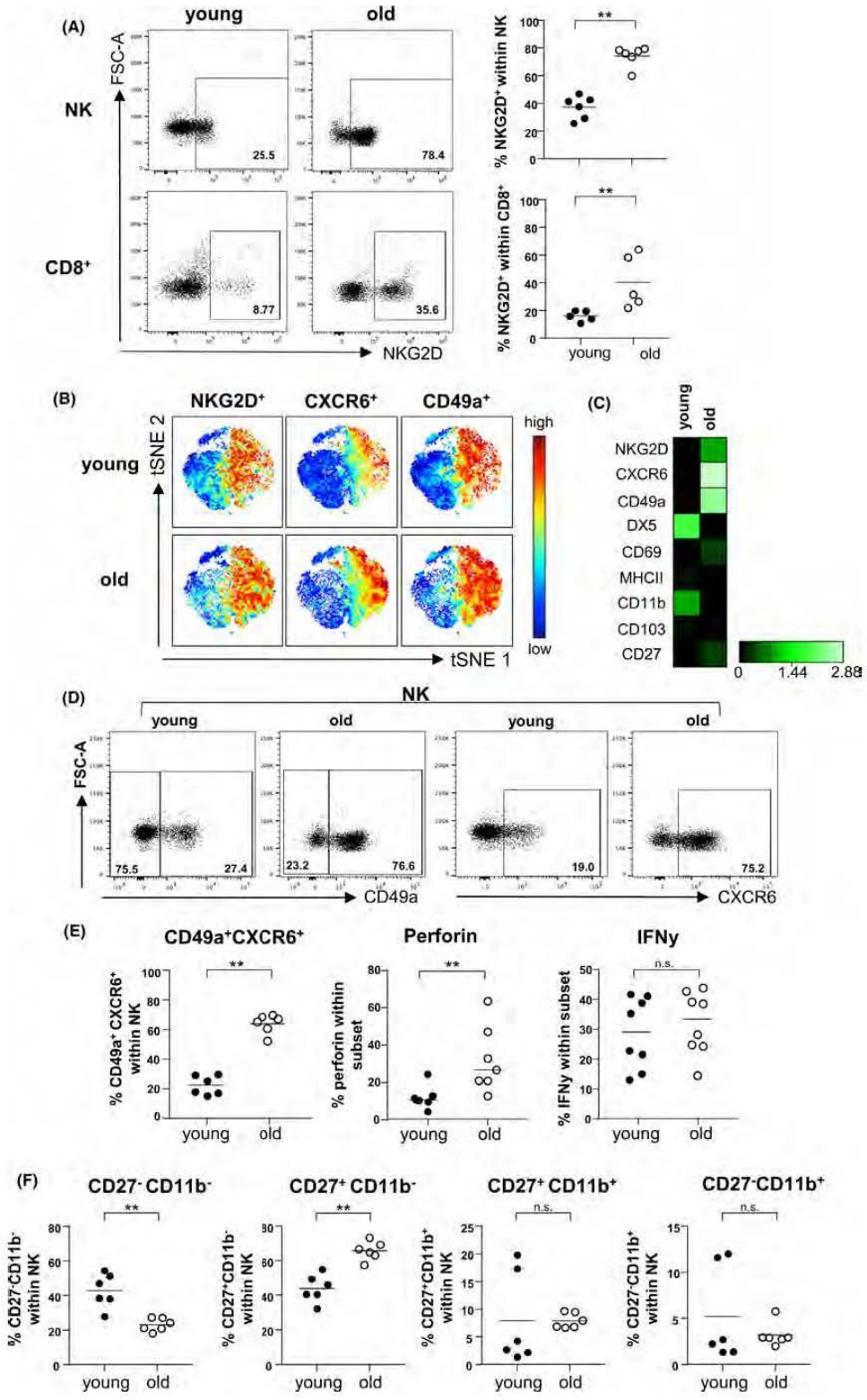
(A)
young
old
NK
CD8+
FSC-A
NKG2D
25.5
78.4
8.77
35.6
% NKG2D+ within NK
% NKG2D+ within CD8+
young
old
(B)
NKG2D+
CXCR6+
CD49a+
young
old
tSNE 2
tSNE 1
high
low
(C)
young
old
NKG2D
CXCR6
CD49a
DX5
CD69
MHCII
CD11b
CD103
CD27
0
1.44
2.88
(D)
NK
young
old
young
old
FSC-A
CD49a
CXCR6
75.5
27.4
23.2
76.6
19.0
75.2
(E)
CD49a+CXCR6+
Perforin
IFNy
% CD49a+ CXCR6+ within NK
% perforin within subset
% IFNy within subset
n.s.
(F)
CD27- CD11b-
CD27+ CD11b-
CD27+ CD11b+
CD27-CD11b+
% CD27-CD11b- within NK
% CD27+CD11b- within NK
% CD27+CD11b+ within NK
% CD27-CD11b+ within NK

FIGURE 2 NKp46$^+$ NK cells upregulating NKG2D, CD49a and CXCR6 accumulate in the senescent murine kidney. (A) Representative FACS dot plots (left panel) and frequencies (right panel) of NKG2D$^+$ NK and CD8$^+$ T cells derived from young and aged C57BL/6 kidneys. (B) viSNE plots of viable NKp46$^+$ CD3$^-$ NK cells showing increased expression of NKG2D$^+$, CXCR6$^+$ and CD49a$^+$ in NK cells isolated from aged compared to young kidneys. Expression is shown by color coding in relative intensity. viSNE plots were generated on concatenated FCS files ($n = 5–6$) considering NKG2D, CXCR6, CD49a, DX5, CD69, MHC II, CD11b, CD103, CD27, an equal amount of 25 111 events were sampled per file. (C) Heatmap plot of flow cytometric analysis for NK cell populations illustrating log 2 transformed median of relative expression levels of measured markers. (D) Exemplary dot plots of CD49a and CXCR6 C57BL/6 expression on NK cells and (E) frequencies of CD49a$^+$CXCR6$^+$ kidney-derived senescent NK cells and their expression of perforin and IFNγ. (F) Frequencies of NK cell subtypes in young and aged C57BL/6 kidneys according to CD27 and CD11b expression, $n = 5–8$ animals/group. Statistically significant differences were tested with Mann–Whitney U test or unpaired t-test and presented as means, $^{**}p < .01$; n.s. = not significant.

survival experiments, the contralateral kidney was removed 1 day before animals were sacrificed, allowing determination of graft function after 24 h of observation. For sensitization of recipients, fully allogeneic BALB/c- (donor) derived hearts were transplanted into C57BL/6 recipients using a heterotopic cardiac transplantation model as described elsewhere.[24]

2.3 | In vivo treatment

ABT-263 (50 mg/kg/day Navitoclax, Hycultech GmbH) was administered in two cycles by oral gavage with a 1-week interval in-between. Control animals received corn oil. Animals were sacrificed either on day 7 (short-term survival) or on day 28 (long-term survival). In the long term group, the contralateral kidney was removed 1 day before animals were sacrificed in order to analyze serum creatinine and urea being indicative for graft function.

2.4 | Serum analysis of kidney function parameters

Serum samples were stored in aliquots at −20°C until serum creatinine and urea were measured using the CREP2 Creatinine Plus version 2 and Urea/BUN assays, respectively, on a Roche/Hitachi Cobas C 701/702 system (Roche Diagnostics).

2.5 | Isolation of cells

For isolating renal MNCs, tissues were mechanically dissociated and digested in 10 ml of RPMI medium supplemented with collagenases II and IV (Gibco/Invitrogen, Worthington) and DNase I (Roche Diagnostics) for 45 min at 37°C. Following digestion, recovered leukocytes were enriched using CD45 Microbeads over MACS LS columns (Miltenyi Biotec, Inc.). Leukocytes from spleen and lymph nodes were isolated by density gradient centrifugation. For analysis and culture of PTECs, kidneys were minced into 2 mm^3 pieces, processed through a 180 μm stainless steel sieve and collected in DMEM/F12 medium. Flow-through was applied to a 100 μm cell strainer from which renal tubular segments and glomeruli were recovered by reverse flushing with medium. After centrifugation, tubular segments were digested using collagenase II for 20 min at 37°C in a shaking waterbath. Thereafter, cells were either immediately analyzed by FACS or transferred to 6 well plates for outgrow cultures; 80% confluence of PTECs was reached after 5–6 days. Glomerular endothelial cells (gECs) were isolated as already published.[25] Briefly, glomeruli were digested using Trypsin–EDTA 0.25% (Life Technologies) for 23 min at 37°C in a shaking waterbath, with pellet resuspension every 5 min. gECs were harvested by filtering the suspension through a 40 μm strainer for immediate FACS analysis.

2.6 | Flow cytometry

Typically 1×10^6 cells were stained with antibodies listed in Table S1. Cells were measured using a FACS Fortessa X20 (BD Bioscience). FACS data analysis was conducted using FlowJo software 10.0 (Tree Star Inc.). A gating strategy for identification of the various lymphocyte subsets is illustrated in Figures S1 and S2. Polyfunctionality was assessed via Boolean gating. Generation of t-Distributed Stochastic Neighbor Embedding (t-SNE) plots, FlowSOM analysis and heatmaps was conducted using Cytobank (Beckman Coulter).

2.7 | In vitro assays

Functional analysis of T and NK was performed as previously described.[23] Cells were rested in 200 U/ml murine IL-2 (Miltenyi Biotec) over night, followed by stimulation with 50 ng phorbol 12-myristate 13-acetate (PMA) and 1 μg ionomycin (Sigma-Aldrich) for 4 h in the presence of 10 μg/ml brefeldin A and 2 μM monensin (Biolegend). CD107a expression was used as a correlate for degranulation. Following activation, cells were surface stained, fixed and permeabilized (Transcription Factor Staining Buffer Set; Thermofisher), followed by intracellular staining (representative raw data shown in Figure S3). To assess alloreactivity, DCs were isolated from young and old BALB/c kidneys by magnetic purification using the MojoSort panDC kit (Biolegend) in combination with MACS LD-type columns for depletion of unwanted cells (Miltenyi Biotec). Splenic CD3$^+$ T cells were equally enriched using the MojoSort T cell kit (Biolegend) from C57BL/6 mice sensitized with a BALB/c heart on day 7 post transplantation, followed by staining with the proliferation dye cell trace violet (CTV, 1 μM, Thermofisher). Allo-induced T cell proliferation

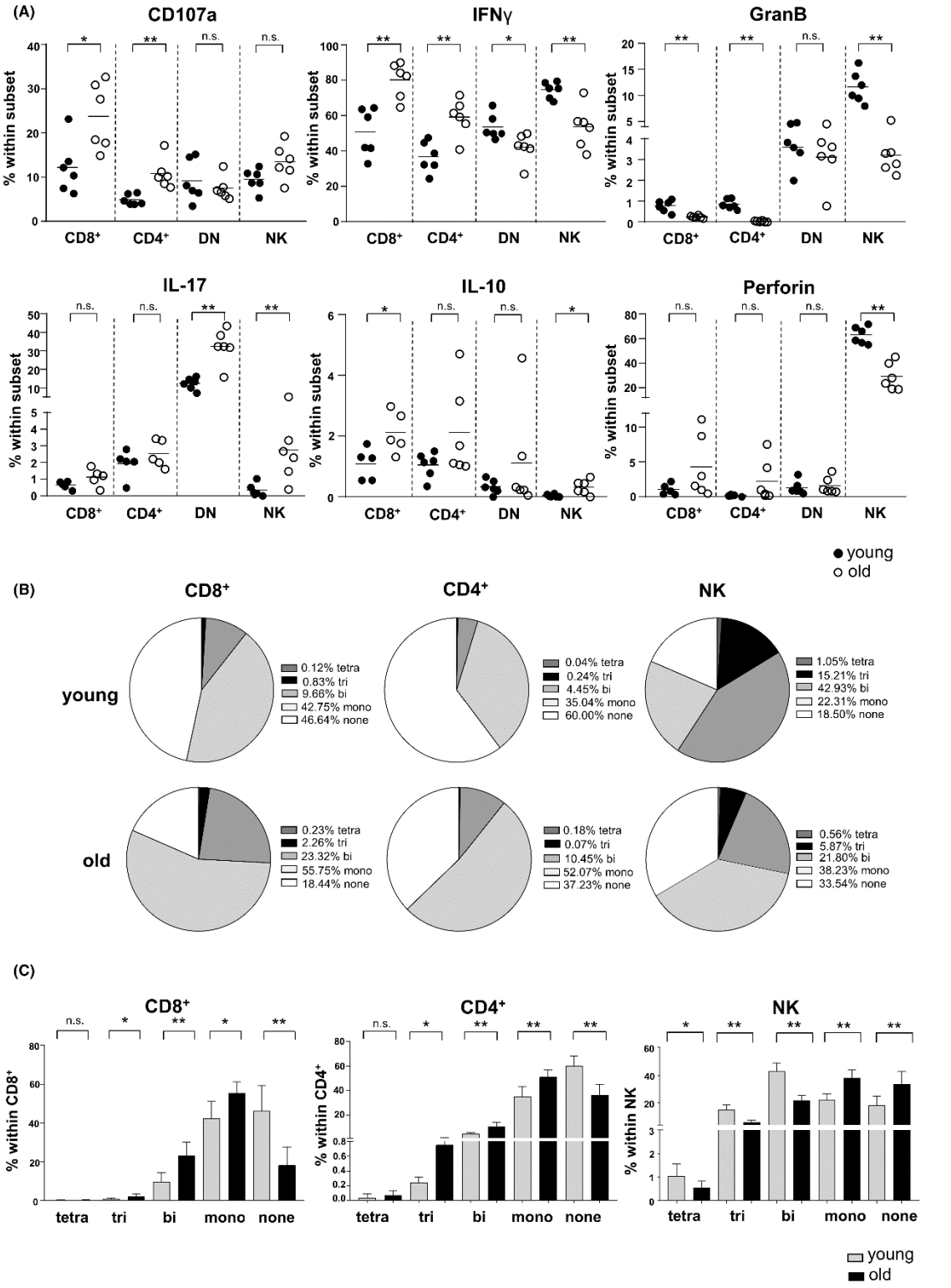
(A)
CD107a
IFNγ
GranB
IL-17
IL-10
Perforin
% within subset
CD8+
CD4+
DN
NK
n.s.
young
old
(B)
CD8+
CD4+
NK
young
0.12% tetra
0.83% tri
9.66% bi
42.75% mono
46.64% none
0.04% tetra
0.24% tri
4.45% bi
35.04% mono
60.00% none
1.05% tetra
15.21% tri
42.93% bi
22.31% mono
18.50% none
old
0.23% tetra
2.26% tri
23.32% bi
55.75% mono
18.44% none
0.18% tetra
0.07% tri
10.45% bi
52.07% mono
37.23% none
0.56% tetra
5.87% tri
21.80% bi
38.23% mono
33.54% none
(C)
CD8+
CD4+
NK
% within CD8+
% within CD4+
% within NK
tetra
tri
bi
mono
none
young
old

FIGURE 3 Kidney-resident lymphocytes derived from aged kidneys show an inflammatory effector profile. (A) Effector profile (CD107a, IFNγ, granzyme B, IL-17, IL-10, and perforin) of $CD8^+$, $CD4^+$, double negative (DN) T cells and NK cells isolated from young or aged C57BL/6 kidneys. (B) Analysis of $CD8^+$, $CD4^+$ T, and NK cell polyfunctionality was performed by boolean gating, including all of the above listed effector molecules. Shown are cells expressing four, three, two, one, or no molecule(s) at a time. Respective mean frequencies from $n = 5–6$ animals/group were used. (C) Statistical analysis of individual data sets as depicted in (B). Statistically significant differences were tested with Mann–Whitney U test and presented as means, $^*p < .05$; $^{**}p < .01$; n.s. = not significant.

was monitored by FACS based on loss of CTV after 4days of co-culture of 10^4 DCs with 10^5T cells.

2.8 | Real-Time RT-PCR

Real-Time PCR was performed as previously described.[26] Total RNA was extracted from snap-frozen samples using RNeasy Mini Kit (Qiagen). RT-PCR was performed for gene expression analysis on ABI 7500 Fast Real-Time PCR System (Applied Biosystems, Life Technologies) using Taqman® gene expression assays (Table S2). Gene expression was normalized ($2^{-\Delta Ct}$ formula) to hypoxanthine-guanine phosphoribosyltransferase (HPRT).

2.9 | Histology

Kidney tissues were formalin-fixed and paraffin-embedded; 1 μm thick sections were prepared, processed and stained with periodic acid schiff (PAS) and counterstained with hematoxilin as previously described.[27] Samples were assessed for necrosis, acute tubular damage, and glomerulitis. Semiquantitative scores in alignment to the Banff criteria were adapted and designed for each lesion. Following scores were used: acute tubular damage: 0 = non, 1 = mild, 2 = moderate, 3 = severe; necrosis: 0 = non, 1 = 1–10% of tissue, 2 = 11–20% of tissue, 3 = more than 20% of tissue; interstitial inflammation in non-fibrotic cortex: 0 = <10%, 1 = 11–25%, 2 = 26–50%, 2 = more than 50%; glomerulitis: 0 = non, 1 = present in at least one glomerulus. Scoring was performed in a blinded fashion based on the whole slide of each sample. Staining of ß-galactosidase was performed according to the manufacturer's instructions (Abcam).

2.10 | Immunofluorescence microscopy

Immunofluorescence microscopy (IF) was done as previously published.[28] Briefly, transplanted kidneys were excised and a ¼ of each kidney was fixed overnight at 4°C with PLP fixative. Following extensive wash with PBS, kidneys were dehydrated in 30% sucrose in PBS overnight at 4°C, snap frozen in OCT and stored at −80°C. 16 μm kidney cryosections were mounted on Superfrost Plus microscope slides (Fisher) and dried overnight at room temperature. Sections were blocked and stained in a humidified box in the dark at room temperature overnight with purified or directly conjugated antibodies (Table S3). Next morning, following washes with PBS sections were stained with the respective secondary antibody for 1 h at room temperature, counterstained with Hoechst and mounted with Fluoromount-G (eBiosciences). Samples were scanned on a Zeiss LSM780 confocal microscope using a dry 20×0.8 N.A. objective. Tiled, z-stacks were acquired at 1024×1024 pixels, with line averaging of 4 and pinhole size 1, and were stitched together using Zen Blue software (Zeiss). Fuji (version 1.53r) was used to process the acquired images and generate maximal intensity projection snapshots.

2.11 | Statistics

Statistical analysis was performed using GraphPad Prism 8 (GraphPad Software). Significant differences between groups were calculated applying either T- or Mann–Whitney U test (two groups) or Kruskal–Wallis test (multiple groups) after testing for normality distribution using the D'Agostino & Pearson test. Statistical significance was considered for the following p values: ns = $p > .05$, $^*p \le .05$, $^{**}p \le .01$, $^{***}p < .001$, $^{****}p \le .0001$.

3 | RESULTS

3.1 | Solid and lymphoid organs are differentially affected by inflamm-aging

Applying a viSNE algorithm approach to assess FACS derived data for T cell diversity, we observed no clear differences between young and aged kidneys (Figure 1A, top). Next, we applied FlowSOM, a technique for unsupervised clustering of FACS data. Generated viSNE maps were overlayed with metaclusters identified in FlowSOM, allowing the identification of multiple T cell subpopulations based on their memory markers present in both young and aged kidneys (Figure 1A, bottom). Based on the annotated clusters, manual gating of FACS data for T cells revealed that frequencies of $CD8^+$ T cells were significantly increased in aged kidneys, spleen and lymph nodes whereas frequencies of $CD4^+$ T cells were decreased. Histology of young and old naïve kidneys did not reveal histopathological changes regarding necrosis, edema or interstitial inflammation (Figure S5A), however aged kidneys showed slightly more acute tubular injury (Figure 1B).

We further observed significantly reduced frequencies of double-negative (DN) T cells as well as $NKp46^+$ NK cells in aged kidneys and spleens compared to young organs, whereas both subsets were significantly increased in lymph nodes. Aged kidneys and lymph nodes were also characterized by significantly higher frequencies of $CD11c^+MHC\text{-}II^+$ dendritic cells (DCs) than their young counterparts (Figure 1C).

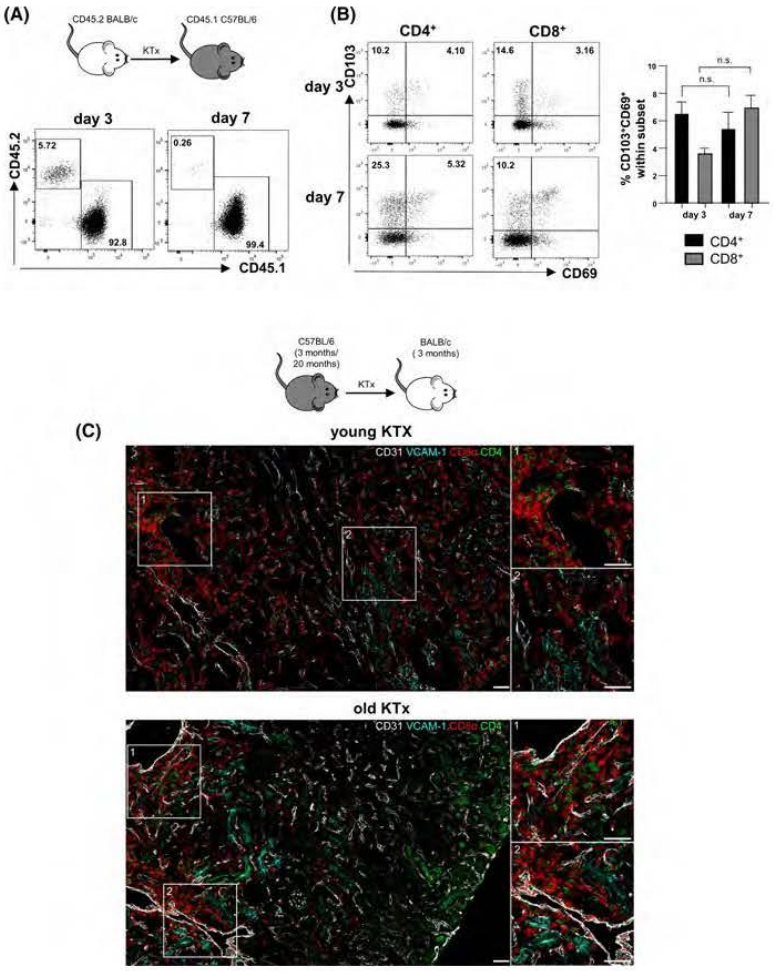

FIGURE 4 Recipient-derived T cells re-populate the allogeneic graft by day 7. (A) Representative FACS dot plots illustrating the intra-renal leukocyte distribution in a congenic BALB/c (donor, CD45.2$^+$) to C57BL/6 (recipient, CD45.1$^+$) combination on day 3 and day 7 post kidney transplantation. (B) Representative FACS dot plots showing the increase of CD69$^+$CD103$^+$ CD4$^+$ and CD8$^+$ T_{rm} cells (left panel). Bar graph represents frequencies of CD4$^+$ and CD8$^+$ T_{rm} cells (right panel, $n = 4$). Statistically significant differences were tested with Mann–Whitney U test and presented as means, n.s. = not significant. (C) Maximal intensity projection of confocal immunofluorescence snapshots from young or aged transplanted kidney cryosections (C57BL/6 into BALB/c, as depicted) stained for the indicated markers. Bars = 50μm.

Both, FlowSOM and manual gating demonstrate that kidney, spleen and lymph nodes harbor significantly higher frequencies of effector memory CD4$^+$ and CD8$^+$ T cells (Figure 1A,D, Figure S5). In contrast, frequencies of natural CD4$^+$CD25$^+$FoxP3$^+$ regulatory T (T_{reg}) cells were significantly reduced in the aged kidney, being characterized by diminished portions of proliferating Ki67$^+$ cells; both features also applied to CD122$^+$ CD8$^+$ regulatory T cells (Figure 1E). As opposed to the kidney, CD8$^+$ T_{reg} frequencies were significantly higher in aged spleens and lymph nodes, but showing less proliferative capacity compared to their young counterparts (Figure S6). Thus, aging results in a change of the intra-renal lymphocyte compartment towards an effector memory phenotype paralleled with a loss of regulatory T cells.

3.2 | A distinct subset of NKp46$^+$ NK cells expressing CD49a and CXCR6 resides in senescent kidneys

We previously described increased mRNA expression of the activating cytotoxicity receptor NKG2D in human renal zero-hour biopsies as being indicative for biological donor age.[29] Here, we identified higher frequencies of NKG2D$^+$ NK and CD8$^+$ T cells in relation to age, confirming that NKG2D is upregulated on senescent renal lymphocytes (Figure 2A). This observation was also corroborated by viSNE analysis for NKp46$^+$ NK cells and equally applied to the chemokine receptor *C-X-C chemokine receptor type 6* (CXCR6) and the *alpha 1 subunit of α1β1 integrin* (CD49a) (Figure 2B). Heatmap analysis confirmed this induction, whereas other NK cell markers including DX5 and CD11b were downregulated (Figure 2C). Interestingly, CXCR6$^+$CD49a$^+$ NK cells have already been identified as tissue-resident NK cells in the human liver,[30] a feature that we confirm for murine kidneys and that quantitatively increases with age (Figure 2D,E). Aged CXCR6$^+$CD49a$^+$ NK cells contain significantly higher portions of perforin$^+$, but not IFNγ$^+$ cells (Figure 2E). Finally, despite lower overall frequencies of NK cells in aged kidneys (Figure 1B), we detected increased frequencies of differentiated CD27$^+$CD11b$^-$ NK cells (Figure 2F), being associated with greater effector function and responsiveness to chemokines.[31]

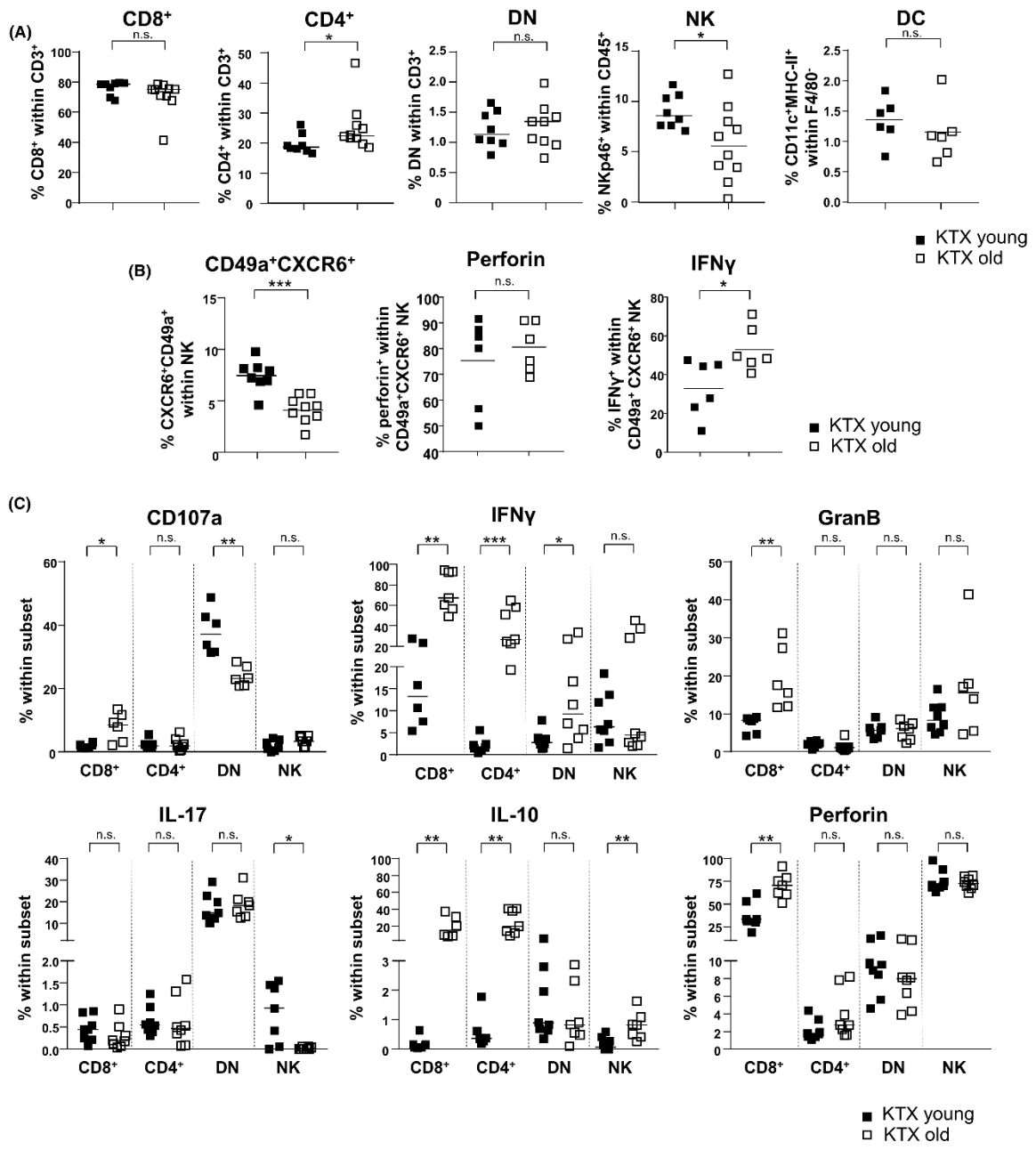

FIGURE 5 Aged kidney grafts provoke an intra-renal inflammatory profile. (A) Frequencies of $CD8^+$, $CD4^+$ T cells, DN, and NK cells isolated from either young or aged C57BL/6 derived grafts, transplanted into BALB/c recipients on day 7 post transplantation ($n = 8–10$). (B) Frequencies of $CD49a^+CXCR6^+$ NK cells isolated from either young or aged grafts and their production of perforin and IFNγ on day 7 post kidney transplantation. (C) Effector profile (CD107a, IFNγ, granzyme B, IL-17, IL-10, and perforin) of $CD8^+$, $CD4^+$ DN T cells, and NK cells isolated from young or aged renal allografts on day 7 post transplantation ($n = 5–9$). Statistically significant differences were tested with Mann–Whitney U test or unpaired *t*-test and presented as means, $^*p < .05$; $^{**}p < .01$; $^{***}p < .001$; n.s. = not significant.

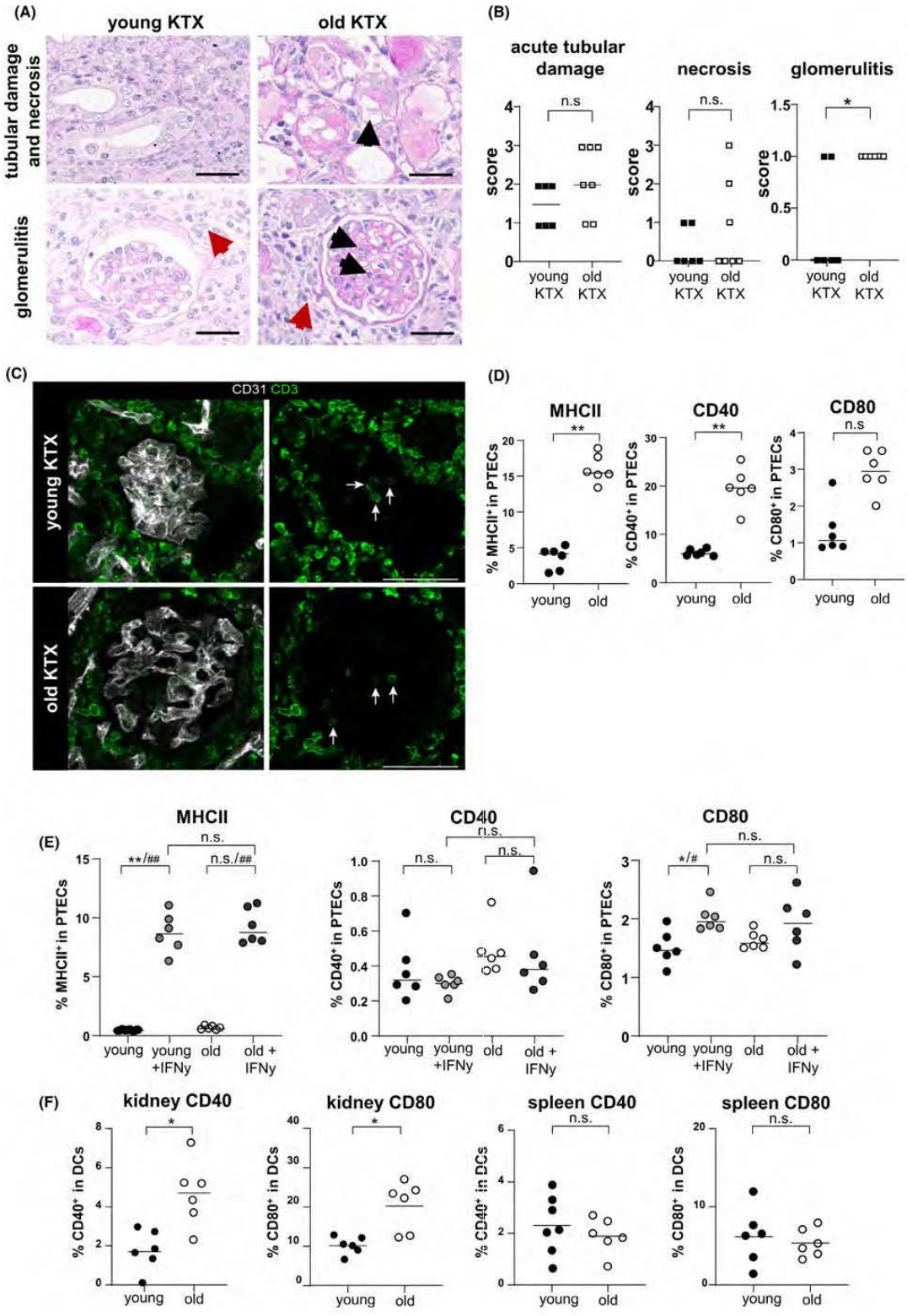
(A)
young KTX
old KTX
tubular damage and necrosis
glomerulitis
(B)
acute tubular damage
necrosis
glomerulitis
score
n.s
n.s.
*
young KTX
old KTX
(C)
CD31 CD3
young KTX
old KTX
(D)
MHCII
CD40
CD80
% MHCII+ in PTECs
% CD40+ in PTECs
% CD80+ in PTECs
**
n.s
young
old
(E)
MHCII
CD40
CD80
% MHCII+ in PTECs
% CD40+ in PTECs
% CD80+ in PTECs
**/##
n.s./##
n.s.
*/#
young
young +IFNy
old
old + IFNy
(F)
kidney CD40
kidney CD80
spleen CD40
spleen CD80
% CD40+ in DCs
% CD80+ in DCs
*
n.s.
young
old

FIGURE 6 Aged PTECs and renal-derived DCs are characterized by induced expression of MHC class II and co-stimulatory molecules. (A) Representative histological images and (B) statistical analysis of tubular damage, necrosis (black arrow), glomerulitis (black arrows), and interstitial inflammation (red arrows) in young versus old C57BL/6 kidney grafts on day 7 post transplantation. 400× magnification, bar represents 20 μm. (C) Confocal immunofluorescence snapshots from young or aged transplanted kidney cryosections stained for CD31 (white) and CD3 (green), bars = 50 μm. (D) Surface expression of MHCII, CD40, and CD80 on freshly isolated PTECs from naïve C57BL/6 kidneys and (E) after 1 week of cell culture followed by IFNγ stimulation. (F) Ex vivo surface expression of CD40 and CD80 on $CD11c^+MHCII^+$ DCs isolated from naïve young or aged C57BL/6 kidneys and spleen. Data from $n = 6–8$ mice/group, respectively. Statistically significant differences were tested with Mann–Whitney U test with # indicating $p < .05$ and ## indicating $p < .01$ in a two-group comparison or, alternatively with Kruskal–Wallis in a multiple group comparison and presented as means and $^*p < .05$; $^{**}p < .01$; n.s. = not significant.

3.3 | Intra-renal lymphocytes display a distinct inflammatory effector function profile according to age

Both aged renal $CD8^+$ and $CD4^+$ populations contained significantly higher frequencies of degranulating $CD107a^+$ as well as $IFN\gamma^+$ cells, whereas portions of granzyme B producers were reduced (Figure 3A). Senescent NK cells less frequently expressed the cytotoxic mediators granzyme B and perforin, along with reduced proportions of $IFN\gamma^+$ cells, indicating an impairment of classical NK effector functions. Increased frequencies of $IL\text{-}17^+$ cells were confined to the senescent $CD4^-CD8^-$ DN T and NK cell compartment (Figure 3A). Aged kidney-derived $CD8^+$ and $CD4^+$ T cells further demonstrated an increase in polyfunctionality reflected by higher portions of cells secreting two or three effector molecules at a time, whereas senescent NK cells lost that ability (Figure 3B,C). In summary, our phenotypic analysis revealed a re-composition and altered effector profile of intra-graft lymphocytes in aged kidneys, which needs to be considered for their potential role as passenger leukocytes.

3.4 | The senescent kidney graft provokes an inflammatory immune response

In order to gain knowledge into the kinetics of graft infiltration, using congenic strains, we transplanted CD45.2 BALB/c kidneys into CD45.1 C57BL/6 recipients. Analysis of the intra-renal leukocyte composition revealed that whereas on day 3 post-transplantation donor-derived leukocytes were still detectable, the kidney was completely re-populated on day 7 by recipient-derived cells (Figure 4A). Thus, the majority of cells isolated from the graft in subsequent experiments are derived from the kidney recipient. Already on day 3, both recipient-derived, graft-infiltrating $CD45.1^+$ $CD4^+$ and $CD8^+$ T cells express the *integrin αE* (CD103) as well as the activation/retention marker CD69 being indicative for tissue-residency (T_{rm}). This expression increased for $CD8^+$ T cells until day 7, demonstrating that graft-infiltrating $CD4^+$ and $CD8^+$ T cells acquire a T_{rm} phenotype after entering the graft (Figure 4B). We hypothesized that aged grafts provoke the formation of higher intra-renal T_{rm} frequencies. However, whereas no differences between young and aged grafts were observed for $CD8^+$ T_{rm}, frequencies of $CD4^+$ T_{rm} were significantly decreased in aged kidney grafts on day 7 post-transplantation (Figure S7A).

Finally, we transplanted kidneys derived from either young (3 months) or aged (20 months) C57BL/6 mice into young (3 months) BALB/c recipients. Although we used in previous experiments BALB/c mice as donors,[23] this was not possible in this experimental set-up, as only aged C57BL/6 mice were available. On day 7 post-transplantation, $CD4^+$ and $CD8^+$ T cells were identified in young and aged organs. Both cell types were located in close proximity to $CD31^+$ (endothelial) cells and, although not exclusively, in close proximity to $VCAM\text{-}1^+$ tubuli in the cortex of kidney grafts (Figure 4C). Higher graft-infiltrating $CD4^+$ T cell frequencies were observed in aged organs, which was not observed for the spleen or lymph nodes (Figure 5A, Figure S7B). On the contrary, frequencies of total NK cells and $CD49a^+CXCR6^+NKp46^+$ NK cells were significantly decreased in aged kidneys compared with young grafts, but contained higher portions of $IFN\gamma^+$ cells (Figure 5B). Furthermore, we observed higher infiltration of effector memory $CD4^+$ T (T_{EM}) cells in aged kidneys (Figure S7C). Recipient-derived $CD8^+$ T cells infiltrating an aged kidney graft showed enhanced degranulation capacity reflected by CD107a, granzyme B, perforin and IFNγ expression with the latter feature also accounting for $CD4^+$ and DN T cells. Surprisingly, recipient-derived $CD4^+$ and $CD8^+$ T cell subsets isolated from a senescent kidney engrafted into a young recipient produced significantly more IL-10 than cells from a young graft (Figure 5C). Taken together, although frequencies of graft infiltrating cells are not dramatically different between young and aged kidneys, old grafts provoke a significantly higher inflammatory immune response mediated by graft-infiltrating recipient-derived T cells.

3.5 | Senescent proximal tubular epithelial cells upregulate MHC class II and co-stimulatory molecules

Aged allografts exhibited a higher incidence of glomerulitis, but not necrosis or tubular damage compared with young grafts (Figure 6A,B). Both young and aged grafts showed the presence of $CD3^+$ T cells in glomeruli (Figure 6C).

We further addressed whether proximal tubule epithelial cells (PTECs) might also contribute to age-related local alloinflammation. Freshly isolated PTECs from naive aged kidneys contained significantly higher portions of MHC class II^+, $CD40^+$ and $CD80^+$ cells than their young counterparts (Figure 6D). To gain sufficient cells for allo-stimulatory assays with T cells, we expanded PTECs from young versus old naïve mice for 5 days in vitro. As shown in

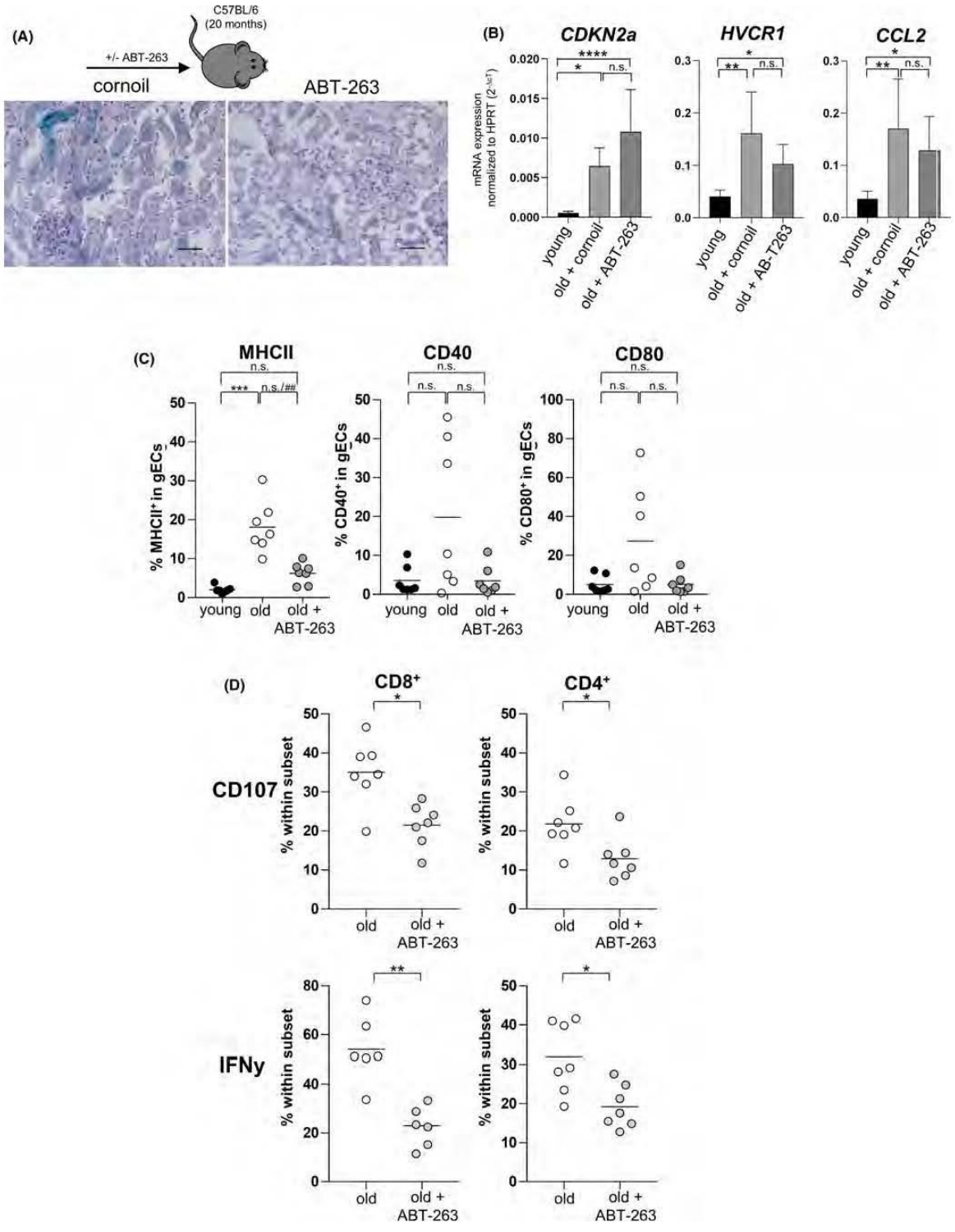
(A)
C57BL/6
(20 months)
+/- ABT-263
cornoil
ABT-263
(B)
CDKN2a
HVCR1
CCL2
mRNA expression
normalized to HPRT (2-ΔCT)
young
old + cornoil
old + ABT-263
old + AB-T263
(C)
MHCII
CD40
CD80
% MHCII+ in gECs
% CD40+ in gECs
% CD80+ in gECs
young
old
old + ABT-263
(D)
CD8+
CD4+
CD107
IFNy
% within subset
old
old + ABT-263

FIGURE 7 Treatment with the senolytic drug ABT-263 modulates graft immunogenicity. (A) Representative histological figures for ß-galactosidase kidney staining for cornoil versus ABT-263 treated old C57BL/6 mice, magnification 200×, bar represents 50 μm. (B) Gene expression analysis for the candidate genes *CDKN2a*, *HVCR1*, and *CCL2* analyzed in kidneys derived from naïve young ($n = 6$), or aged cornoil ($n = 8$) versus ABT-236 treated aged C57BL/6 mice ($n = 11$). (C) Ex vivo surface expression of MHCII, CD40, and CD80 on glomerular endothelial cells isolated from naïve young ($n = 6$), or aged cornoil ($n = 7$) versus ABT-236 treated aged C57BL/6 mice ($n = 6$). (D) Frequencies of $CD107a^+$ and $IFN\gamma^+$ $CD8^+$ and $CD4^+$ T cells isolated from aged cornoil ($n = 7$) versus ABT-236 treated aged C57BL/6 mice ($n = 7$). Statistically significant differences were tested with Mann–Whitney U where ## indicates $p < .01$ in a two-group comparison or, alternatively by Kruskal–Wallis-test in a multiple group comparison and presented as means. $^*p < .05$; $^{**}p < .01$; $^{***}p < .001$; $^{****}p < .0001$; n.s. = not significant.

Figure 6E, however, PTECs lose MHC class II and CD40 during culture as compared to ex vivo expression (Figure 6D). To re-induce costimulatory molecules, the expansion culture medium was supplemented with IFNγ, resulting in significant MHC class II upregulation; however, no differences between young and aged PTECs could be observed under these conditions (Figure 6E). CD80 expression was upregulated following IFNγ treatment solely on young kidney-derived PTECs but did not demonstrate higher expression levels than aged kidney-derived PTECs (Figure 6E). As an alternative cell-type for stimulation of allo-specific T cells, DCs were isolated. In line with data from PTECs, aged renal DCs showed significantly higher expression of CD40 and CD80 (Figure 6F), a feature not accounting for splenic DCs. However, the allo-stimulatory capacity of aged versus young kidney-derived DCs by adding allo-sensitized T cells was comparable (Figure S8).

3.6 | ABT-263 pre-treatment reduces inflammation in the aged graft

ABT-263 (Navitoclax) is a Bcl-2/w/xL inhibitor targeting the Bcl-2 pathway in senescent cells, resulting in cellular apoptosis.[32] Currently, ABT-263 is used in phase 1/2 clinical trials for both hematologic and solid organ malignancies, suggesting additional potential in other conditions requiring depletion of senescent cells, such as kidney transplantation.[33] We therefore treated naïve aged C57BL/6 mice with ABT-263 dosages. To examine potential effects of ABT-263 on renal senescent cells, we analyzed the contralateral kidney for classical markers indicative for renal senescence, tubular injury and inflammation.[18,34,35] Staining with ß-galactosidase, a classical senescence marker, demonstrated a reduction of senescent PTECs in ABT-263 pre-treated animals confirming recent data (Figure 7A).[34] Both aged mice treated with ABT-263 and untreated controls demonstrated a significantly higher mRNA expression of *CDKN2a* (p16INK4a), *HAVCR1* (kidney injury molecule 1, KIM 1) and *CCL2* (Monocyte Chemoattractant Protein-1, MCP-1) compared to untreated young kidneys (Figure 7B). Intriguingly, p16INK4a was induced, whereas KIM-1 and MCP-1 showed a reduced mRNA expression in ABT-263 kidneys. In order to evaluate the impact of ABT-236 treatment of renal endothelial cells, we isolated glomerular endothelial cells (gECs) from naïve young, old untreated and old ABT-263 treated mice. Comparable with PTECs, aged renal gECs demonstrated a significantly higher expression of MHCII compared with young gECs, which was partially observed for CD40 and CD80. This expression was downregulated in kidneys from ABT-263 pre-treated mice, although not statistically significant (Figure 7C). Interestingly, $CD4^+$ and $CD8^+$ T cells isolated from ABT-263 pre-treated untransplanted kidneys showed significantly less degranulation capacity and IFNγ production (Figure 7D).

On day 7 post kidney transplantation, higher frequencies of DN T cells and NK cells infiltrated ABT-263 pre-treated allografts. Despite the overall increase of NK cells, frequencies of $CD49a^+CXCR6^+$ $NKp46^+$ NK cells were significantly lower in grafts from ABT-263 treated mice (Figure 8A). Moreover, gECs isolated on day 7 post kidney transplantation from ABT-263 pre-treated mice showed still reduced levels of MHCII, CD40 and CD80 compared with aged untreated controls although not statistically significant (Figure 8B). Although no difference for graft function was detected on day 7 post transplantation (Figure 8C), recipient-derived, graft-infiltrating cells demonstrated a significant reduction of IFNγ and IL-10 for all T cell subsets (Figure 8D). We did not detect any histological changes between the ABT-263 treated and non-treated groups (Figure 8E). To prove a long-term effect of ABT-263 treatment, we repeated the aforementioned experiments, sacrificing the animals on day 28. Again, no dramatic changes for the various intra-renal lymphocyte populations analyzed were detected (Figure 9A), but creatinine and urea levels were significantly lower in the ABT-263 treated versus non- treated group, indicating an improvement of graft function after ABT-263 pre-treatment despite of unaltered histology (Figure 9A–C). Figure 10 summarizes the main findings of the study.

4 | DISCUSSION

Strategies to address the current organ shortage request a critical re-examination of donor eligibility, especially including the elderly.[36,37] Immune activation within a renal allograft may be mediated via the vasculature and/or passenger immune cells, yet no experimental studies have determined the impact of aging on any of these compartments. As molecular mechanisms of senescence have already been documented,[38–40] we aimed to understand the immunological component first, by assessing the intra-renal cellular composition according to kidney senescence. A shift of the CD4:CD8 ratio has already been described in association with aging and obesity in humans,[41] however, our analysis confirms higher frequencies of $CD8^+$ T cells, paralleled by a reduction of

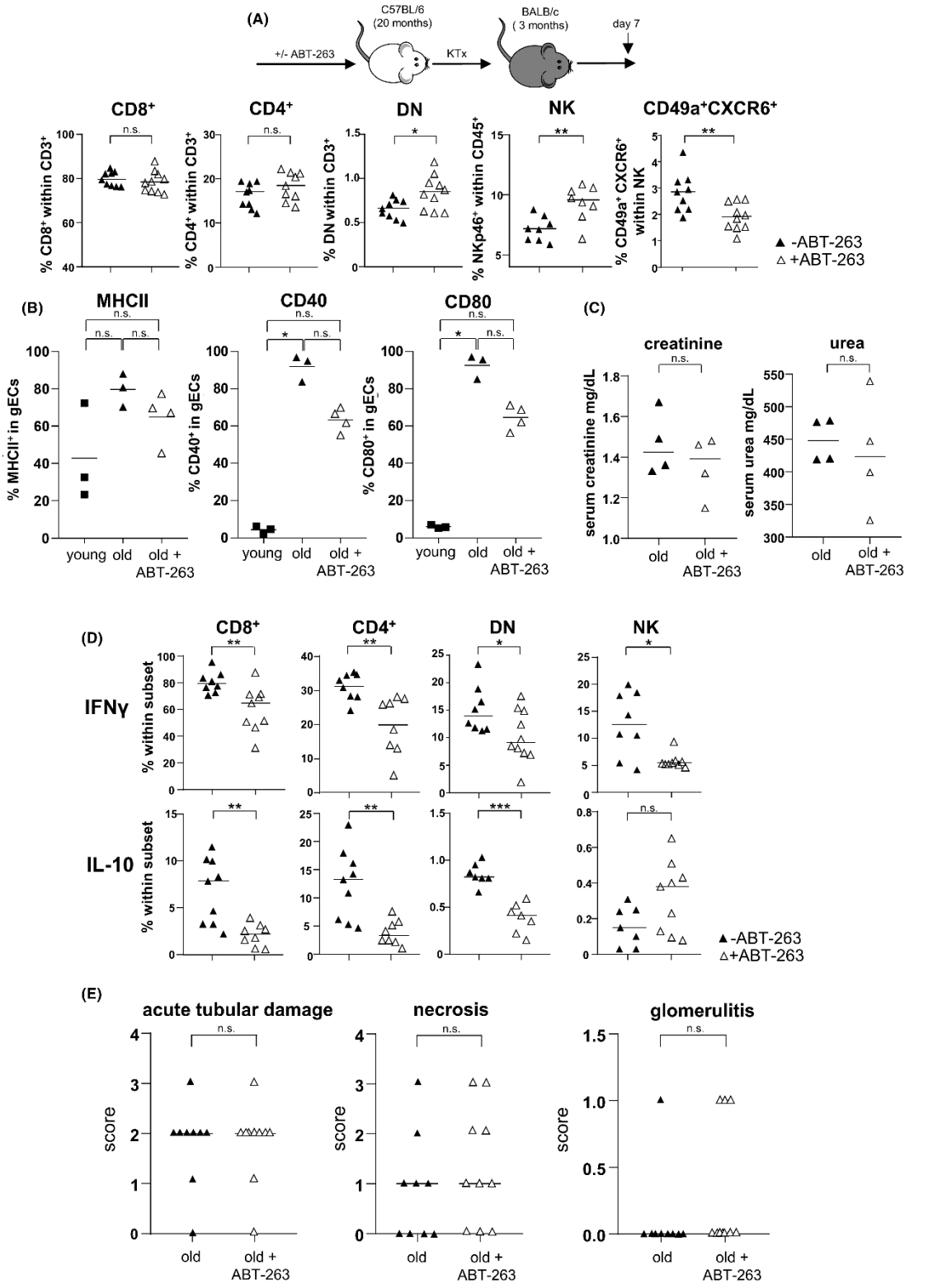
(A)
C57BL/6 (20 months)
BALB/c (3 months)
+/- ABT-263
KTx
day 7
CD8+
CD4+
DN
NK
CD49a+CXCR6+
% CD8+ within CD3+
% CD4+ within CD3+
% DN within CD3+
% NKp46+ within CD45+
% CD49a+ CXCR6+ within NK
n.s.
*
**
▲ -ABT-263
△ +ABT-263
(B)
MHCII
CD40
CD80
% MHCII+ in gECs
% CD40+ in gECs
% CD80+ in gECs
young
old
old + ABT-263
(C)
creatinine
urea
serum creatinine mg/dL
serum urea mg/dL
(D)
IFNγ
IL-10
% within subset
***
(E)
acute tubular damage
necrosis
glomerulitis
score

FIGURE 8 ABT-263 treatment ameliorates intra-graft inflammation of senescent kidneys (A) Frequencies of $CD8^+$, $CD4^+$, DN, NK, and $CD49a^+CXCR6^+$ NK cells isolated from either cornoil or ABT-263 pre-treated aged C57BL/6 derived grafts on day 7 post transplantation (8–10 animals/group). (B) Ex vivo surface expression of MHCII, CD40, and CD80 on glomerular endothelial cells isolated from young ($n = 3$) or aged cornoil ($n = 3$) versus ABT-236 treated aged C57BL/6 grafts ($n = 4$) transplanted into BALB/c recipient mice on day 7 post transplantation. (C) Functional parameters (serum creatinine, urea) from aged cornoil ($n = 3$) versus ABT-236 treated aged C57BL/6 grafts ($n = 4$) on day 7 post kidney transplantation. (D) IFNγ and IL-10 expression of $CD8^+$, $CD4^+$, DN T, NK cells isolated from either cornoil or ABT-263 pre-treated grafts. (E) Histopathological scoring for acute tubular damage, necrosis and glomerulitis between cornoil and ABT-263 pre-treated senescent grafts derived from day 7 post kidney transplantation. Statistically significant differences were tested with Mann–Whitney *U*-test, unpaired *t*-test or Kruskal–Wallis test and presented as means. $^*p<.05$; $^{**}p<.01$; n.s. = not significant.

$CD4^+$ T cells, in the aged kidney. According to studies performed in human peripheral blood and murine studies, we detected a significantly higher portion of $CD4^+$ and $CD8^+$ T_{EM}, whereas naïve T cells were decreased.[42,43] Our findings further demonstrate that renal NK cells were significantly reduced in naïve, older kidneys displaying reduced cytotoxicity and impaired polyfunctionality. Although an age-dependent decline of peripheral blood NK cells in humans has been described,[44,45] alternative studies document a significant increase in the percentage and/or absolute number of $CD3^-$ $CD56^+$ NK cells according to age.[46,47] We could also identify the presence of $CD49a^+CXCR6^+$ NK cells in the aged kidney. Both CD49a and CXCR6 have been originally described as markers of murine and human liver NK cells, the latter being critical for their long-term homeostasis.[48,49] These liver $CXCR6^+$ NK cells can mediate intense skin inflammation, suggesting that $CXCR6^+$ NK cells possess a memory potential.[48] As NK cells are emerging as powerful drivers of immune-mediated kidney allograft rejection,[50–53] future studies will be necessary to determine which defined NK cell subpopulation might be responsible for these effects. In summary, our findings document that the aging renal compartment is characterized by a defined composition of lymphocytes, which is not necessarily reflected in spleen or lymph nodes. Thus, inflammaging is an organ-specific characteristic, which needs to be considered in future studies addressing senescence.

The interaction between senescent cells and the intra-renal immune milieu post-transplantation is complex. Potential targets of recipient-derived graft-infiltrating cells including PTECs or gECs were characterized by significantly higher expression of activating and co-stimulatory markers indicating a premature aging phenotype. Although it can be assumed that senescence can also be triggered actively when cells are exposed to excessive inflammatory stimuli, such as IFNγ, aged versus young PTECs did not demonstrate a significant difference in their expression of MHC class II or CD80 in vitro. Similarly, we did not detect a difference in the stimulatory capacity of young versus aged renal-derived DCs towards allo-sensitized T cells. Thus, these data suggest that a subtle chronic inflammatory status shapes and maintains a senescent intra-renal micromilieu in vivo resulting in a mature phenotype of PTECs and gECs, which is difficult to mimic in vitro, in contrast to recently published data within a heart transplantation setting.[54] With the exception of infiltrating $CD4^+$ and $CD8^+$ T cells acquiring a T_{rm} phenotype,[55] we did not detect dramatic differences in lymphocyte frequencies infiltrating a young versus an aged organ. However, recipient-derived T cells isolated from aged donor grafts were characterized by an inflammatory phenotype. Based on the observation that a higher activation status was still observed for old gECs on day 7 post kidney transplantion, we postulate that recipient-derived T cells will become activated by the higher stimulatory capacity of the local endothelium/epithelium present in aged grafts.

Murine studies have shown that depletion of senescent cells delays age-associated disease.[56] We therefore pre-treated aged kidneys by the direct inhibition of the pro-survival Bcl-2 pathway applying ABT-263 to donor animals. This resulted in a depletion of senescent PTECs and gECs as well as in a reduction of activated graft-resident $CD4^+$ and $CD8^+$ T cells. Thus, it can be assumed that in naïve aged kidneys, activated PTECs and gECs maintain a pro-inflammatory phenotype of resident T cells. Interestingly, a reduction of allostimulatory gECs as a consequence of ABT-263 donor-pretreatment was still detected on day 7 post kidney transplantation. Targeting of renal senescent cells resulted in reduced IFNγ and IL-10 production by graft-infiltrating lymphocyte subsets, although graft histology and renal function were not influenced. Similar observations were made for day 28, however, an improvement of graft function could be observed for the ABT-263 pretreamtent group.

The application of senolytics has already been demonstrated to ameliorate numerous conditions in experimental models, including diabetes, cardiac dysfunction or acute kidney injury[32,34,57] as well as experimental heart transplantation.[58] Here, we demonstrate that targeting of renal senescence might also be a valuable approach to improve donor organ function, bearing the potential to reduce maintenance immunosuppression.

We are aware that our study has several limitations. First, it remains unclear why *p16INK4a* mRNA expression is not lower in ABT-263 pre-treated kidneys compared to controls, although this has been shown e.g. in lungs of aged ABT-263 treated mice.[32] As p16INK4A is not found in all senescent cells and can also be expressed in some non-senescent cells, the induced expression remains to be clarified.[59,60] Although the effectiveness of alternative senolytics, such as Dasatinib and Quercetin has been proven in experimental models as well as in clinical studies,[54,61–63] it needs to be evaluated whether their application might result in comparable—or even better results. Second, we failed with potential co-culture assays to understand the direct interaction between recipient-derived graft-infiltrating cells and potential target cells explaining their enhanced effector functions. Finally, it remains to be determined how very subtle changes in tissue integrity could be uncovered by advanced histological techniques.

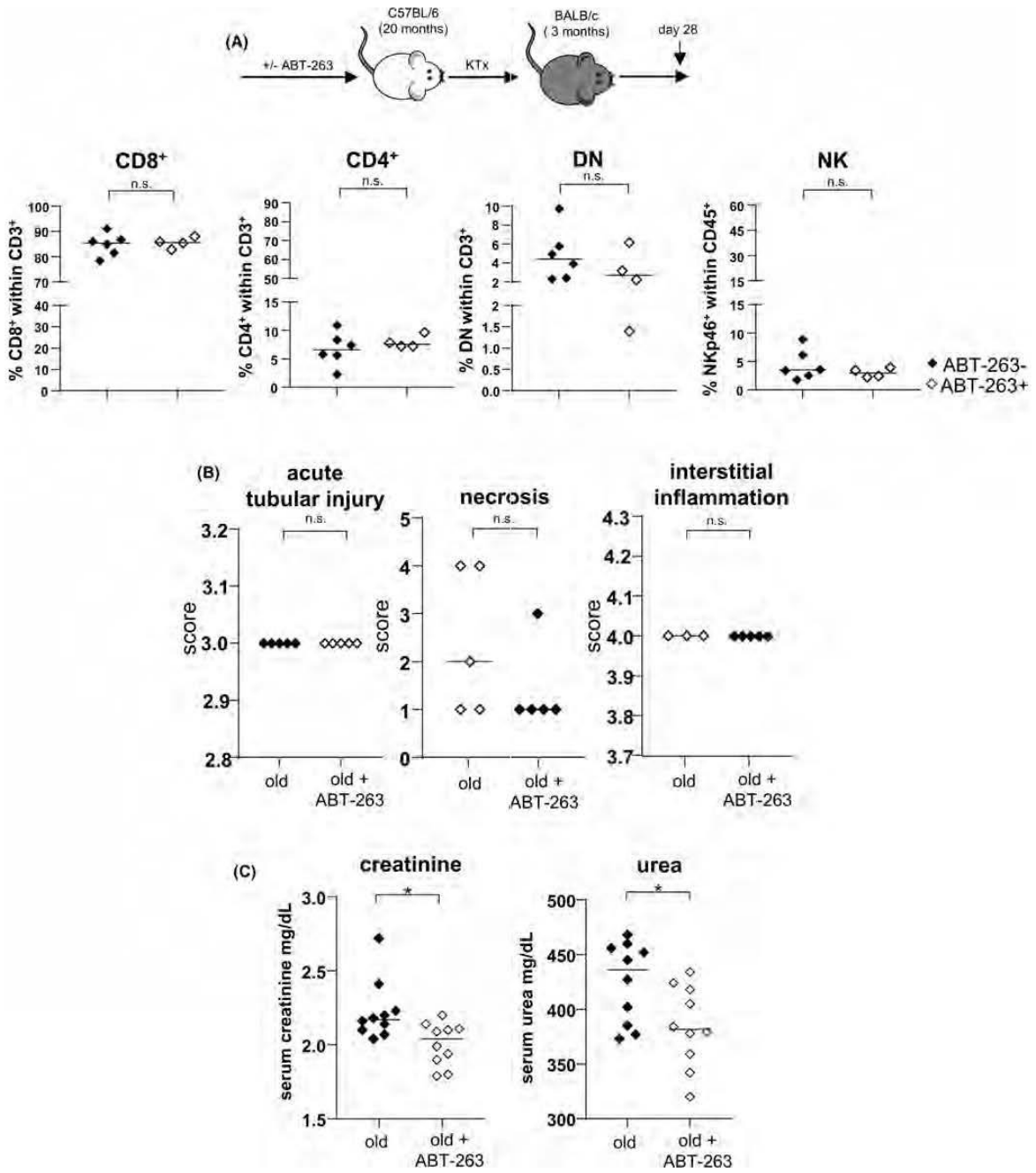

FIGURE 9 ABT-263 pre-treatment of senescent kidneys improves graft function in the long term but does not change graft histology. (A) Frequencies of $CD8^+$, $CD4^+$, DN T, and NK cells isolated from either cornoil or ABT-263 pre-treated aged C57BL/6 derived grafts on day 28 post transplantation ($n = 4$–6 animals/group). (B) Histopathological scoring for acute tubular damage, necrosis, and glomerulitis between cornoil and ABT-263 pre-treated senescent grafts derived from day 28 post kidney transplantation (3–5 animals/group). (C) Functional parameters (serum creatinine, urea) on day 28 post kidney transplantation ($n = 10$–11 animals/group). Statistically significant differences were tested with Mann–Whitney U test or unpaired *t*-test and presented as means. $^*p < .05$; n.s. = not significant.

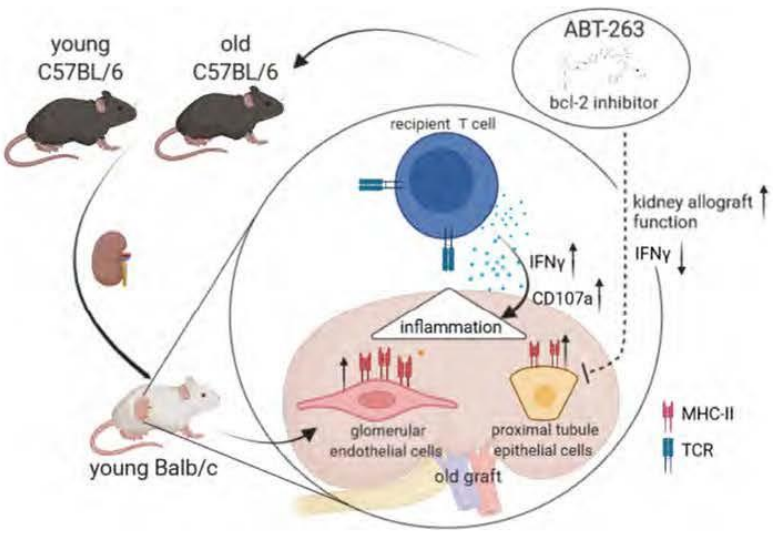

FIGURE 10 Graphical summary of the main manuscript findings.

Our current understanding of the influence of age on the size of the memory compartment entirely relies on studies of peripheral blood and lacks information on resident memory cells. It is therefore mandatory to better understand the molecular and cellular pathways that are responsible for linking the aging immune system with the kidney. On that background, pre-conditioning of senescent organs, as demonstrated here, bears a high potential for clinical translation due to its regulation of the inflammatory cellular response and improvement of organ function.

ACKNOWLEDGMENTS

A.H., A.SAR., L.M.L.T., J.S., A.S., M.I.A., V.P., C.S., T.D., Y.B., P.V.R., S.E., K.W.H., E.G.S., R.D.B., and P.B. carried out experiments; A.H., A.SAR., L.M.L.T., and A.S. analyzed the data; made the figures; A.H., A.SAR., and K.K. drafted and revised the paper; K.K. designed the study; all authors approved the final version of the manuscript. Open Access funding enabled and organized by Projekt DEAL.

FUNDING INFORMATION

This work was funded by grants from Deutsche Forschungsgemeinschaft (DFG-Ko2270/4-1, DFG-Ko2270/5-1), Sonnenfeldstiftung and Sanofi Genzyme GmbH to K.K. and A.H. is funded by a grant from Chinese Scholarship Council (CSC). P.B. is supported by the Deutsche Forschungsgemeinschaft (Project-IDs 322900939, 454024652, 432698239, and 445703531 and 445703531), European Research Council (ERC) Consolidator Grant AIM.imaging.CKD (no. 101001791), and the Federal Ministry of Education and Research (STOP-FSGS-01GM1901A). EGS is supported by Deutsche Forschungsgemeinschaft (STA 1657/2-1).

DISCLOSURE

The authors of this manuscript have no conflicts of interest to disclose as described by the *American Journal of Transplantation*.

DATA AVAILABILITY STATEMENT

The data that support the findings of this study are available from the corresponding author upon reasonable request.

ORCID

An He https://orcid.org/0000-0002-7592-7527
Attia Sarwar https://orcid.org/0000-0002-0923-6373
Linda Marie Laura Thole https://orcid.org/0000-0003-0926-841X
Janine Siegle https://orcid.org/0000-0003-2230-493X
Ame Sattler https://orcid.org/0000-0003-2572-5641
Muhammad Imtiaz Ashraf https://orcid.org/0000-0002-6789-5393
Vanessa Proß https://orcid.org/0000-0003-1489-9494
Theresa Dornieden https://orcid.org/0000-0003-0911-4568
Paul Viktor Ritschl https://orcid.org/0000-0003-4610-1766
Susanne Ebner https://orcid.org/0000-0002-0394-9620
Efstathios Gregorios Stamatiades https://orcid.org/0000-0002-2785-9005
Roman David Bülow https://orcid.org/0000-0002-8527-7353
Peter Boor https://orcid.org/0000-0001-9921-4284
Katja Kotsch https://orcid.org/0000-0002-3803-0964

REFERENCES

1. Tonelli M, Riella M. Chronic kidney disease and the ageing population. *Nephron Clin Pract*. 2014;128:319-322. doi:10.1159/000362458
2. Liu P, Quinn RR, Lam NN, et al. Progression and regression of chronic kidney disease by age among adults in a population-based cohort in Alberta, Canada. *JAMA Netw Open*. 2021;4:e2112828. doi:10.1001/jamanetworkopen.2021.12828
3. Heylen L, Thienpont B, Busschaert P, et al. Age-related changes in DNA methylation affect renal histology and post-transplant fibrosis. *Kidney Int*. 2019;96:1195-1204. doi:10.1016/j.kint.2019.06.018
4. Favi E, Puliatti C, Iesari S, Monaco A, Ferraresso M, Cacciola R. Impact of donor age on clinical outcomes of primary single kidney transplantation from Maastricht category-III donors after

circulatory death. *Transplant Direct*. 2018;4:e396. doi:10.1097/TXD.0000000000000835
5. Summers DM, Johnson RJ, Hudson A, Collett D, Watson CJ, Bradley JA. Effect of donor age and cold storage time on outcome in recipients of kidneys donated after circulatory death in the UK: a cohort study. *Lancet*. 2013;381:727-734. doi:10.1016/S0140-6736(12)61685-7
6. Martin JE, Sheaff MT. Renal ageing. *J Pathol*. 2007;211:198-205. doi:10.1002/path.2111
7. Tan JC, Busque S, Workeneh B, et al. Effects of aging on glomerular function and number in living kidney donors. *Kidney Int*. 2010;78:686-692. doi:10.1038/ki.2010.128
8. Denic A, Glassock RJ, Rule AD. Structural and functional changes with the aging kidney. *Adv Chronic Kidney Dis*. 2016;23:19-28. doi:10.1053/j.ackd.2015.08.004
9. Tan JC, Workeneh B, Busque S, Blouch K, Derby G, Myers BD. Glomerular function, structure, and number in renal allografts from older deceased donors. *J Am Soc Nephrol*. 2009;20:181-188. doi:10.1681/ASN.2008030306
10. O'Sullivan ED, Hughes J, Ferenbach DA. Renal aging: causes and consequences. *J Am Soc Nephrol*. 2017;28:407-420. doi:10.1681/ASN.2015121308
11. Docherty MH, O'Sullivan ED, Bonventre JV, Ferenbach DA. Cellular senescence in the kidney. *J Am Soc Nephrol*. 2019;30:726-736. doi:10.1681/ASN.2018121251
12. Wiggins JE, Goyal M, Sanden SK, et al. Podocyte hypertrophy, "adaptation," and "decompensation" associated with glomerular enlargement and glomerulosclerosis in the aging rat: prevention by calorie restriction. *J Am Soc Nephrol*. 2005;16:2953-2966. doi:10.1681/ASN.2005050488
13. Schroth J, Thiemermann C, Henson SM. Senescence and the aging immune system as major drivers of chronic kidney disease. *Front Cell Dev Biol*. 2020;8:564461. doi:10.3389/fcell.2020.564461
14. Zhu Y, Armstrong JL, Tchkonia T, Kirkland JL. Cellular senescence and the senescent secretory phenotype in age-related chronic diseases. *Curr Opin Clin Nutr Metab Care*. 2014;17:324-328. doi:10.1097/MCO.0000000000000065
15. Sis B, Tasanarong A, Khoshjou F, Dadras F, Solez K, Halloran PF. Accelerated expression of senescence associated cell cycle inhibitor p16INK4A in kidneys with glomerular disease. *Kidney Int*. 2007;71:218-226. doi:10.1038/sj.ki.5002039
16. Schmitt R, Melk A. Molecular mechanisms of renal aging. *Kidney Int*. 2017;92:569-579. doi:10.1016/j.kint.2017.02.036
17. Kirkland JL, Tchkonia T. Senolytic drugs: from discovery to translation. *J Intern Med*. 2020;288:518-536. doi:10.1111/joim.13141
18. Melk A, Schmidt BM, Vongwiwatana A, Rayner DC, Halloran PF. Increased expression of senescence-associated cell cycle inhibitor p16INK4a in deteriorating renal transplants and diseased native kidney. *Am J Transplant*. 2005;5:1375-1382. doi:10.1111/j.1600-6143.2005.00846.x
19. Reutzel-Selke A, Jurisch A, Denecke C, et al. Donor age intensifies the early immune response after transplantation. *Kidney Int*. 2007;71:629-636. doi:10.1038/sj.ki.5002098
20. Carrasco E, Gómez de Las Heras MM, Gabandé-Rodríguez E, Desdín-Micó G, Aranda JF, Mittelbrunn M. The role of T cells in age-related diseases. *Nat Rev Immunol*. 2021;22:97-111. doi:10.1038/s41577-021-00557-4
21. Stavropoulou E, Kantartzi K, Tsigalou C, et al. Microbiome, Immunosenescence, and Chronic Kidney Disease. *Front Med (Lausanne)*. 2021;8:661203. doi:10.3389/fmed.2021.661203
22. Dornieden T, Sattler A, Pascual-Reguant A, et al. Signatures and specificity of tissue-resident lymphocytes identified in human renal peri-tumor and tumor tissue. *J Am Soc Nephrol*. 2021;32:2223-2241. doi:10.1681/ASN.2020101528
23. Ashraf MI, Sarwar A, Kühl AA, et al. Natural killer cells promote kidney graft rejection independently of cyclosporine A therapy. *Front Immunol*. 2019;10:2279. doi:10.3389/fimmu.2019.02279
24. Resch T, Ashraf MI, Ritschl PV, et al. Disturbances in iron homeostasis result in accelerated rejection after experimental heart transplantation. *J Heart Lung Transplant*. 2017;36:732-743. doi:10.1016/j.healun.2017.03.004
25. Dumas SJ, Meta E, Conchinha NV, et al. Protocols for endothelial cell isolation from mouse tissues: kidney, spleen, and testis. *STAR Protoc*. 2021;28:100523. doi:10.1016/j.xpro.2021.100523
26. Ritschl PV, Ashraf MI, Oberhuber R, et al. Donor brain death leads to differential immune activation in solid organs but does not accelerate ischaemia-reperfusion injury. *J Pathol*. 2016;239:84-96. doi:10.1002/path.4704
27. Buhl EM, Djudjaj S, Klinkhammer BM, et al. Dysregulated mesenchymal PDGFR-beta drives kidney fibrosis. *EMBO Mol Med*. 2020;12:e11021. doi:10.15252/emmm.201911021
28. Stamatiades EG, Tremblay ME, Bohm M, et al. Immune monitoring of trans-endothelial transport by kidney-resident macrophages. *Cell*. 2016;166:991-1003. doi:10.1016/j.cell.2016.06.058
29. Günther J, Resch T, Hackl H, et al. Identification of the activating cytotoxicity receptor NKG2D as a senescence marker in zero-hour kidney biopsies is indicative for clinical outcome. *Kidney Int*. 2017;91:1447-1463. doi:10.1016/j.kint.2016.12.018
30. Stegmann KA, Robertson F, Hansi N, et al. CXCR6 marks a novel subset of T-bet(lo)Eomes(hi) natural killer cells residing in human liver. *Sci Rep*. 2016;6:26157. doi:10.1038/srep26157
31. Chiossone L, Chaix J, Fuseri N, Roth C, Vivier E, Walzer T. Maturation of mouse NK cells is a 4-stage developmental program. *Blood*. 2009;113:5488-5496. doi:10.1182/blood-2008-10-187179
32. Chang J, Wang Y, Shao L, et al. Clearance of senescent cells by ABT263 rejuvenates aged hematopoietic stem cells in mice. *Nat Med*. 2016;22:78-83. doi:10.1038/nm.4010
33. Mohamad Anuar NN, Nor Hisam NS, Liew SL, Ugusman A. Clinical review: navitoclax as a pro-apoptotic and anti-fibrotic agent. *Front Pharmacol*. 2020;11:564108. doi:10.3389/fphar.2020.564108
34. Mylonss KJ, O'Sullivan ED, Humphries D, et al. Cellular senescence inhibits renal regeneration after injury in mice, with senolytic treatment promoting repair. *Sci Transl Med*. 2021;13:eabb0203. doi:10.1126/scitranslmed.abb0203
35. Clements ME, Chaber CJ, Ledbetter SR, Zuk A. Increased cellular senescence and vascular rarefaction exacerbate the progression of kidney fibrosis in aged mice following transient ischemic injury. *PLoS One*. 2013;8:e70464. doi:10.1371/journal.pone.0070464
36. Vanholder R, Domínguez-Gil B, Busic M, et al. Organ donation and transplantation: a multi-stakeholder call to action. *Nat Rev Nephrol*. 2021;17:554-568. doi:10.1038/s41581-021-00425-3
37. Dreyer GJ, Hemke AC, Reinders ME, de Fijter JW. Transplanting the elderly: balancing aging with histocompatibility. *Transplant Rev (Orlando)*. 2015;29:205-211. doi:10.1016/j.trre.2015.08.003
38. Rodwell GE, Sonu R, Zahn JM, Lund J, Wilhelmy J, Wang L, et al. A transcriptional profile of aging in the human kidney. *PLoS Biol* 2: e427, 2004. 10.1371/journal.pbio.0020427
39. Rowland J, Akbarov A, Eales J, et al. Uncovering genetic mechanisms of kidney aging through transcriptomics, genomics, and epigenomics. *Kidney Int*. 2019;95:624-635. doi:10.1016/j.kint.2018.10.029
40. Epping MT, Meijer LA, Krijgsman O, Bos JL, Pandolfi PP, Bernards R. TSPYL5 suppresses p53 levels and function by physical interaction with USP7. *Nat Cell Biol*. 2011;13:102-108. doi:10.1038/ncb2142
41. Kalathookunnel Antony A, Lian Z, Wu H. T cells in adipose tissue in aging. *Front Immunol*. 2018;9:2945. doi:10.3389/fimmu.2018.02945
42. Li M, Yao D, Zeng X, et al. Age related human T cell subset evolution and senescence. *Immun Ageing*. 2019;16:24. doi:10.1186/s12979-019-0165-8

43. Yang X, Wang X, Lei L, et al. Age-related gene alteration in naïve and memory t cells using precise age-tracking model. *Front Cell Dev Biol*. 2021;8:624380. doi:10.3389/fcell.2020.624380
44. Chidrawar SM, Khan N, Chan YL, Nayak L, Moss PA. Ageing is associated with a decline in peripheral blood CD56bright NK cells. *Immun Ageing*. 2006;3:10. doi:10.1186/1742-4933-3-10
45. Gounder SS, Abdullah BJJ, Radzuanb NEIBM, et al. Effect of aging on NK cell population and their proliferation at ex vivo culture condition. *Anal Cell Pathol (Amst)*. 2018;2018:7871814. doi:10.1155/2018/7871814
46. Hazeldine J, Hampson P, Lord JM. Reduced release and binding of perforin at the immunological synapse underlies the age-related decline in natural killer cell cytotoxicity. *Aging Cell*. 2012;11:751-759. doi:10.1111/j.1474-9726.2012.00839.x
47. Lutz CT, Moore MB, Bradley S, Shelton BJ, Lutgendorf SK. Reciprocal age related change in natural killer cell receptors for MHC class I. *Mech Ageing Dev*. 2005;126:722-731. doi:10.1016/j.mad.2005.01.004
48. Paust S, Gill HS, Wang BZ, et al. Critical role for the chemokine receptor CXCR6 in NK cell-mediated antigen-specific memory of haptens and viruses. *Nat Immunol*. 2010;11:1127-1135. doi:10.1038/ni.1953
49. Hydes T, Noll A, Salinas-Riester G, et al. IL-12 and IL-15 induce the expression of CXCR6 and CD49a on peripheral natural killer cells. *Immun Inflamm Dis*. 2018;6:34-46. doi:10.1002/iid3.190
50. Zhang ZX, Huang X, Jiang J, et al. Natural killer cells mediate long-term kidney allograft injury. *Transplantation*. 2015;99(5):916-924. doi:10.1097/TP.0000000000000665
51. Kohei N, Tanaka T, Tanabe K, et al. Natural killer cells play a critical role in mediating inflammation and graft failure during antibody-mediated rejection of kidney allografts. *Kidney Int*. 2016;89(6):1293-1306. doi:10.1016/j.kint.2016.02.030
52. Yagisawa T, Tanaka T, Miyairi S, et al. In the absence of natural killer cell activation donor-specific antibody mediates chronic, but not acute, kidney allograft rejection. *Kidney Int*. 2019;95(2):350-362. doi:10.1016/j.kint.2018.08.041
53. Kildey K, Francis RS, Hultin S, et al. Specialized roles of human natural killer cell subsets in kidney transplant rejection. *Front Immunol*. 2019;10:1877. doi:10.3389/fimmu.2019.01877
54. Iske J, Seyda M, Heinbokel T, et al. Senolytics prevent mt-DNA-induced inflammation and promote the survival of aged organs following transplantation. *Nat Commun*. 2020;11(1):4289. doi:10.1038/s41467-020-18039-x
55. Abou-Daya KI, Tieu R, Zhao D, et al. Resident memory T cells form during persistent antigen exposure leading to allograft rejection. *Sci Immunol*. 2021;6(57):eabc8122. doi:10.1126/sciimmunol.abc8122
56. Xu M, Pirtskhalava T, Farr JN, et al. Senolytics improve physical function and increase lifespan in old age. *Nat Med*. 2018;24(8):1246-1256. doi:10.1038/s41591-018-0092-9
57. Palmer AK, Xu M, Zhu Y, et al. Targeting senescent cells alleviates obesity-induced metabolic dysfunction. *Aging Cell*. 2019;18(3):e12950. doi:10.1111/acel.12950
58. Lewis-McDougall FC, Ruchaya PJ, Domenjo-Vila E, et al. Aged-senescent cells contribute to impaired heart regeneration. *Aging Cell*. 2019;18(3):e12931. doi:10.1111/acel.12931
59. Hernandez-Segura A, de Jong TV, Melov S, Guryev V, Campisi J, Demaria M. Unmasking transcriptional heterogeneity in senescent cells. *Curr Biol*. 2017;27(17):2652-2660.e4. doi:10.1016/j.cub.2017.07.033
60. Hall BM, Balan V, Gleiberman AS, et al. p16(Ink4a) and senescence-associated beta-galactosidase can be induced in macrophages as part of a reversible response to physiological stimuli. *Aging (Albany NY)*. 2017;9(8):1867-1884. doi:10.18632/aging.101268
61. Zhu Y, Tchkonia T, Pirtskhalava T, et al. The Achilles' heel of senescent cells: from transcriptome to senolytic drugs. *Aging Cell*. 2015;14(4):644-658. doi:10.1111/acel.12344
62. Kim SR, Puranik AS, Jiang K, et al. Progressive cellular senescence mediates renal dysfunction in ischemic nephropathy. *J Am Soc Nephrol*. 2021;32(8):1987-2004. doi:10.1681/ASN.2020091373
63. Hickson LJ, Langhi Prata LGP, Bobart SA, Evans TK, Giorgadze N, Hashmi SK, et al.: Senolytics decrease senescent cells in humans: preliminary report from a clinical trial of Dasatinib plus Quercetin in individuals with diabetic kidney disease. *EBioMedicine*. 2020;52:102-595. doi: 10.1016/j.ebiom.2019.12.004 EBioMedicine 47:446-456, 2019 doi: 10.1016/j.ebiom.2019.08.069.

SUPPORTING INFORMATION

Additional supporting information can be found online in the Supporting Information section at the end of this article.

How to cite this article: He A, Sarwar A, Thole LML, et al. Renal inflamm-aging provokes intra-graft inflammation following experimental kidney transplantation. *Am J Transplant*. 2022;00:1-19. doi:10.1111/ajt.17154

ESOT | Transplant International

BRIEF RESEARCH REPORT
published: 04 August 2022
doi: 10.3389/ti.2022.10677

SARS-CoV2 mRNA Vaccine-Specific B-, T- and Humoral Responses in Adolescents After Kidney Transplantation

Arne Sattler[1]†, Julia Thumfart[2†], Laura Tóth[1], Eva Schrezenmeier[3,4,5], Vanessa Proß[1], Carolin Stahl[1], Janine Siegle[1], An He[1], Linda Marie Laura Thole[1], Carolin Ludwig[8,9], Henriette Straub-Hohenbleicher[3], Frank Friedersdorff[6,7], Bernd Jahrsdörfer[8,9], Hubert Schrezenmeier[8,9], Philip Bufler[2] and Katja Kotsch[1]**

[1]Department of General and Visceral Surgery, Charite-Universitätsmedizin Berlin, Corporate Member of Freie Universität Berlin and Humboldt-Universität zu Berlin, Berlin, Germany, [2]Department of Pediatric Gastroenterology, Nephrology and Metabolic Diseases, Charité-Universitätsmedizin Berlin, Corporate Member of Freie Universität Berlin and Humboldt-Universität zu Berlin, Berlin, Germany, [3]Department of Nephrology and Medical Intensive Care, Charité-Universitätsmedizin Berlin, Corporate Member of Freie Universität Berlin and Humboldt-Universität zu Berlin, Berlin, Germany, [4]Department of Rheumatology and Clinical Immunology, Charité-Universitätsmedizin Berlin, Corporate Member of Freie Universität Berlin and Humboldt-Universität zu Berlin, Berlin, Germany, [5]Berlin Institute of Health at Charité-Universitätsmedizin Berlin, BIH Academy, Clinician Scientist Program Universitätsmedizin Berlin, Berlin, Germany, [6]Department of Urology, Evangelisches Krankenhaus Königin Elisabeth Herzberge, Berlin, Germany, [7]Department of Urology, Charite-Universitätsmedizin Berlin, Corporate Member of Freie Universität Berlin and Humboldt-Universität zu Berlin, Berlin, Germany, [8]Institute of Transfusion Medicine, Ulm University, Ulm, Germany, [9]Institute for Clinical Transfusion Medicine and Immunogenetics, German Red Cross Blood Transfusion Service Baden-Württemberg—Hessen and University Hospital Ulm, Ulm, Germany

OPEN ACCESS

***Correspondence:**
Arne Sattler
arne.sattler@charite.de
Katja Kotsch
katja.kotsch@charite.de

[†]These authors have contributed equally to this work

Received: 27 May 2022
Accepted: 11 July 2022
Published: 04 August 2022

Citation:
Sattler A, Thumfart J, Tóth L, Schrezenmeier E, Proß V, Stahl C, Siegle J, He A, Thole LML, Ludwig C, Straub-Hohenbleicher H, Friedersdorff F, Jahrsdörfer B, Schrezenmeier H, Bufler P and Kotsch K (2022) SARS-CoV2 mRNA Vaccine-Specific B-, T- and Humoral Responses in Adolescents After Kidney Transplantation. Transpl Int 35:10677. doi: 10.3389/ti.2022.10677

Protection of adult kidney transplant recipients against SARS-CoV2 was shown to be strongly impaired owing to low reactogenicity of available vaccines. So far, data on vaccination outcomes in adolescents are scarce due to later vaccination approval for this age group. We therefore comprehensively analyzed vaccination-specific humoral-, T- and B-cell responses in kidney transplanted adolescents aged 12–18 years in comparison to healthy controls 6 weeks after standard two-dose BNT162b2 ("Comirnaty"; Pfizer/BioNTech) vaccination. Importantly, 90% (18/20) of transplanted adolescents showed IgG seroconversion with 75% (15/20) developing neutralizing titers. Still, both features were significantly diminished in magnitude compared to controls. Correspondingly, spike-specific B cells were quantitatively reduced and enriched for non-isotype-class-switched IgD^+27^+ memory cells in patients. Whereas spike specific $CD4^+$ T cell frequencies were similar in both groups, cytokine production and memory differentiation were significantly impaired in transplant recipients. Although our data identify limitations in all arms of vaccine-specific immunity, the majority of our adolescent patients showed robust humoral responses despite antimetabolite-based treatment being associated with poor vaccination outcomes in adults.

Keywords: kidney transplantation, vaccination, immunity, SARS-CoV2, adolescents

Abbreviations: ARPKD, autosomal recessive polycystic kidney disease; CAKUT, congenital anomalies of kidney and urinary tract; CS, corticosteroids; Eve, everolimus; HC, healthy control(s); IS, immunosuppression; KTx, kidney transplantation; KTR, kidney transplant recipients; MPA, mycophenolic Acid; NS, nephrotic syndrome; PBMC, peripheral blood mononuclear cells; RBD, receptor binding domain; Rapa, rapamycin; Tac, tacrolimus.

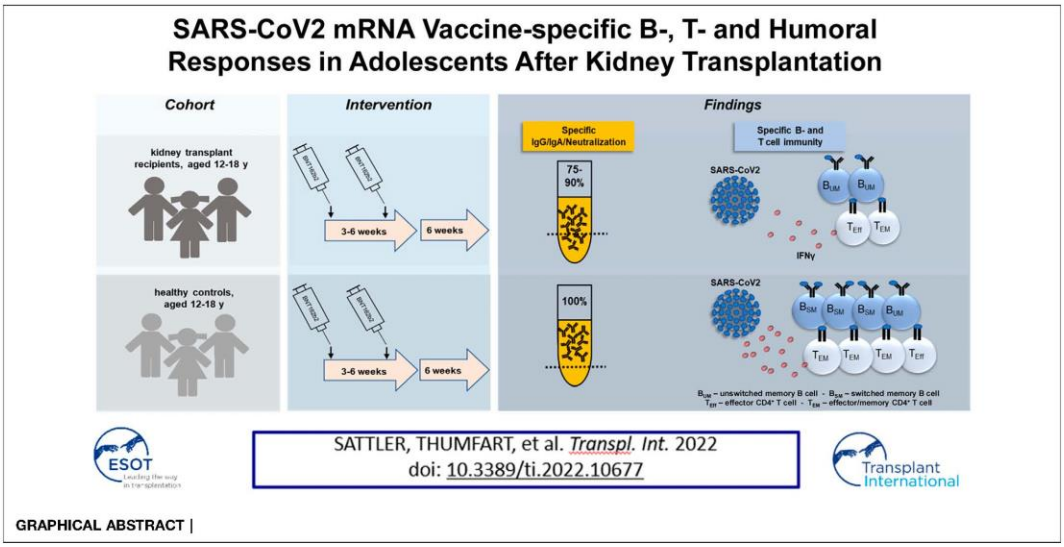

GRAPHICAL ABSTRACT |

INTRODUCTION

Children and adolescents frequently experience asymptomatic SARS-CoV-2 infections or exhibit mild respiratory symptoms with fever, headache, and cough. Nevertheless, both groups can suffer from severe COVID-19 with respiratory failure or pediatric inflammatory multisystem syndrome (1). Children on renal replacement therapy or after kidney transplantation (KTx) have an increased risk for hospitalization after infection (2). Even if mortality is low, pediatric COVID-19 can seriously burden health care systems in times of pandemic, as treatment resources may become scarce. It should also be noted that parents are particularly concerned about the health of their chronically ill children, resulting in higher rates of homeschooling, with adverse consequences for social interaction with peers (3). Vaccination against SARS-CoV-2, being recommended by the World health organization for children and adolescents with underlying chronic diseases (4), is therefore key for protection of pediatric at-risk groups. However, many studies (5–7) revealed that adult solid organ recipients show a broad impairment in CoV2-vaccination-induced immunity, affecting both humoral and cellular responses, likely due to mycophenolate (MPA)-based immunosuppression (IS) (8). To provide comprehensive data on mRNA vaccine induced responses in kidney transplant recipients (KTR) aged 12–18 years, we conducted an observational study after approval for this age group where vaccine-specific IgG, IgA and virus neutralizing capacity was assessed in concert with comprehensive quantification and functional characterization of spike protein-specific B- and T cells. Our results suggest that the majority of pediatric patients, despite being on antimetabolite treatment, mount robust vaccine-specific humoral responses, with selective impairments in various adaptive immune compartments.

MATERIALS AND METHODS

Study Design and Medication

For this observational study, adolescent KTx patients were recruited at the Charité Department of Pediatric Gastroenterology, Nephrology and Metabolic Diseases. As per medical center guideline, patients had initially received triple IS therapy consisting of corticosteroids (CS), Tac and MPA immediately after KTx. Except for patient 1 (**Table 2**), none of the patients had received induction therapy. After the first year, CS had been discontinued according to the standard protocol of the center. Healthy controls included age- and sex-matched individuals without any documented acute or chronic disease conditions (**Table 1**). They were routinely vaccinated according to the national vaccination program. The inclusion criteria for the study groups were age between 12 and 18 years, absence of previous SARS-CoV2 or other severe infections prior to vaccination and completion of the 2-dose vaccination protocol with BNT162b2 vaccine (Comirnaty; BioNTech/Pfizer) according to the manufacturer's recommended dose (30 μg) and time schedule (two doses at a 3–6 weeks interval). All patients received the 2nd dose between June and October 2021. Blood and serum samples were collected approximately 6 weeks after the second dose with no significant differences between groups. IS trough levels (**Table 2**) were analyzed at the same time point. The study was approved by the local ethical committee of the Charité Universitätsmedizin (EA2/227/21). All

TABLE 1 | Basic characteristics of KTx patients and healthy controls.

Variable	KTx (n =20)	HC (n = 13)	p value
Age (mean yrs ±SD)	14.17 (1.31)	13.99 (1.99)	0.7595
Females (n, %)	7 (35.00)	5 (38.46)	>0.9999
Caucasians (n, %)	16 (80.00)	12 (92.00)	0.6253
Time since 2nd vaccination dose (mean days±SD)	39.30 (11.06)	44.54 (16.87)	0.2306

(K)Tx, (Kidney) Transplantation; HC, healthy control.

TABLE 2 | Detailed characteristics of KTx patients.

Patient	Gender	Underlying disease	Age (years)	Time since KTx (years)	Current IS[b]	Tac trough level (µg/l)[b]	MPA trough level (mg/l)[§]	Former rejection episodes (date)
1[a]	F	unknown	17.5	0.9	Tac, MMF, CS	5.1	3.3	Yes (2021/2, 2021/3)
2	F	CAKUT	13.1	9.2	Tac, MMF	2.7	8.3	No
3	M	CAKUT	12.6	9.6	Tac, MMF	3.3	0.9	No
4	M	CAKUT	12.5	10.0	Tac, MMF	3.3	1.3	No
5	M	CAKUT	13.2	7.1	Tac, MMF	3.3	2.1	No
6	M	ARPKD	12.8	1.8	Tac, MMF	4.8	1.8	No
7	M	CAKUT	14.9	13.2	Tac, MMF	4.2	3.5	No
8	M	CAKUT	15.0	8.3	Tac, MMF	3.6	0.8	No
9	F	NS	14.6	10.2	Tac, MMF	5	2.5	No
10	F	NS	15.1	10.2	Tac, CS	3.3	n.a	No
11	F	NS	14.1	2.6	Tac, Eve	5.7	n.a	Yes (2019/4)
12	M	HNF1 Beta	14.9	2.1	Tac, MMF	4.7	1.2	No
13	M	NS	16.1	10.6	Tac, CS	4.9	n.a	No
14	F	Papillorenal syndrome	13.1	1.0	Tac, MMF	3.6	4.3	No
15	M	NS	15.3	7.4	Rapa, MMF, CS		4.5	No
16	M	Sartan nephropathy	14.2	10.5	Tac, CS	2.8	n.a	No
17	M	CAKUT	14.0	11.7	Tac, MMF	4.1	0.4	Yes (2012/10)
18	F	NS	14.3	9.2	Tac, MMF, CS	5.7	1.7	Yes (2014/9, 2014/12)
19	M	Cystinosis	12.6	2.1	Tac, Eve	1.8	n.a	No
20	M	CAKUT	13.4	3.3	Tac, MMF	3.7	1.8	No
Mean ± SD			14.2 ± 1.3	7.0 ± 4.1		4.0 ± 1.1	1.8 ± 2.0	

(K)Tx, (Kidney) Transplantation; IS, immunosuppression; Tac-Tacrolimus; MPA-Mycophenolic Acid; CS-Corticosteroids; Eve-Everolimus; Rapa-Rapamycin; CAKUT, congenital anomalies of kidney and urinary tract; NS, nephrotic syndrome; ARPKD-Autosomal recessive polycystic kidney disease; SD, standard deviation; n.a., not applicable.

[a]*Patient 1 had received her 2nd transplant with induction therapy (basiliximab).*

[b]*At time of humoral and cellular analysis.*

individuals (over 14 years) and their legal guardians signed informed consent.

Assessment of Humoral Immunity

Previous or current SARS-CoV2 infection was excluded based on medical history data available from our clinic, continuous negative point of care antigen tests conducted thrice-weekly during school visits and a negative SARS-CoV2 nucleoprotein specific ELISA (Euroimmun) (**Supplementary Figure S1A**). SARS-CoV-2 S1 domain specific IgG (QuantiVac, Euroimmun) and IgA (Euroimmun) was determined by ELISA. For IgA quantification, serum samples exceeding O.D. ratios of 6 were pre-diluted tenfold and re-measured. Serum samples with OD ratios of ≥1.1 (Nucleoprotein and IgA) or ≥35.2 BAU/ml (IgG) were considered positive according to the manufacturer´s guidelines. OD ratios were calculated based on the ratio of the OD of the respective sample over the OD of the calibrator provided with the ELISA kit. For quantification of virus neutralizing capacity in our study, a blocking ELISA (sVNT kit, GenScript) was used that mimics the virus neutralization process. In detail, serum antibodies are tested for blocking the binding of recombinant SARS-CoV2 RBD (alpha = vaccine variant) to human ACE2 receptor protein. A neutralization capacity of more than 30% was defined as positive as per the manufacturer's recommendation.

Assessment of SARS-CoV2 Vaccine-Specific B and T Cells

Peripheral blood mononuclear cells (PBMCs) were isolated from EDTA blood by density gradient centrifugation using Ficoll-Paque PLUS (GE Healthcare Bio-Sciences, Chicago, IL, United States). Within 5–10 × 10^6 PBMC, B cells were detected by flow cytometry and gated as $CD19^+CD3^-CD14^-CD56^-$

among single live lymphocytes (gating strategy depicted in **Supplementary Figure S1B**). SARS-CoV2-specific B cells were identified as shown before (8, 9) by double staining with AlexaFluor488 coupled recombinant receptor binding domain (RBD) protein and biotinylated recombinant full spike protein (both alpha-variant, RnD Systems, Minneapolis, MN, United States) with the latter being detected by streptavidin-APC (Biolegend, San Diego, CA, United States). For flow cytometric analysis, the following fluorochrome-labeled antibodies were used: CD19 (SJ25C1, BL), CD3 (SK7, BL), CD56 (NCAM, BL), CD14 (M5E2, BL), IgD (IA6-2, BL), IgG (G18-145, BD) and CD27 (M-T271, BL). For identification of vaccine-specific T cells, 3×10^6 PBMC were stimulated or not for 16 h with overlapping 15-mers covering the complete SARS-CoV2 spike (alpha-variant) protein. A combination of overlapping 15-mer peptide mixes including cytomegalovirus (CMV, "Peptivator pp65," Miltenyi Biotech, Bergisch Gladbach), Epstein Barr virus (EBV, "Peptivator consensus", Miltenyi Biotech) and influenza H1N1 ("Peptivator matrix protein 1," and "Peptivator nucleoprotein," Miltenyi Biotech) served as control and is termed CEF throughout. Antigens were used at a final concentration of 0.5 µg/ml per peptide. Specific $CD4^+$ T helper cells were identified based on CD137 and CD154 coexpression as shown in **Supplementary Figure S2**. A response was defined as positive when stimulated cultures contained at least twofold higher frequencies of $CD137^+CD154^+$ cells as compared to the respective unstimulated control with at least twenty events, as resported earlier (5). For surface labelling, antibodies against CD3 (SK7, Biolegend), CD4 (SK3, BD), CD8 (SK1, Ebioscience, San Diego, CA, United States), CD45RO (UCHL1, BL), CD62L (DREG-56, BL) and PD1 (EH12.1, BD) were used. A dump channel excluded unwanted cells and contained $CD14^+$ (M5E2, BL), $CD19^+$ (HIB19, BL), and dead (fixable live/dead, BL) events. Cells were fixed with FACS Lysing Solution (BD) after surface staining, followed by permeabilization in FACS Perm II Solution (BD) and stained intracellularly with anti-CD154 (24–31, BL), anti-CD137 (4B4-1, BL), anti-TNF-α (MAb11, BL), anti-IFN-γ (4SB3, Ebioscience), anti-IL-2 (MQ1-17H12, BL), and anti-IL-4 (MP4-25D2, BL). Data was acquired using a BD FACS Fortessa X20.

Data Analysis and Statistics

FACS data analysis was conducted with FlowJo 10 (BD). Gating strategies for analysis of antigen-reactive B- and T cells are illustrated in **Supplementary Figures S1, S2**. Depicted frequencies of spike-specific $CD4^+$ T cells were background (=unstimulated control) -substracted. Co-expression of cytokines was quantified by Boolean gating in Flowjo. Statistical analysis and graph preparation was performed in GraphPad Prism 8 (GraphPad, La Jolla, CA, United States). Data distribution was assessed using the Kolmogorov-Smirnov test. Given that all data sets did not show normal distribution, a Mann-Whitney test was used throughout for two-group comparisons. For analysis of contingency tables, Fisher's exact test was applied.

RESULTS

Patient Characteristics

Twelve patients received dual IS therapy with Tac and MPA according to the standard protocol of the center after the first year after KTx. Two patients received triple IS therapy (Tac, MPA and CS) due to former rejection episodes. Three patients received Tac and CS due to side effects of MPA. Two patients were treated with Everolimus and Tac because of ongoing Epstein-Barr- and polyoma virus BK viremia. One patient received triple IS (Rapamycin, MPA and corticosteroids) due to calcineurin inhibitor toxicity. Mean trough levels were 4.0 ± 1.1 for Tac and 1.8 ± 2.0 for MPA at the time point of immunity analysis (**Table 2**); no changes in medication were undertaken from 2 months before vaccination until time point of humoral and cellular analyses. Last rejection episodes with methylprednisolone treatment were at least 4 months before first vaccination. After vaccination, no rejection episodes were observed in the KTx cohort. No other adjunctive immunosuppressive drugs were taken within the last 6 months prior to analysis. As per inclusion criteria, all patients and controls were virus-naïve at the timepoint of analyses and none of the individuals became SARS-CoV2-positive until the end of the study (12/2021).

Characterization of SARS-CoV2-Vaccination-Specific Humoral and B Cell Immunity

Humoral BNT162b2-vaccination-specific immunity above threshold was detected in all healthy individuals and in 90% (18/20) of KTR for IgG, 85% (17/20) for IgA and in 75% (15/20) with respect to neutralizing capacity. Two of three patients receiving triple IS therapy showed no or low IgG and neutralizing antibody levels. One of the two patients under Everolimus treatment showed low IgG and no neutralizing antibody titers whereas both did not develop IgA responses. Overall, KTx patients showed significantly reduced spike-specific IgG, IgA- and neutralization capacity levels as compared to controls (**Figure 1A**). Employing a robust FACS-based assay (9), transplant recipients were further characterized by significantly reduced frequencies of spike protein receptor binding domain (RBD)-specific B cells (**Figure 1B**, left) that were approximately ten-fold higher in humoral responders as compared to non-responders (**Figure 1B**, right). Antigen-specific B cells in patients contained reduced portions of isotype class switched IgD^-CD27^+ memory-type cells (**Figure 1C**, left), being in line with diminished frequencies of specific IgG^+ cells (**Figure 1C**, right). An exemplary gating strategy for B cell characterization is depicted in **Supplementary Figure S1**.

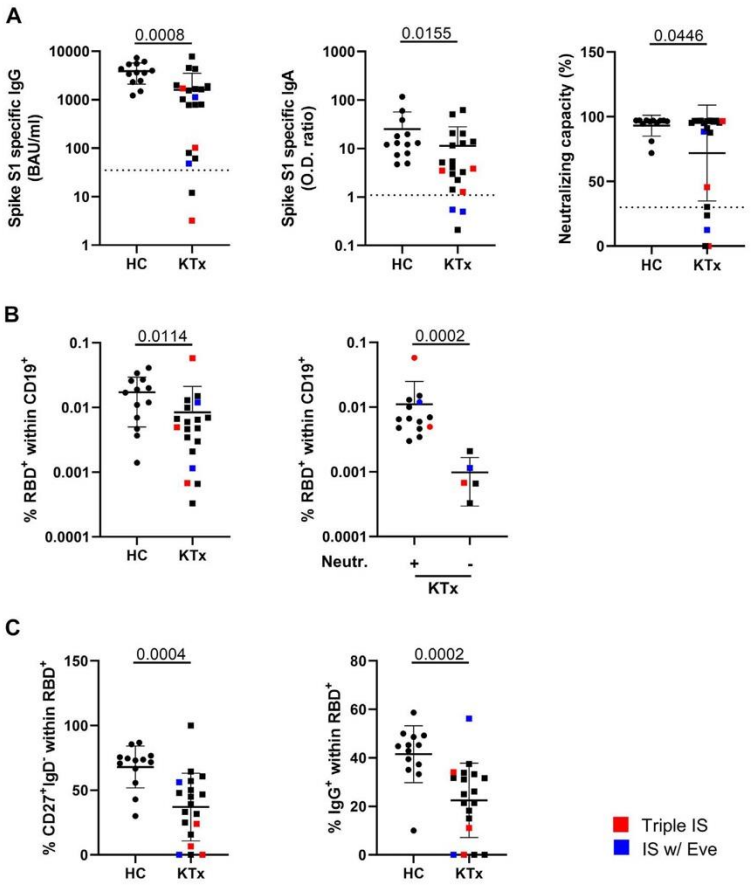

FIGURE 1 | Humoral immune responses and vaccination-specific B cell immunity. **(A)** Humoral vaccine-specific immune responses were assessed for anti-spike protein S1 domain specific IgG, IgA and virus neutralization capacity in healthy controls (HC) and KTx patients around 6 weeks after administration of the second standard BNT162b2 dose. Thresholds defining a positive response are indicated by dotted lines. **(B)** Relative frequencies of RBD-specific CD19$^+$ B cells identified by FACS in HC vs KTx (left) and in KTx that were stratified according to responders (+) and non-responders (–) regarding neutralizing capacity above threshold (right). **(C)** Memory-type of spike-RBD-specific B-cells according to IgD and CD27 expression (left) and portions of class-switched IgG$^+$ cells (right). In all analyses, $n = 20$ KTx and $n = 13$ HC were enrolled. Mann-Whitney test was applied throughout based on non-normal distribution of values. Graphs show means ± SD. Patients receiving triple immunosuppressive (IS) therapy are depicted in red, those under Everolimus-containing IS in blue.

Quantitative and Qualitative Features of Vaccination-Specific CD4$^+$ T Cells

Vaccination-specific SARS-CoV2 spike protein- and CEF control antigen-reactive CD4$^+$ T cells were identified based on CD154 and CD137 coexpression after peptide mix stimulation with the gating strategy illustrated in **Supplementary Figure S2**. We detected spike-specific CD4$^+$ T cells in all individuals included in the study (**Figure 2A**, left) with frequencies being similar in patients and controls (**Figure 2A**, right). However, KTx patients were characterized by significantly reduced portions of IFNγ$^+$-, but not TNFα$^+$, IL-2$^+$ or IL-4$^+$ T cells (**Figure 2B**). Furthermore, antigen-reactive polyfunctional T cells co-expressing IFNγ, TNFα and IL-2 were less frequently detected in transplanted individuals, along with higher frequencies of cytokine non-producing cells (**Figure 2C**). IL-4 was excluded from polyfunctionality analyses due to comparably low frequencies of positive cells.

With respect to subset classification of antigen-specific cells, we found a significant increase of CD45RO$^-$CD62L$^-$ effector T cells in patients in concert with lower portions of CD45RO$^+$CD62L$^-$ effector/memory-type T cells (**Figure 2D**).

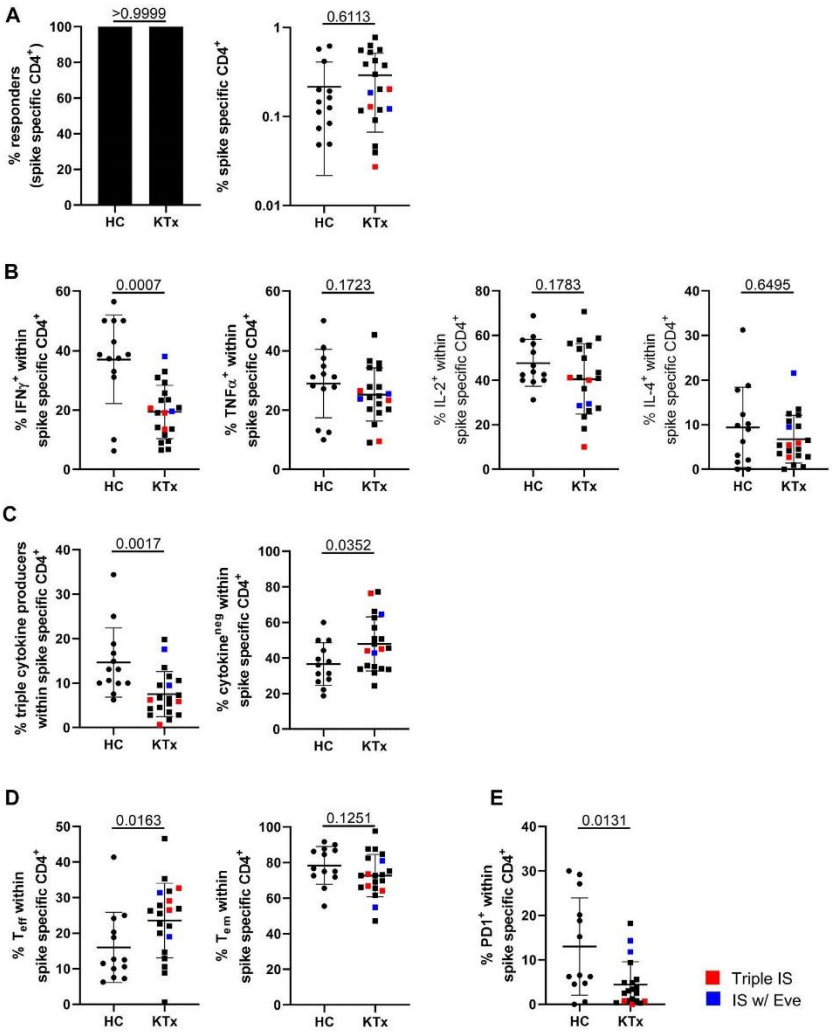

FIGURE 2 | Assessment of spike-specific T cell responses. PBMC were stimulated with spike peptide mix or left unstimulated. Specific $CD4^+$ T cells were detected by flow cytometry according to co-expression of CD154 and CD137. **(A)** Depicts responder rates (left) and portions of spike-specific $CD4^+$ T cells in HC vs. KTx after unstimulated control background substraction (right), **(B)** frequencies of cytokine producers as indicated within the antigen-specific population. **(C)** Quantifies $IFN\gamma^+TNF\alpha^+IL\text{-}2^-$ "triple+" polyfunctional (left) and cytokine-non-producing (right) cells. **(D)** Analysis of effector and effector/memory-type differentiation of antigen-specific $CD4^+$ T cells. **(E)** Portions of specific, recently *in vivo* activated PD-1^+ T cells. N in all experiments as in **Figure 1**. Mann-Whitney test was applied throughout based on non-normal distribution of values. Graphs show means ± SD. Patients receiving triple immunosuppressive therapy are depicted in red, those under Everolimus-containing IS in blue.

Furthermore, healthy donors showed significantly elevated portions of antigen-specific $PD1^+$ cells than KTx, reflecting recent *in vivo* activation (**Figure 2E**). Overall frequencies of antigen-specific T cells were within the lower range in one patient, and *in vivo* activated PD-1^+ cells were rarely found in all three patients under triple IS treatment. Of note, CEF control antigen mix specific $CD4^+$ T cell responses did not significantly differ between healthy controls and patients except for slightly reduced frequencies of IL-2^+ T cells in the latter (**Supplementary Figures S3A–E**).

DISCUSSION

A plethora of studies suggests that vaccination of adult KTx patients against SARS-CoV2 results in blunted antiviral immunity (6, 7), mirrored by the broad inability to develop neutralizing antibody titers in individuals receiving standard triple IS including antimetabolites (5, 9). So far, reactogenicity of mRNA vaccines in pediatric patients has only been examined for individuals with a mean age of 18 years and only with respect to IgG responses in the absence of matched healthy controls (10, 11). Importantly, our data presented herein demonstrate that 85–90% of our KTx patient cohort between 12 and 18 years of age developed IgA and IgG responses, respectively, while 75% reached neutralizing antibody titers. According to recent literature, the latter data based on sVNT assay measurement might potentially even underestimate neutralizing capacity as compared to the Plaque Reduction Neutralization Test (12).

Whereas these results are encouraging and suggest that high humoral responder rates can be achieved despite MPA treatment, our data at the same time reveal that all arms of adaptive immunity are compromised in young patients as compared to controls. This includes frequencies of spike-reactive B cells and their capacity to undergo class switching to IgG, a phenomenon already reported for adult cohorts (9) and likely resulting from Everolimus- (13) or MPA-based suppression of B cell differentiation and plasma blast formation (14, 15). In fact, we could recently show that short-term pausing of MPA during SARS-CoV2 re-vaccination enables previous non-responders to mount robust anti-viral immunity including expansion of antigen-specific B cells (8). The absence of antimetabolites also supported specific T cell proliferation and *ex vivo* activation, whereas cytokine production capacity was only marginally affected (8). Interestingly, pediatric KTx patients showed selective limitations within spike-specific T cells as compared to controls that mainly included memory differentiation, IFNγ production and polyfunctionality. Whereas the exact role of multifunctional T cells is not completely understood, they might contribute to a better protection given that quantities are elevated in individuals experiencing mild as compared to severe SARS-COV2 infections (16), a feature also observed in other infections such as tuberculosis (17).

With respect to cytokine production, adolescent KTx patients obviously show less impairment than their adult counterparts where production of all spike- induced, but not CEF-induced cytokines, was strongly blunted (5). As one limitation of our study, it remains to be determined whether these differences predominantly depend on patient age, as has been already discussed for HBV vaccination in transplant recipients (18) or arise from different treatment regimens, given that the default medication recommendation of adult transplant recipients comprises triple IS including corticosteroids, whereas 60% of our pediatric patients received dual IS with Tac and MPA. In support of the latter hypothesis, two of three adolescents under triple IS in our study showed no or low specific IgG levels; the same applied to frequencies of class-switched memory B-cells. Given the potential risk of rejection episodes, however, therapeutic modifications including MPA hold are probably not reasonable in pediatric KTx patients.

The main limitation of our study is the relatively small study cohort. However, due to ethical guidelines limiting blood donation volumes from young individuals for cellular assays and a high dissemination of CoV2-infection in this group (thereby preventing inclusion of more virus-naive individuals), studies on adolescents will likely remain comparably small. Additionally, the overall number of adolescent KTx patients is substantially lower and vaccine approval was delayed as compared to adults. These facts may explain the comparably small size of other pediatric studies (10, 11). Due to the completion of our study by the end of 2021, we were not able to include data after a third vaccination of our cohort that is meanwhile standard of care. Given that recent literature demonstrates a considerable impact of a booster immunization on IgG levels in adolescent transplant recipients (19), it will not only be important to examine all arms of immunity after a third dose to better understand differential vaccine-specific immunity of young vs adult KTx patients, but also include neutralization data on virus variants of concern that have emerged meanwhile and have not been considered in this study.

In summary, based on comprehensive SARS-CoV2 vaccine-specific serological and cellular analysis, our data demonstrate that the majority of pediatric KTx patients under dual IS therapy in our cohort develops robust humoral immunity, but shows distinct differentiation- and function-related impairments within B- and T helper cell compartments.

DATA AVAILABILITY STATEMENT

The raw data supporting the conclusion of this article will be made available by the authors, without undue reservation.

ETHICS STATEMENT

The studies involving human participants were reviewed and approved by the local ethical committee of the Charité Universitätsmedizin (EA2/227/21). Written informed consent to participate in this study was provided by the participants' legal guardian/next of kin.

AUTHOR CONTRIBUTIONS

AS, JT, PB, and KK designed the study, supervised experiments, analyzed data and wrote the manuscript. LT, ES, VP, CS, JS, AH, LLT, and CL performed experiments and

analyzed data. HS-H, FF, BJ, and HS designed the study and supervised experiments.

FUNDING

AS and KK received funding by the Sonnenfeldstiftung Berlin, Germany. KK was supported by grants from the Deutsche Forschungsgemeinschaft (KO-2270/71 and KO-2270/4-1) and unconditional project funding from Chiesi GmbH. The funder was not involved in the study design, collection, analysis, interpretation of data, the writing of this article or the decision to submit it for publication. ES is funded by the Federal Ministry of Education and Research (BMBF) grant (BCOVIT and 01KI20161) and is enrolled in the Charité Clinician Scientist Program funded by the Charité–Universitätsmedizin Berlin and the Berlin Institute of Health. HS receives funding by the Ministry for Science, Research and Arts of Baden-Württemberg, Germany and the European Commission (HORIZON2020 Project SUPPORT-E, 101015756).

CONFLICT OF INTEREST

The authors declare that the research was conducted in the absence of any commercial or financial relationships that could be construed as a potential conflict of interest.

ACKNOWLEDGMENTS

The authors thank all participants for their willingness to donate blood, thereby greatly supporting this study. We further thank Sofia Friedersdorff for special support.

SUPPLEMENTARY MATERIAL

The Supplementary Material for this article can be found online at: https://www.frontierspartnerships.org/articles/10.3389/ti.2022.10677/full#supplementary-material

REFERENCES

1. Case SM, Son MB. COVID-19 in Pediatrics. *Rheum Dis Clin North Am* (2021) 47:797–811. doi:10.1016/j.rdc.2021.07.006
2. Canpolat N, Yildirim ZY, Yildiz N, Tasdemir M, Goknar N, Evrengul H, et al. COVID-19 in Pediatric Patients Undergoing Chronic Dialysis and Kidney Transplantation. *Eur J Pediatr* (2022) 181:117–23. doi:10.1007/s00431-021-04191-z
3. Downes KJ, Statler VA, Orscheln RC. *Return to School and COVID-19 Vaccination for Pediatric Solid Organ Transplant Recipients in the United States: Expert Opinion for 2021-2022*. Philadelphia, PA: J Pediatric Infect Dis Soc (2021).
4. Europe WHOROf. *European Technical Advisory Group of Experts on Immunization (ETAGE) Interim Recommendations, June 2021: Inclusion of Adolescents Aged 12–15 Years in National COVID-19 Vaccination Programmes* (2021).
5. Sattler A, Schrezenmeier E, Weber UA, Potekhin A, Bachmann F, Straub-Hohenbleicher H, et al. Impaired Humoral and Cellular Immunity after SARS-CoV-2 BNT162b2 (Tozinameran) Prime-Boost Vaccination in Kidney Transplant Recipients. *J Clin Invest* (2021) 150175. doi:10.1172/JCI150175
6. Boyarsky BJ, Werbel WA, Avery RK, Tobian AAR, Massie AB, Segev DL, et al. Antibody Response to 2-Dose SARS-CoV-2 mRNA Vaccine Series in Solid Organ Transplant Recipients. *JAMA* (2021) 325:2204–6. doi:10.1001/jama.2021.7489
7. Stumpf J, Siepmann T, Lindner T, Karger C, Schwobel J, Anders L, et al. Humoral and Cellular Immunity to SARS-CoV-2 Vaccination in Renal Transplant versus Dialysis Patients: A Prospective, Multicenter Observational Study Using mRNA-1273 or BNT162b2 mRNA Vaccine. *Lancet Reg Health Eur* (2021) 9:100178. doi:10.1016/j.lanepe.2021.100178
8. Schrezenmeier E, Rincon-Arevalo H, Jens A, Stefanski AL, Hammett C, Osmanodja B, et al. Temporary Antimetabolite Treatment Hold Boosts SARS-CoV-2 Vaccination-specific Humoral and Cellular Immunity in Kidney Transplant Recipients. *JCI Insight* (2022) 7:e157836. doi:10.1172/jci.insight.157836
9. Rincon-Arevalo H, Choi M, Stefanski AL, Halleck F, Weber U, Szelinski F, et al. Impaired Humoral Immunity to SARS-CoV-2 BNT162b2 Vaccine in Kidney Transplant Recipients and Dialysis Patients. *Sci Immunol* (2021) 6:eabj1031. doi:10.1126/sciimmunol.abj1031
10. Haskin O, Ashkenazi-Hoffnung L, Ziv N, Borovitz Y, Dagan A, Levi S, et al. Serological Response to the BNT162b2 COVID-19 mRNA Vaccine in Adolescent and Young Adult Kidney Transplant Recipients. *Transplantation* (2021) 105:e226–e233. doi:10.1097/TP.0000000000003922
11. Crane C, Phebus E, Ingulli E. Immunologic Response of mRNA SARS-CoV-2 Vaccination in Adolescent Kidney Transplant Recipients. *Pediatr Nephrol* (2022) 37:449–53. doi:10.1007/s00467-021-05256-9
12. Hofmann N, Grossegesse M, Neumann M, Schaade L, Nitsche A. Evaluation of a Commercial ELISA as Alternative to Plaque Reduction Neutralization Test to Detect Neutralizing Antibodies against SARS-CoV-2. *Sci Rep* (2022) 12:3549. doi:10.1038/s41598-022-07597-3
13. Haneda M, Owaki M, Kuzuya T, Iwasaki K, Miwa Y, Kobayashi T, et al. Comparative Analysis of Drug Action on B-Cell Proliferation and Differentiation for Mycophenolic Acid, Everolimus, and Prednisolone. *Transplantation* (2014) 97:405–12. doi:10.1097/01.TP.0000441826.70687.f6
14. Karnell JL, Karnell PG, 3rd, Stephens GL, Rajan B, Morehouse C, Li Y, et al. Mycophenolic Acid Differentially Impacts B Cell Function Depending on the Stage of Differentiation. *J Immunol* (2011) 187:3603–12. doi:10.4049/jimmunol.1003319
15. Eickenberg S, Mickholz E, Jung E, Nofer JR, Pavenstadt HJ, Jacobi AM, et al. Mycophenolic Acid Counteracts B Cell Proliferation and Plasmablast Formation in Patients with Systemic Lupus Erythematosus. *Arthritis Res Ther* (2012) 14:R110. doi:10.1186/ar3835
16. Sekine T, Perez-Potti A, Rivera-Ballesteros O, Stralin K, Gorin JB, Olsson A, et al. Robust T Cell Immunity in Convalescent Individuals with Asymptomatic or Mild COVID-19. *Cell* (2020) 183:158–68. doi:10.1016/j.cell.2020.08.017
17. Lindenstrom T, Agger EM, Korsholm KS, Darrah PA, Aagaard C, Seder RA, et al. Tuberculosis Subunit Vaccination Provides Long-Term Protective Immunity Characterized by Multifunctional CD4 Memory T Cells. *J Immunol* (2009) 182:8047–55. doi:10.4049/jimmunol.0801592
18. Chaichotjinda K, Anurathapan U, Boonsathorn S, Chaisavaneeyakorn S, Treepongkaruna S, Techasaensiri C, et al. Immune Responses to Hepatitis B Vaccination after Hematopoietic Stem Cell Transplantation in Pediatric and Young Adult Patients. *Clin Transpl* (2020) 34:e14024. doi:10.1111/ctr.14024
19. Cirillo L, Citera F, Mazzierli T. *Response to Third Dose of Vaccine against SARS-CoV-2 in Adolescent and Young Adult Kidney Transplant Recipients*. Philadelphia, PA: Transplantation (2022).

Curriculum Vitae

My curriculum vitae does not appear in the electronic version of my paper for reasons of data protection

Publication list

Renal inflamm-aging provokes intra-graft inflammation following experimental kidney transplantation. He A*, Sarwar A*, Thole LML, Siegle J, Sattler A, Ashraf MI, Proß V, Stahl C, Dornieden T, Bergmann Y, Ritschl PV, Ebner S, Hublitz KW, Stamatiades EG, Bülow RD, Boor P, Kotsch K.. Am J Transplant. 2022 Nov;22(11):2529-2547, * equally contributing first authors
IF 9.369

SARS-CoV2 mRNA Vaccine-Specific B-, T- and Humoral Responses in Adolescents After Kidney Transplantation. Sattler A*, Thumfart J*, Tóth L, Schrezenmeier E, Proß V, Stahl C, Siegle J, **He A**, Thole LML, Ludwig C, Straub-Hohenbleicher H, Friedersdorff F, Jahrsdörfer B, Schrezenmeier H, Bufler P, Kotsch K. Transpl Int. 2022 Aug 4;35:10677.
* equally contributing first authors
IF 3.842

Acknowledgments

Saying time passes by quickly is a cliché, but always a good way to start the farewell to the end of a period in life. “白驹过隙”, which is an ancient Chinese idiom means “a white steed flits past a crack, how time flies!’’.

In September 2018, I came to Berlin with my wife to pursue our Ph.D. The past five years have been quite memorable: got a nice apartment in Prenzlauer Berg; learned the challenging mouse kidney transplantation model; raised a very cute dog; delivered a beautiful daughter and our son is around the corner; experienced Berlin’s exciting summer and depressed winter; made through three years of the pandemic; experienced completely different cultures, landscapes and great beers; all these amazing things happened along with the interesting, struggling, as well as disappointed and delighted research life in the lab which is full of adventures.

I stepped into the clinical transplantation field in 2013, and since then I have always been interested in transplantation immunology, which is why I am extremely grateful to complete my doctoral thesis on this topic. At this point, with my whole heart, I would like to thank everyone who made my doctorate possible to complete successfully. Especially, I would like to thank my doctoral mother Prof. Dr. Katja Kotsch, for her consistent and comprehensive support in the past years. I came to the lab as “naïve”, leave the lab as “treated”, I believe the improvement is significant. Special thanks to Dr. Arne Sattler for the scientific guidance and caring both in science and in life, always be there for me, to raise me up. I also would like to thank Dr. Muhammad Imtiaz Ashraf for the great training in the challenging murine kidney transplantation model. Of course, I would also like to thank the entire lovely AG Kotsch, who were always at my side when I had questions, whose help I could always count on, and who made my work full of fun. I would also like to thank all other working groups for their cooperation during this time and their constant help with materials and knowledge.

Of course, I would like to say a special thank you to my family, especially my wife, who has always had my back and has always supported and encouraged me throughout.